

This is to certify that the

dissertation entitled

INTERCALATION OF CATALYTICALLY ACTIVE METAL  
COMPLEXES IN MICA-TYPE SILICATES:  
RHODIUM HYDROFORMYLATION CATALYSTS

presented by

FAEZEH FARZANEH

has been accepted towards fulfillment  
of the requirements for

PH. D. degree in CHEMISTRY

THOMAS J. PINNAVIA

Major professor

Date 8-27-81



**OVERDUE FINES:**  
25¢ per day per item

**RETURNING LIBRARY MATERIALS:**  
Place in book return to remove  
charge from circulation records

--	--

INTERCALATION OF CATALYTICALLY ACTIVE METAL  
COMPLEXES IN MICA-TYPE SILICATES:  
RHODIUM HYDROFORMYLATION CATALYSTS

By

Faezeh Farzaneh

A DISSERTATION

Submitted to

Michigan State University

in partial fulfillment of the requirements

for the degree of

DOCTOR OF PHILOSOPHY

Department of Chemistry

1981

ABSTRACT

INTERCALATION OF CATALYTICALLY ACTIVE METAL  
COMPLEXES IN MICA-TYPE SILICATES:  
RHODIUM HYDROFORMYLATION CATALYSTS

By

Faezeh Farzaneh

Cationic rhodium complexes such as  $[\text{Rh}(\text{NBD})(\text{PPh}_3)_2]^+ \text{PF}_6^-$  (I) and  $[\text{Rh}(\text{COD})(\text{PPh}_3)_2]^+ \text{A}^-$ ; ( $\text{A}^- = \text{PF}_6^-, \text{BF}_4^-$ ) (II) are active catalyst precursors for hydroformylation of 1-hexene even at room temperature and 1 atm pressure. The rate of hydroformylation in DMF is appreciably faster than in acetone. Solvated sodium ions in the layered silicate hectorite are readily exchanged by complexes I and II; IR and X-ray studies confirm this result. Hydroformylation of 1-hexene in the intercalated system shows n-heptanal to 2-methyl hexanal ratio of 3:1, which is similar to the homogeneous results. It was found that these complexes are not well suited for intercalation in layer silicates, because of the reactive intermediate appears to be a neutral monohydride complex  $\text{RhH}(\text{CO})_x(\text{PPh}_3)_2$  (III) which is readily

desorbed from the silicate surface during the course of the catalytic reaction. The effects of acid ( $\text{HClO}_4$ ) and base ( $\text{NEt}_3$ ) on the activity of the homogeneous catalysts in the hydroformylation of 1-hexene also support the presence of a neutral monohydride rhodium complex ( $\overset{\text{I}}{\underset{\text{III}}{\text{Rh}}}$ ).

Positively charged analogs of ( $\overset{\text{I}}{\underset{\text{III}}{\text{Rh}}}$ ), suitable for intercalation in layered silicate, are obtained by reaction of the positively charged ligand  $\text{Ph}_2\text{P}(\text{CH}_2)_2\text{P}^+\text{Ph}_2(\text{CH}_2\text{Ph})$ , abbreviated  $\text{P-P}^+$  with rhodium ( $\overset{\text{I}}{\text{Rh}}$ ) complexes such as  $[\text{Rh}(\text{diene})\text{Cl}]_2$ ,  $\text{Rh}(\text{dien})^+$  where diene = COD, NBD and  $[\text{Rh}(\text{CO})\text{Cl}]_2$  in a ratio of  $\text{P-P}^+:\text{Rh}$ ,  $\geq 2:1$ . These positively charged catalysts were all active in homogeneous and intercalated systems. In all of the supported catalysts, the rates of hydroformylation are lower than for the homogeneous system, but the normal to branched (n/b) aldehyde ratio is increased and isomerization of 1-hexene to 2-hexene is decreased. When  $\text{RhCOD}^+/\text{P-P}^+/\text{Hect}$  is the catalyst for hydroformylation of olefin, no isomerization is observed, which is in favor of the hydroformylation reaction. The inhibition of isomerization may be attributed to the steric crowding at the rhodium center by the bulky positively charged ligand.  $^{31}\text{P}$  nmr studies indicated that the behavior of the positively charged  $\text{P-P}^+$  ligand is similar to triphenylphosphine in its ability to coordinate to rhodium. The complex  $[\text{RhCl}(\text{CO})(\text{S})_2(\text{P-P}^+)_2](\text{BF}_4)_2$ , where S = acetone, has been identified as a catalyst precursor for olefin hydroformylation.

To Heroic People of Iran

## ACKNOWLEDGMENTS

I wish to express my deepest gratitude to Professor Thomas J. Pinnavaia, for his guidance, encouragement, understanding and friendship throughout the course of this study. I am also grateful for the editorial assistance given by my second reader, Professor Carl Brubaker.

I would like to acknowledge the financial support of the People of Iran, administered through the Free University of Iran.

Thanks are extended to the National Science Foundation and Michigan State University for financial support during this study.

## TABLE OF CONTENTS

Chapter	Page
LIST OF TABLES . . . . .	viii
LIST OF FIGURES . . . . .	xii
I. INTRODUCTION . . . . .	1
A. Homogeneous Catalysts . . . . .	1
B. Historical Background of Supported Metal Complexes . . . . .	7
1. Background of Supported Metal Complex . . . . .	
2. Polymers As a Support for Homogeneous Catalysis . . . . .	14
3. Inorganic Support for Homo- geneous Catalysts . . . . .	20
4. Advantages of Inorganic Oxide Over Polymer as Supports . . . . .	20
5. Inorganic Oxides as a Support . . . . .	21
6. Structural Features of Layered Silicates . . . . .	30
C. Hydroformylation . . . . .	38
II. EXPERIMENTAL . . . . .	49
A. Materials . . . . .	49
B. Physical Methods . . . . .	50
1. Infrared Spectra . . . . .	50
2. X-Ray Diffraction Studies . . . . .	51
3. Proton NMR Studies . . . . .	51

Chapter	Page
4. Phosphorus-31 NMR Studies . . . . .	52
5. Gas Chromatography. . . . .	53
6. Elemental Analysis and Melting Points. . . . .	53
C. Synthesis . . . . .	54
1. $[\text{RhCl}(\text{COD})]_2$ . . . . .	54
2. $[\text{Rh}(\text{NBD})\text{Cl}]_2$ . . . . .	54
3. $[\text{Rh}(\text{COD})(\text{PPh}_3)_2]\text{PF}_6$ , $[\text{Rh}(\text{COD})(\text{PPh}_3)_2]\text{BF}_4$ . . . . .	55
4. $[\text{Rh}(\text{NBD})(\text{PPh}_3)_2]\text{PF}_6$ . . . . .	55
5. $[\text{Rh}(\text{COD})(\text{diphos})]\text{ClO}_4$ . . . . .	55
6. $\text{RhCl}(\text{COD})(\text{PPh}_3)$ . . . . .	56
7. $\text{Ph}_2\text{PCH}_2\text{CH}_2\text{PPh}_2\text{CH}_2\text{PhBr}$ . . . . .	56
8. $\text{BF}_4^-$ - Resin. . . . .	56
9. $(\text{Ph}_2\text{PCH}_2^1\text{CH}_2^2\text{PPh}_2\text{CH}_2^3\text{Ph})\text{BF}_4$ . . . . .	56
10. $[\text{RhCl}(\text{COD})(\text{Ph}_2\text{PCH}_2^1\text{CH}_2^2\text{PPh}_2\text{CH}_2^3\text{Ph})]\text{BF}_4$ . . . . .	57
11. $[\text{Rh}(\text{CO})_2\text{Cl}(\text{P}-\text{P}^+)]\text{BF}_4$ and $[\text{Rh}(\text{CO})\text{Cl}(\text{P}-\text{P}^+)_2](\text{BF}_4)_2$ . . . . .	58
12. $[\text{RhCl}(\text{CO})(\text{S})_x(\text{P}-\text{P}^+)_2](\text{BF}_4)_2$ , S = Aceton, X = 2,3 . . . . .	59
13. $[\text{Rh}(\text{COD})^+]\text{BF}_4$ . . . . .	60
14. $[\text{Rh}(\text{NBD})]^+\text{BF}_4$ . . . . .	60
15. $[\text{Rh}(\text{COD})(\text{PPh}_3)_2]^+$ -hectorite . . . . .	60
16. $[\text{Rh}(\text{NBD})(\text{PPh}_3)_2]$ -hectorite. . . . .	60
17. $\text{RhCl}(\text{COD})\text{P}-\text{P}^+/\text{Hectorite}$ . . . . .	61

Chapter	Page
18. Oriented Film Samples of Hectorite and Montmorillonite . . . . .	61
19. Oriented Films of Rhodium Exchanged Hectorite . . . . .	61
20. P-P <sup>+</sup> /Hectorite. . . . .	62
D. Hydroformylation Procedures and Apparatus . . . . .	62
1. Method I - Homogeneous Catalysts. . . . .	66
2. Method I, Heterogeneous Catalysts . . . . .	66
3. Method II, Homogeneous Catalyst . . . . .	67
4. Method II, Heterogeneous System . . . . .	68
5. Method III, Heterogeneous Catalyst. . . . .	68
III. RESULTS AND DISCUSSION. . . . .	70
A. Characterization of Rhodium Exchanged Hectorite . . . . .	70
1. Interpretation of Infrared Spectra . . . . .	71
2. X-Ray Diffraction Studies . . . . .	76
B. Homogeneous Hydroformylation. . . . .	79
C. Hydroformylation with Intercalated Rh(diene)(PPh <sub>3</sub> ) <sub>2</sub> <sup>+</sup> . . . . .	85
D. Further Characterization of Homogeneous Rh(COD)(PPh <sub>3</sub> ) <sub>2</sub> <sup>+</sup> Catalyst Precursor. . . . .	91
E. Utilization of P-P <sup>+</sup> a Cationic Phosphine Ligand. . . . .	97
1. [RhCl(COD)] <sub>2</sub> + P-P <sup>+</sup> Precursor Catalyst System . . . . .	97
2. Hydroformylation of 1-Hexene with Intercalated Catalysts . . . . .	105

Chapter	Page
3. Solvent Effects . . . . .	112
4. Characterization of the Homo- geneous Hydroformylation Catalysts Containing P-P <sup>+</sup> . . . . .	117
5. Rh(diene) <sup>+</sup> , P-P <sup>+</sup> Precursor System. . . . .	134
6. [Rh(CO) <sub>2</sub> Cl] <sub>2</sub> + P-P <sup>+</sup> Catalyst Precursor System. . . . .	141
SUMMARY . . . . .	146
REFERENCES. . . . .	148

## LIST OF TABLES

Table		Page
1	Industrial Process Involving Homogeneous Catalysts . . . . .	3
2	Advantages and Disadvantages of Homogeneous and Heterogeneous Catalysis . . . . .	6
3	Some Heterogeneous Catalysts of Industrial Importance . . . . .	9
4	Application of Polymer Supported Catalysts . . . . .	18
5	Grafting of Homogeneous Catalysts on Inorganic Support (Silica) . . . . .	23
6	Examples of Organometallic Pre- cursor Supported on Inorganic Supports. . . . .	27
7	Physisorption and Ion Exchange Re- actions in Zeolites and Layered Silicates . . . . .	29
8	Some Minerals Having the Three- fold Sheets Found in Micas. . . . .	31
9	Hydroformylation Catalysts and Their Variants. . . . .	40

Table	Page
10	Hydroformylation with Immobilized Catalysts . . . . . 45
11	Complexes Containing Positively Charged Ligands . . . . . 48
12	Infrared Bands ( $\text{cm}^{-1}$ ) of $[\text{Rh}(\text{NBD})-(\text{PPh}_3)_2]\text{PF}_6$ , $\text{Na}^+$ -hectorite and $\text{Rh}(\text{NBD})(\text{PPh}_3)_2$ -hectorite. . . . . 75
13	001 Basal Spacings of $\text{Na}^+$ -Hectorite and $\text{Na}^+$ -Hectorite Partially Exchanged with Cationic Rhodium Complexes . . . . . 78
14	Homogeneous Hydroformylation of 1-Hexene with $[\text{Rh}(\text{diene})(\text{PPh}_3)_2]\text{PF}_6$ as Catalyst Precursors. . . . . 80
15	Homogeneous Hydroformylation of 1-Hexene with $[\text{Rh}(\text{COD})(\text{PPh}_3)_2]\text{PF}_6$ as Catalyst Precursor . . . . . 81
16	Homogeneous Hydroformylation of 1-Hexene with $[\text{Rh}(\text{COD})(\text{PPh}_3)_2]\text{PF}_6$ as Catalyst Precursor . . . . . 83
17	Hydroformylation of 1-hexene with $\text{Rh}(\text{COD})(\text{PPh}_3)_2^+$ Intercalated in Hectorite at $25^\circ\text{C}$ . . . . . 84
18	Physical Constants for Acetone and DMF . . . . . 89

Table	Page
19	Homogeneous Hydroformylation of 1-hexene with $[\text{RhCl}(\text{COD})\text{P}-\text{P}^+]\text{BF}_4$ as Catalyst Precursor. . . . . 99
20	Homogeneous Hydroformylation of 1-Hexene with $\text{ClRh}(\text{COD})\text{P}-\text{P}^+$ as Catalyst Precursor. . . . . 100
21	Homogeneous and Heterogeneous Hydro- formylation of 1-Hexene with $\text{ClRh}(\text{COD})-$ $\text{P}-\text{P}^+$ . . . . . 107
22	Homogeneous and Heterogeneous Hydro- formylation of 1-Hexene with $\text{ClRh}(\text{COD})-$ $\text{P}-\text{P}^+$ as Catalyst Precursor in DMF, and $\text{C}_6\text{H}_6$ . . . . . 113
23	001 Basal Spacing of $\text{Na}^+$ -Hectorite After Partial Exchanged with $\text{RhCl}(\text{COD})-$ $\text{P}-\text{P}^+ + \text{P}-\text{P}^+$ Under Hydroformylation Condition . . . . . 115
24	$^{31}\text{P}$ nmr Data for 1:1 $\text{RhCl}(\text{COD}) \text{P}-\text{P}^+$ : $\text{P}-\text{P}^+$ Under Hydroformylation Conditions. . . 126
25	Hydroformylation of 1-Hexene with $\text{Rh}(\text{diene})^+$ Complexes as Catalyst Pre- cursors in Homogeneous and Inter- calated Systems . . . . . 136
26	Hydroformylation of 1-Hexene with $\text{Rh}(\text{diene})^+$ as Catalyst Precursor in

Table	Page
Homogeneous and Intercalated System. . . . .	138
27 Hydroformylation of 1-Hexene with RhCl(CO) <sub>2</sub> (P-P <sup>+</sup> ), 2P-P <sup>+</sup> as Catalyst Precursor. . . . .	143

## LIST OF FIGURES

Figure		Page
1	A representative structural element of the multifunctional catalyst. . . . .	17
2	Grafting of homogeneous catalysis on silica . . . . .	22
3	Direct interaction of organo-metallic compounds with silica surface . . . . .	26
4	General types of possible surface reactions (adapted from Reference 34e). . . . .	28
5	Layer structure of smectites illustrating the intracrystalline space which contains the exchangeable cations. (Adopted from Reference 73a.) . . . . .	36
6	Cobalt clusters for hydroformylation . . . . .	44
7	Hydroformylation apparatus (schematic) for reaction carried out at 1 atm pressure . . . . .	63

Figure	Page
8	600 ml autoclave used for hydroformylation reactions at 600 psi. . . . . 65
9	Infrared spectra (KBr pellet) of [Rh(NBD)(PPh <sub>3</sub> ) <sub>2</sub> ]PF <sub>6</sub> in the region 1600-250 cm <sup>-1</sup> . . . . . 72
10	Infrared spectra of (A) Na <sup>+</sup> -hectorite and (B) [Rh(NBD)(PPh <sub>3</sub> ) <sub>2</sub> ]-hectorite as oriented films. . . . . 74
11	<sup>31</sup> P nmr spectra of (A) [Rh(COD)(PPh <sub>3</sub> ) <sub>2</sub> ]PF <sub>6</sub> 0.01M in acetone at 25°C; (B) [Rh(COD)(PPh <sub>3</sub> ) <sub>2</sub> ] <sup>+</sup> + CO, 0.01 M in acetone at 25°C, (C) at -30°C number of accumulated scans = 10000 . . . . . 94
12	<sup>31</sup> P nmr spectra of [Rh(COD)(PPh <sub>3</sub> ) <sub>2</sub> ]PF <sub>6</sub> + CO-H <sub>2</sub> , 0.01M in acetone under hydroformylation condition (A) after 2 hr; (B) after 16 hrs. . . . . 96
13	Dissociative (I) and Associative (II) mechanism of hydroformylation reactions (according to G. Wilkinson, et al. 1968). . . . . 102
14	Mechanism of the hydroformylation with possible isomerization steps (HM = HM(CO) <sub>m</sub> ). . . . . 108
15	Possible pathways for hydroformylation and isomerization of 1-hexene between the silicate sheets . . . . . 110

Figure	Page
16	$^{31}\text{P}$ nmr spectra (A,B) of $\text{RhCl}-(\text{COD})\text{P}-\text{P}^+\text{BF}_4$ 0.01M in acetone ( $d_6$ ) at $-30^\circ\text{C}$ , number of accumulated scans, NS = 10000 . . . . . 119
17	$^{31}\text{P}$ nmr spectrum of $\text{RhCl}(\text{COD})-\text{P}-\text{P}^+-\text{P}-\text{P}^+$ in 0.01M solution of acetone ( $d_6$ ), NS = 10000. . . . . 122
18	$^{31}\text{P}$ nmr spectra of (A) $\text{RhCl}(\text{COD})-\text{P}-\text{P}^++\text{P}-\text{P}^++\text{CO}-\text{H}_2$ (1:1) 0.01M in Acetone ( $d_6$ ) at $-30^\circ\text{C}$ . (B) $\text{RhCl}-(\text{COD})\text{PPh}_3 + \text{PPh}_3 + \text{CO}/\text{H}_2$ (1:1), 0.01M in benzene at $25^\circ\text{C}$ . NS = 10000 . . . 125
19	Infrared spectra of (A) 1:1 mixture of $\text{RhCl}(\text{COD})\text{P}-\text{P}^+:\text{P}-\text{P}^+$ in acetone under hydroformylation condition (A) crystallized in pentane; (B) recrystallized in $\text{CHCl}_3$ . . . . . 131
20	Infrared spectra of 1:1 mixture of $\text{RhCl}(\text{COD})\text{P}-\text{P}^+:\text{P}-\text{P}^+ + 1\text{-hexene}$ under hydroformylation condition (recrystallized in $\text{CHCl}_3$ ) . . . . . 133
21	Infrared spectra (KBr disks) of A, Na-hectorite, and (B) the $\text{P}-\text{P}^+-\text{hectorite} + \text{RhCOD}^+$ system before hydroformylation. Spectrum C

Figure		Page
	is for the P-P <sup>+</sup> -hectorite + Rh(COD) <sup>+</sup> system after hydro- formylation . . . . .	140
22	Infrared spectra of [RhCl(CO) <sub>2</sub> - (P-P <sup>+</sup> )]BF <sub>4</sub> . . . . .	145

## LIST OF SYMBOLS AND ABBREVIATIONS

$\text{BF}_4^-$ -Resin	Tetrafluoroborate anion exchange resin
COD	1,5 cyclooctadiene
diphos	bis(1,2-diphenylphosphino)ethane
d	doublet
dt	doublet of triplets
L	Ligand (usually phosphine)
$\text{L}^+$	cationic ligand
M	metal
Me	methyl
m	multiplet
NBD	norbornadiene
NMR	Nuclear Magnetic Resonance
NS	Number of accumulating scans
P	Phosphorus nucleus (usually in a phosphine)
$\text{P}^+$	Phosphonium phosphorus nucleus
Ph	Phenyl group
$\text{P}-\text{P}^+$	1-diphenyl phosphino-2-benzoyldiphenyl phosphonium ethane
$\text{P}-\text{P}^+\text{BF}_4$	$\text{P}-\text{P}^+$ tetrafluoroborate
$\text{P}-\text{P}^+\text{Br}$	$\text{P}-\text{P}^+$ bromide
$\text{P}-\text{P}^+/\text{Hect.}$	$\text{P}-\text{P}^+$ exchanged form of hectorite
S	solvent

SIL

silica

t

triplet

$\delta$

chemical shift

## I. INTRODUCTION

### A. Homogeneous Catalysts

The field of homogeneous catalysts includes vast areas of active research ranging from simple acid-base catalysis to extremely complex metalloenzyme catalysis. It is one of the most rapidly expanding fields of chemistry. Before the last two decades only a few homogeneous catalysts were used on a laboratory or on industrial scale. The past several years, however, have seen the emergence of a variety of novel and useful homogeneous catalyst systems. This rapid enrichment seems to be only the beginning of further growth of this field.<sup>1</sup>

Examples of some of these developments include relevant metal ions which have been found to function as superacids (or superelectrophiles) to accelerate some reactions to great extent. Redox properties of some transition metal ions (e.g.,  $\text{Cu}^+$  and  $\text{Cu}^{2+}$ ) have been advantageously utilized to catalyze electron transfer reactions. The development of coordination chemistry has greatly helped the understanding of these metal ion catalysts. Soluble metal complexes, especially those of transition metals, are now extensively used in industry to catalyze syntheses of organic compounds. Some of the best known catalyst

processes involving organometallic compounds are:<sup>2</sup>

- (a) hydrogenation of olefins in the presence of compounds of low valent metals such as rhodium [e.g.,  $\text{RhCl}(\text{PPh}_3)_3$ , Wilkinson's catalyst];
- (b) hydroformylation of olefins using a cobalt or rhodium catalyst (oxo process);
- (c) oxidation of olefins to aldehyde and ketones (Wacker process);
- (d) polymerization of propylene by using an organo-aluminum titanium catalyst (Ziegler-Natta catalyst) to give stereoregular polymers.
- (e) cyclopolymerization of acetylenes by using nickel catalysts (Reppé's or Wilke's catalysts); and
- (f) olefin isomerization by using nickel catalysts.

During a rapid development in the organic chemistry of the transition metals, Fischer and Wilkinson and Ziegler and Natta were doing the research that won them Nobel prizes in chemistry. In fact, their work became a basis for producing many industrial products. In Table 1, examples of major industrial applications of homogeneous catalysis are listed.

In addition, conversions of coal to CO is now very important process<sup>25</sup> and selective hydrogenation of CO is being investigated actively.<sup>26</sup> Metal clusters are novel homogeneous catalysts for various reactions. For example,

Table 1. Industrial Process Involving Homogeneous Catalysts. 3

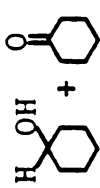
Reaction	Catalyst	Ref.
<u>Carbonylation</u>		
$\text{CH}_3\text{CH}=\text{CH}_2 + \text{CO} + \text{H}_2 \rightarrow \text{C}_3\text{H}_7\text{CHO}$	$\text{CO}_2(\text{CO})_8 + \text{PR}_3$ $\text{RhH}(\text{CO})(\text{PR}_3)_3$ $\text{RhH}(\text{CO})_2(\text{PR}_3)_2$	4 5,6 7
$\text{RCH}=\text{CH}_2 + \text{CO} + \text{H}_2 \rightarrow \text{R}-(\text{CH}_2)_2-\text{CH}_2\text{OH}$ $\text{CH}_3\text{OH} + \text{CO} \rightarrow \text{CH}_3\text{COOH}$	$\text{CO}_2(\text{CO})_8 + \text{PR}_3$ $\text{CO}_2(\text{CO})_8 + \text{RI}$ $\text{RhCl}_3 + \text{MeI}$	4,8 9 10
<u>Oxidation</u>		
$\text{CH}_2=\text{CH}_2 + \text{O}_2 \rightarrow \text{CH}_3\text{CHO}$	$\text{PdCl}_2 + \text{CuCl}_2$	11
$\text{cyclo-C}_6\text{H}_{12} + \text{O}_2 \rightarrow$  $+ \text{HNO}_3$ $\downarrow$ $\text{HOOC}(\text{CH}_2)_4\text{COOH}$	Cobalt naphthenate Cobalt acetate or copper/ manganese acetate or VV salts	12 13
$\text{Cyclo-C}_{12}\text{H}_{24} + \text{O}_2 \rightarrow \text{cyclo-C}_{12}\text{H}_{23}\text{OH} + \text{cyclo-C}_{12}\text{H}_{22}\text{O}$ $\downarrow \text{HNO}_3$ (adipic acid)	$\text{H}_3\text{BO}_3$ or $\text{H}_2\text{MoO}_5$ Copper/manganese acetate or VV Salts	14 15

Table 1. Continued.

Reaction	Catalyst	Ref.
$  \begin{array}{c}  \text{CH}_3 \\    \\  \text{C}_6\text{H}_2 \\    \\  \text{CH}_3  \end{array}  + \text{O}_2 \rightarrow  \begin{array}{c}  \text{COOH} \\    \\  \text{C}_6\text{H}_2 \\    \\  \text{COOH}  \end{array}  $	COBr <sub>2</sub> or MnBr <sub>2</sub>	16
$  n\text{-C}_4\text{H}_{10} + \text{O}_2 \rightarrow \text{CH}_3\text{COOH}  $	Co(II) acetate	17
$  \text{CH}_3\text{CHO} + \text{O}_2 \rightarrow \text{CH}_3\text{COOH}  $	Mn <sup>II</sup> salts	18
$  \text{CH}_3\text{CH}=\text{CH}_2 + \text{ROOH} \rightarrow \text{CH}_3\text{CH}(\text{O})-\text{CH}_2 + \text{ROH}  $	Mo Salts	19
<p>Reaction of dienes</p> $  \begin{array}{c}  \text{H}_2 \\  \downarrow \\  \text{cyclo-C}_{12}\text{H}_{24}  \end{array}  $	Et <sub>3</sub> Al <sub>2</sub> Cl <sub>3</sub> +TiCl <sub>4</sub>	20
$  \begin{array}{c}  \text{CH}_2\text{CH}_2 + \text{CH}_2\text{CH}=\text{CH}_2 \\  + 2\text{HCN} \rightarrow \text{NC}(\text{CH}_2)_4\text{CN}  \end{array}  $	RhCl <sub>3</sub> , 3H <sub>2</sub> O Ni(P(OAr) <sub>3</sub> ) <sub>4</sub>	21 22
<p>Olefin Isomerization</p> $  \text{CH}_2=\text{CHCHClCH}_2\text{Cl} \rightarrow \text{ClCH}_2\text{CH}=\text{CHCH}_2\text{Cl}  $	CuCl	23
<p>Manufacture of 1,4-dicyanobut-2-ene</p> $  \text{ClCH}_2\text{CH}=\text{CHCH}_2\text{Cl} + 2\text{NaCN} \rightarrow \text{NCCH}_2\text{CN}=\text{CHCH}_2\text{CN}  $	CuCN	24

the reduction of CO to methane, methanol, ethylene glycol and others has been reported recently.<sup>26,27</sup>

Homogeneous catalysts show potential for solving environment problems in the future. Catalytic conversion of poisonous NO and CO gases into nonpoisonous N<sub>2</sub>O and CO<sub>2</sub> has been successfully performed by using [RhCl<sub>2</sub>(CO)<sub>2</sub>]<sup>-</sup> as a homogeneous catalyst in an aqueous acidic ethanol solution.<sup>28</sup> Homogeneous catalysts are also utilized in the fine chemicals industry, where delicate control of organic reactions is important. For example, asymmetric hydrogenation is currently being used for the production of L-dopa; a drug used to treat Parkinson's disease.<sup>29</sup> Micelles, cyclopolymers, and similar macromolecular catalysts<sup>30</sup> have been used to accelerate many organic reactions, especially in the syntheses of fine chemicals.

The heterogenizing of homogeneous catalysts is currently a very active and relatively new area of research.<sup>31</sup> The term heterogenizing refers to the process whereby a homogeneous transition metal complex is immobilized or anchored to an inert polymer or inorganic support.<sup>31a</sup> In order to appreciate the reasons for the present interest in supported complex catalysts, it is useful to look at the advantages and disadvantages of heterogeneous and homogeneous catalysts.

By looking to Table 2 one can see that homogeneous catalysts suffer from three major problems which are

Table 2. Advantages and Disadvantages of Homogeneous and Heterogeneous Catalysis. 32

Process	Advantages	Disadvantages
Homogeneous Catalysis	<ol style="list-style-type: none"> <li>1) High activity due to very ready availability of metal</li> <li>2) Facile electronic and steric variability, no mass transfer problems</li> <li>3) High substrate selectivity and product specificity</li> </ol>	<ol style="list-style-type: none"> <li>1) Process for catalyst separation necessary</li> <li>2) Sensitive to extreme temperature.</li> <li>3) Solubility or solvent problem.</li> </ol>
Heterogeneous Catalysis	<ol style="list-style-type: none"> <li>1) Catalyst readily separable from substrate.</li> <li>2) Stable to high temperatures.</li> </ol>	<ol style="list-style-type: none"> <li>1) Active sites make only part of the metal content available.</li> <li>2) Unlimited specificity.</li> <li>3) Mass transfer problems in pores.</li> </ol>

sufficient to preclude their use in most industrially important processes. The major disadvantage of homogeneous catalysts is the problem of separating the catalyst from the products at the end of the reaction. The thermal stability of heterogeneous catalysts such as pure metals and metal oxides, is often much higher than that of homogeneous catalysts. Whereas the range of suitable solvents for a homogeneous catalyst is often limited by the solubility characteristics of the catalyst, this clearly presents no problem for a heterogeneous catalyst.

#### B. Historical Background of Supported Metal Complexes

The first heterogeneous catalytic process of industrial significance, introduced in about 1875, utilized platinum to oxidize  $\text{SO}_2$  to  $\text{SO}_3$ , which was then converted to sulfuric acid by absorption in an aqueous solution of the acid. Other inorganic chemical catalytic processes followed, notably the development by Ostwald in about 1903 of the oxidation of ammonia on a platinum gauze to form nitrogen oxides for conversion to nitric acid. Also, the synthesis of ammonia from the elements by the Born-Haber process was initiated in the early 1900's. The conversion of methanol to formaldehyde was introduced in about 1890. Benzene oxidation to maleic anhydride occurred in 1928. The partial oxidation of ethylene to ethylene oxide was commercialized by Union Carbide in 1937. In the processing

of petroleum for fuels, the first catalytic process, catalytic cracking, appeared in about 1937. This first used acid-treated clay, then later a synthetic silica alumina catalyst, and more recently Zeolite catalysts incorporated in a silica-alumina matrix. Reforming, which originally used molybdena-alumina catalyst to increase the octane number of gasoline by cyclization of paraffins and dehydrogenation to aromatics, was superseded by reforming process that used a Pt/alumina catalyst. Catalytic hydrocracking and hydrodesulfurization and hydrotreating have grown rapidly the past two decades and are now of major importance in petroleum processing. Table 3 lists these and some of the other major industrial reactions which utilize a heterogeneous catalyst.

A homogeneous catalyst can be heterogenized in a variety of ways.<sup>34</sup> The common method is to attach the catalyst to a solid support by an ionic or covalent bond. Alternatively, the metal complex may be physically dispersed within the pore structure of a support, e.g., silica or other suitable material, by impregnation of a carrier solution of the complex, followed by solvent evaporation. Such evaporations have been termed dry or solid support. The complex may also be dispersed by using a relatively involatile solvent, which remains in the solid after the evaporation steps and which the complex is effectively dispersed. Such supported liquid phase (SLPC) catalyst preparations,<sup>35</sup> have

Table 3. Some Heterogeneous Catalysts of Industrial Importance. 33

Reaction	Catalyst and Reactor Type (Continuous Operation Unless Otherwise Noted)
$C_4H_{10} \rightarrow$ (butane) butenes and $C_4H_6 \rightarrow$ (butadiene)	<u>Dehydrogenation</u> $Cr_2O_3-Al_2O_3$ (fixed bed, cyclic)
Butenes $\rightarrow C_4H_6$ (butadiene)	$Fe_2O_3$ promoted with $Cr_2O_3$ and $K_2CO_3$ , or $Ca_8Ni(PO)_4$ (fixed bed, continuous, in presence of steam)
$C_6H_5C_2H_5 \rightarrow C_6H_5CH=CH_2$ (ethyl benzene $\rightarrow$ styrene)	$Fe_2O_3$ promoted with $Cr_2O_3$ and $K_2CO_3$ (fixed bed)
$CH_4$ or other hydrocarbons $+ H_2O \rightarrow$	Supported Ni (fixed bed)
$CO + H_2$ (steam reforming)	ZnO
$(CH_3)_2CHOH \rightarrow CH_3COCH_3 + H_2$ (isopropanol $\rightarrow$ acetone $+ H_2$ )	<u>Hydrogenation</u>
$CH_3CH(OH)C_2H_5 \rightarrow CH_3COC_2H_5 + H_2$	Raney Ni, or Ni on a support (slurry reactor, batch or continuous) Pd on C or other support (slurry reactor, batch or continuous) (other supported metals may also be used)
Of edible fats and oils	
Various hydrogenations of fine organic chemicals	

Table 3. Continued.

Reaction	Catalyst and Reactor Type (Continuous Operation Unless Otherwise Noted)
$C_6H_6 + 3H_2 \rightarrow C_6H_{12}$ $N_2 + 3H_2 \rightarrow 2NH_3$ (selective hydrogenation of $C_2H_2$ impurity in $C_2H_4$ from thermal-cracking plant)	Ni or noble metal on support (fixed bed) Fe promoted with $Al_2O_3$ , $K_2O$ , $CaO$ , and $MgO$ (adiabatic fixed bed)
$SO_2 + \frac{1}{2}O_2 \rightarrow SO_3$	<u>Oxidation</u> $V_2O_5$ plus $K_2SO_4$ on $SiO_2$ (adiabatic, fixed beds)
$2NH_3 + \frac{5}{2}O_2 \rightarrow 2NO + 3H_2O$	90% Pt-10% Rh wire gauze, oxidizing conditions
$NH_3 + CH_4 + air \rightarrow HCN$ (Andrussov process)	90% Pt-10% Rh wire gauze, under net reducing conditions
$C_{10}H_8$ or $1,2-C_6H_4(CH_3)_2 + O_2 \rightarrow$ $C_6H_4(CO)_2O$	Supported $V_2O_5$ (multitube fixed bed)
(naphthalene or o-xylene + air $\rightarrow$ maleic anhydride)	
$n-C_4H_8$ or $C_6H_6 + O_2$ $C_4H_2O_3$ (butene or benzenes + air maleic anhydride)	Supported $V_2O_5$ (multitube fixed bed)

Table 3. Continued.

Reaction	Catalyst and Reactor Type (Continuous Operation Unless Otherwise Noted)
$\text{CH}_3\text{OH} + \text{O}_2 \rightarrow \text{CH}_2\text{O} + \text{H}_2\text{O}$ and/or $\text{H}_2\text{O}$	Ag or $\text{Fe}_2\text{O}_3\text{-MoO}_3$
$\text{C}_3\text{H}_6 + \text{O}_2 \rightarrow \text{CH}_2=\text{CHCHO}$ (acrolein) and/or $\text{CH}_2=\text{CHCOOH}$ (acrylic acid)	$\text{Cu}_2\text{O}$ or multimetallic oxide compositions
$\text{C}_3\text{H}_6 + \text{NH}_3 + \frac{3}{2}\text{O}_2 \rightarrow \text{CH}_2=\text{CHCN} + 3\text{H}_2\text{O}$	Complex metal molybdates or multimetallic oxide compositions (fluid bed)
Complete oxidation of CO, hydrocarbons, in pollution control, as of auto exhaust	Pt or Pt-Pd, pellet or monolith support
$\text{C}_2\text{H}_4 + \frac{1}{2}\text{O}_2 + \text{CH}_3\text{COOH} \rightarrow$	Pd on acid-resistant support (vapor phase, multitube fixed bed)
$\text{CH}_3\text{COOCH}=\text{CH}_2$ (vinyl acetate)	Promoted ferrite spinels
$\text{C}_4\text{H}_8 + \frac{1}{2}\text{O}_2 \rightarrow \text{C}_4\text{H}_6 + \text{H}_2\text{O}$	<u>Acid-Catalyzed Reactions</u>
Catalytic cracking	Zeolite (molecular sieve) in $\text{SiO}_2\text{-Al}_2\text{O}_3$ matrix (fluid bed)
Hydrocracking	Metal (e.g., Pd) on zeolite (adiabatic fixed beds)
Isomerization	Metal on acidified $\text{Al}_2\text{O}_3$ (fixed bed), zeolites

Table 3. Continued.

Reaction	Catalyst and Reactor Type (Continuous Operation Unless Otherwise Noted)
Catalytic reforming	Pt, Pt-Re, or Pt-Ir on acidified $Al_2O_3$ (adiabatic, fixed or moving bed)
Polymerization	$H_3PO_4$ on clay (fixed bed)
Hydration, e.g., propylene to isopropyl alcohol	Mineral acid or acid-type ion-exchange resin (fixed bed)
$CO+2H_2 \rightarrow CH_3OH$	<u>Reactions of Synthesis Gas</u>
$CO+3H_2 \rightarrow CH_4+H_2O$ (methanation)	ZnO promoted with $Cr_2O_3$ , or $Cu^{I}-ZnO$ promoted with $Cr_2O_3$ or $Al_2O_3$ (adiabatic, fixed beds or multitube fixed bed)
$CO+H_2 \rightarrow$ paraffins, etc. (Fischer-Tropsch synthesis)	Supported Ni (fixed bed) Fe with promoters (fluid bed)
Oxychlorination (e.g., $C_2H_4+2HCl+\frac{1}{2}O_2 \rightarrow C_2H_4Cl_2+H_2O$ )	<u>Other</u>
Hydrodesulfurization	$CuCl_2/Al_2O_3$ with KCl promoter Co-Mo/ $Al_2O_3$ or Ni-Mo/ $Al_2O_3$ (adiabatic, fixed beds)

Table 3. Continued.

Reaction	Catalyst and Reactor Type (Continuous Operation Unless Otherwise Noted)
$\text{SO}_2 + 2\text{H}_2\text{S} + 3\text{S} + 2\text{H}_2\text{O}$ (Claus process)	$\text{Al}_2\text{O}_3$ (fixed beds)
$\text{H}_2\text{O} + \text{CO} + \text{CO}_2 + \text{H}_2$ (water-gas shift)	$\text{Fe}_3\text{O}_4$ promoted with $\text{Cr}_2\text{O}_3$ (adiabatic fixed bed); for a second, lower temperature stage, Cu-ZnO supported on $\text{Al}_2\text{O}_3$ or $\text{SiO}_2$

Adapted from Reference 33.

received some attention<sup>36</sup> though this has been limited.

Each general method has its advantages and limitations. The ionic or covalent anchoring procedures are preferred in general since the dry or SLP catalysts may be easily desorbed by immersion in solvents or liquid solvents. For use in gas solid reactions, all three methods could in principle be used.

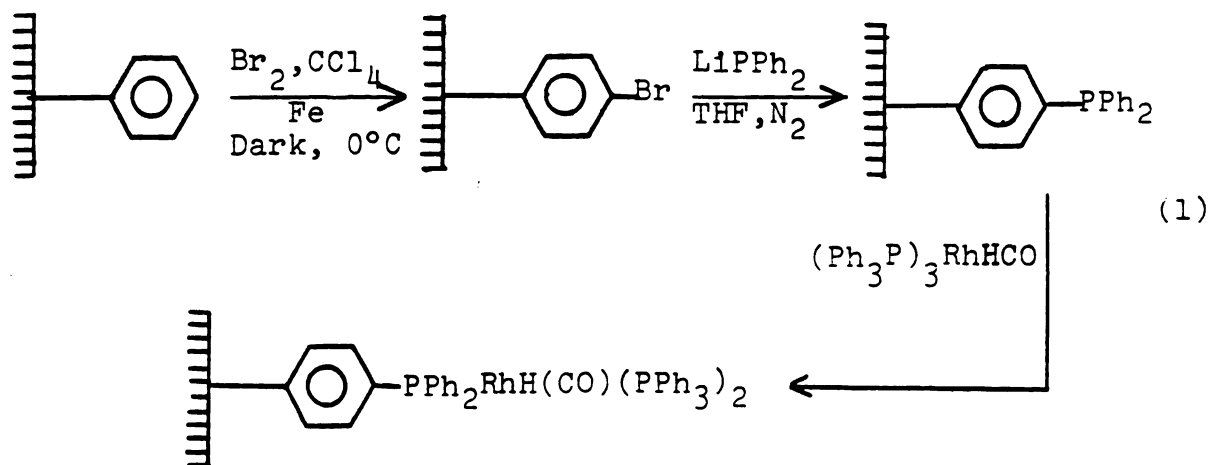
Supports which have been applied for the heterogenizing of homogeneous catalysts<sup>31a,32a</sup> may be organic or inorganic:

Organic supports: polyamino acids  
acrylic polymers  
styrene polymers  
cellulose  
cross-linked dextrans

Inorganic Supports: silica  
glass  
metal oxides  
Zeolite  
clay

## 2. Polymers As a Support for Homogeneous Catalysis

This field has certainly been the most intensively studied from a fundamental point of view. A great deal of work has been carried out by Grubbs et al.<sup>37</sup> as well as by Pittman et al.,<sup>38</sup> Eraca et al.,<sup>39</sup> Graziani et al.,<sup>40</sup> using polystyrene-divinyl-benzene cross-linked polymers. The most common technique involves linking diphenyl phosphine group to a benzene ring of the polymer as indicated in Equation (1).



Then by simple ligand exchange it is possible to graft the metal complex onto the polymer, e.g., zero valent nickel complexes, bivalent nickel complexes, Wilkinson complex, ruthenium<sup>II</sup> complexes,  $\text{RhH}(\text{CO})(\text{PPh}_3)_3$ , Vaska's complex, and so on. Many catalytic reactions have been carried out with these supported complexes.

An interesting feature of these supported complexes is related to the possibility of multifunctionality obtained by grafting on the same polymer with two different catalysts capable of catalyzing two different reactions in a two step process. For example, it is possible to cyclooligomerize butadiene on a nickel(0) complex and then to hydrogenate the cyclic dimers to the saturated hydrocarbons with the Wilkinson catalyst.

An important contribution to the field of multifunctional



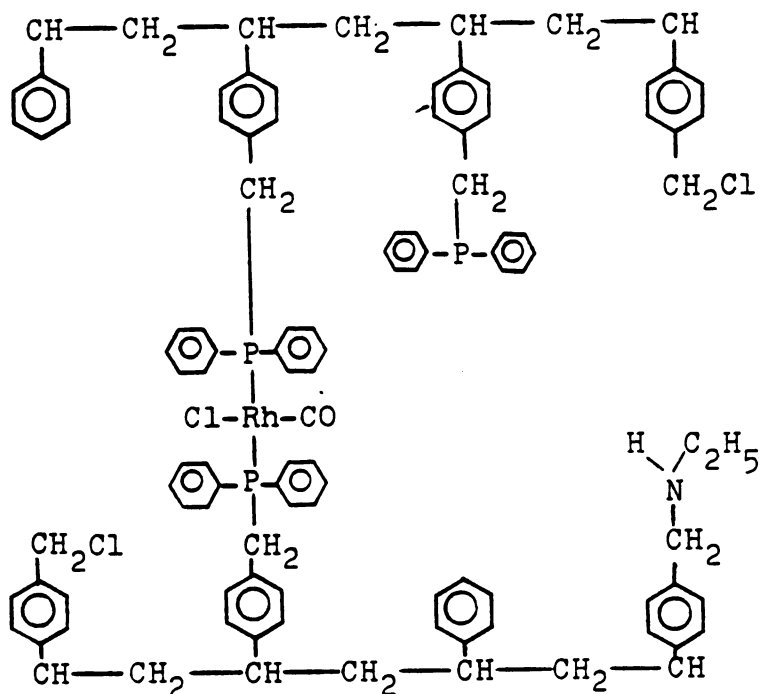


Figure 1. A representative structural element of the multifunctional catalyst.<sup>41</sup>

(Examples of polymer supported catalyst applications are provided in Table 4.)

Table 4. Application of Polymer Supported Catalysts.

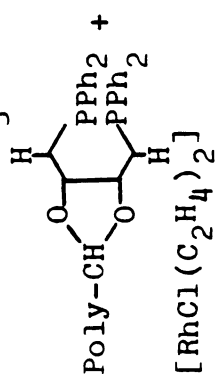
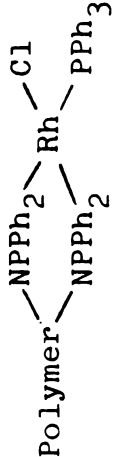
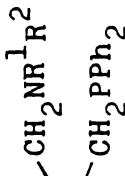
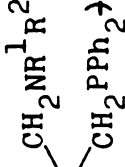
Support (a)	Proposed Supported Complex	Catalytic Action	Ref.
Poly-Cp	Poly-CpTiR <sub>x</sub> R = Cl, Me, X = 1,2,3	Hydrogenation	37(b)
Poly	Poly $\pi$ -Cr(CO) <sub>3</sub>	Hydrogenation	42
Poly-CH <sub>2</sub> -Cl	 Poly-CH-CH <sub>2</sub> -Cl + [RhCl(C <sub>2</sub> H <sub>4</sub> ) <sub>2</sub> ]	Asymmetric Hydrogenation	43
Phosphinated Poly-(m-phenylene isophthalamide) (Nomex)	 Polymer $\left\{ \begin{array}{l} \text{NPPH}_2 \\ \text{NPPH}_2 \end{array} \right\} \text{Rh} \begin{array}{l} \text{Cl} \\ \text{PPh}_3 \end{array}$	Hydrogenation (Alkenes)	44
Poly-PPh <sub>2</sub>	(Poly-PPh <sub>2</sub> ) <sub>x</sub> -RhCl(PPh <sub>3</sub> ) <sub>3-x</sub> (Poly-PPh <sub>2</sub> ) <sub>x</sub> -IrCoCl(PPh <sub>3</sub> ) <sub>z-x</sub> (Poly-PPh <sub>2</sub> ) <sub>x</sub> -RuCl <sub>2</sub> (CO) <sub>2</sub>	Hydrogenation Hydrogenation Hydrogenation	(38b) 45 38a
Poly-PPh <sub>2</sub>	(Poly PPh <sub>2</sub> ) <sub>x</sub> RhHCO(PPh <sub>3</sub> ) <sub>3-x</sub>	Hydroformylation	46

Table 4. Continued.

Support	Proposed Supported Complex	Catalytic Action	Ref.
Poly-CH <sub>2</sub> NMe <sub>2</sub> (cross-linked)	Poly-CH <sub>2</sub> -NMe <sub>2</sub> RhCl <sub>3</sub>	Hydroformylation	47
Poly(vinylpyridine)	Poly-  , Rh <sub>4</sub> (CO) <sub>12</sub> or CO <sub>4</sub> (CO) <sub>12</sub>	Hydroformylation	48
Poly- 	Poly-  R <sup>1</sup> R <sup>2</sup> R <sup>1</sup> =R <sup>2</sup> =H, R <sup>1</sup> =H, R <sub>2</sub> =C <sub>2</sub> H <sub>5</sub> R <sup>1</sup> =R <sup>2</sup> =C <sub>2</sub> H <sub>5</sub>	Hydrof. & Aldox conden.	41
Poly (partially hydrogenated)	 -PdCl <sub>2</sub>	Polymerization	49
Poly CH <sub>2</sub> NMe <sub>2</sub>	Poly-CH <sub>2</sub> NMe <sub>2</sub> , [Rh(CO) <sub>2</sub> Cl] <sub>2</sub>	Hydroosilation	50
Poly CH <sub>2</sub> NMe <sub>2</sub>	PolyCH <sub>2</sub> , H <sub>2</sub> PtCl <sub>6</sub>	Hydroosilation	51
Poly-PPh <sub>2</sub>	(Poly PPh <sub>2</sub> ) <sub>x</sub> Pd(PPh <sub>3</sub> ) <sub>4-x</sub>	Linear dimerization	52
Poly-PPh <sub>2</sub>	(PolyPPh <sub>2</sub> ) <sub>2</sub> Ni(CO) <sub>2</sub>	Cyclooligomerization	38b
Poly-PPh <sub>2</sub>	Poly  <sub>x</sub> Ni(CO) <sub>2</sub>  <sub>x</sub> RuCl	Cyclooligomerization	38b

<sup>a</sup>poly =  in poly(styrene-dyb) copolymers.

five-fold greater for hydroformylation, 15 fold greater for condensation and 30-fold greater for hydrogenation.

### 3. Inorganic Support for Homogeneous Catalysts

Inorganic supports suitable for use in the attachment of metal complexes may be classified into the following groups:

1. High surface area oxides (mainly  $\text{SiO}_2$ ,  $\text{Al}_2\text{O}_3$ , aluminasilicate type).
2. Layered structures (mica-type silicates (clay), tantalum disulfide and related sulfides, graphite).
3. Cage-type lattices (zeolites).
4. Advantages of Inorganic Oxide Over Polymer as Supports

Unlike polymers, which are flexible and can be swelled to varying degrees depending on solvent, temperature and pressure, metal oxides have rigid structures. Also, metal oxides are less susceptible than organic polymers to chemical or thermal degradation. A stable structurally rigid support limits the number of surface attached liganding groups capable of binding to the metal complex. Thus, it should be easier to control the degree of coordination unsaturation of the metal center on metal oxide surface, than in the pores of a flexible polymer matrix. Structural

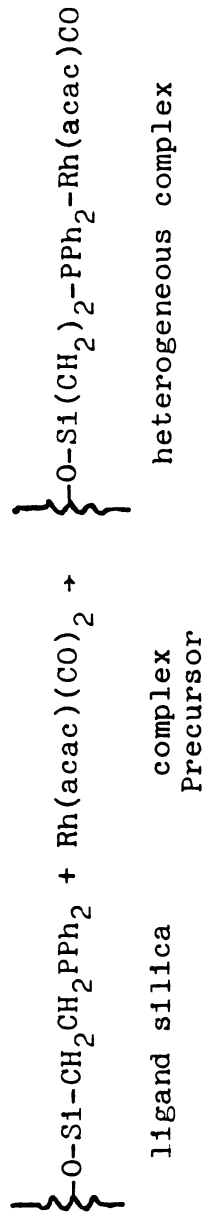
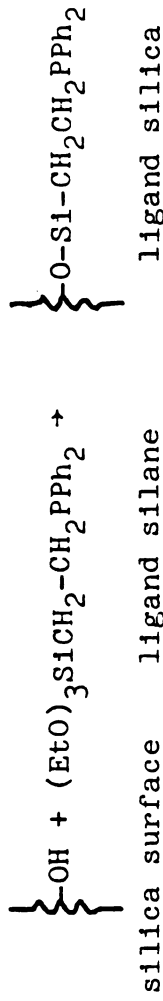
rigidity is also desirable in large scale applications, because the size and porosity of the catalyzed remains constant through the catalytic reaction. Although polymers can be stiffened by crosslinking, they become increasingly brittle with increasing crosslinking and attrition of the polymer particles becomes a particle problem.<sup>34b</sup>

### 5. Inorganic Oxides as a Support

Much work<sup>53</sup> has been carried out by British Petroleum which has been intensively studying a wide range of catalytic reactions. The most interesting aspect of the work is related to development of new methods for grafting many homogeneous catalysts on silica. These methods seem to be general.<sup>53</sup>

The first method (A) involves reaction of a coupling reagent, e.g.,  $(Et-O)_3Si-(CH_2)_n-PPh_2$ , with the silanol groups present on silica to obtain a grafted phosphine. It is then possible by ligand exchange to graft any kind of precursor complex. The method (B) involves first forming a metal complex with the  $(EtO)_3-Si(CH_2)_n-PPh_2$  coupling agent or ligand. It is then possible to control the number of silane ligands before grafting the complex to the support (Figure 2). Similar functionalization procedures have been adapted by Moreto et al. and Kochloeff et al. (silica) and by Capka and Hetflejs (silica,  $\gamma$ -alumina, glass and molecular sieve zeolite).<sup>34c</sup>

METHOD A



METHOD B

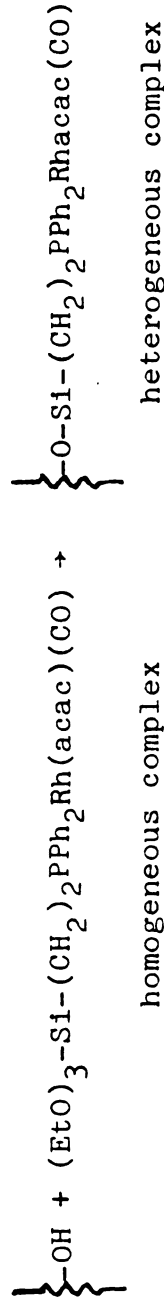
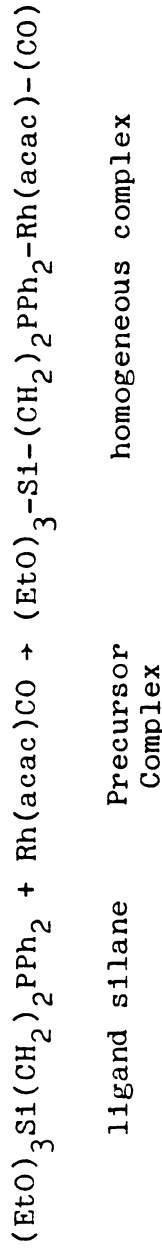


Figure 2. Grafting of homogeneous catalysis on silica.

Table 5. Grafting of Homogeneous Catalysts on Inorganic Support (Silica).

Support	Proposed Supported Complex	Catalytic Action	Method	Ref.
≡Si-OH	$\text{CpTiCl}_2 (\text{C}_5\text{H}_4\text{-SIL})$	Hydrogenation	B	54
	$\text{TiCl}_2 (\text{C}_5\text{H}_4\text{-SIL})_2$	Hydrogenation	B	54
	$\text{RhCl} (\text{PPh}_2 (\text{CH}_2)_2\text{-SIL})_3$	Hydrof. & hydrog.	A,B	53
	$\text{Rh}(\text{CO})\text{PPh}_2\text{-(CH}_2)_2\text{-SIL)}_2$	Hydrof.	B	53
	$\text{RhCl}_3/\text{PPh}_2 (\text{CH}_2)_2\text{SIL}$	Hydrosilation	A	55
	$\text{PtCl}_4^{2-}/\text{SnCl}_4/\text{PPh}_2 (\text{CH}_2)_2\text{-SIL}$	Isomerization	A	56
	$\text{H}_2\text{PtCl}_6/\text{NMe}_2 (\text{CH}_2)_3\text{SIL}$	Hydrosilation	A	55
	$\text{PdCl}_2 (\text{PPh}_2 (\text{CH}_2)_2\text{SIL})$	carbonylation & Hydrosilation	A	55,57
	$\text{Pd} (\text{acac})_2/\text{PPh}_2 (\text{CH}_2)_8\text{-SIL}$	Carbonylation	A	57
	$\text{Co}_2 (\text{CO})_2 (\text{C}_5\text{H}_4\text{-SIL})$	Hydroformylation	A,B	57,58
	$\text{Co} (\text{acac})_2 / (\text{PPh}_2 (\text{CH}_2)_2\text{SIL})$	Hydroformylation	A	57,58
	$\text{NiCl}_2 (\text{PPh}_2 (\text{CH}_2)_2\text{-SIL})_2$	oligomerization	A	59
	$\text{Ni} (\text{COD}) (\text{PPh}_2 (\text{CH}_2)_2\text{-SIL})_2$	Oligomerization	A	59
	$\text{IrCl} (\text{PPh}_2 \text{C}_6\text{H}_4 (\text{CH}_2)_4\text{-SIL})_2$	Hydrogenation	A	60,56
	$\text{RuCl}_2 (\text{PPh}_2 (\text{CH}_2)_2\text{-SIL})$	Hydrogenation	A	56

Another method of catalyst immobilization on inorganic supports involves the direct reaction of an organometallic complex with hydroxyl groups on the surface of the support. This method of immobilization is significantly different from the preceding one which uses a coupling agent, since the method of grafting is such that the support acts as a ligand directly bonded to the transition metal. In many cases the formation of  $\text{Si-O-M}_T$  bond or  $\text{Al-O-M}_t$  bond are involved. It does not seem that in this case, the molecular nature of the catalyst is kept at least in the sense of a homogeneous complex, but the resulting catalyst may exhibit very high activity and selectivity compared with the homogeneous counterpart. Very intense research in this field is due to Ballard and coworkers<sup>31c,61</sup> and to Yermakov and coworkers.<sup>62</sup> The general method involves the reaction of an organometallic with the surface groups of alumina or silica (Figure 3, Table 6).

Another alternative in immobilization has been developed by Yermakov<sup>63</sup> and closely resembles the usual techniques of heterogeneous catalysis synthesis. After grafting the organometallics to the surface, drastic reducing treatments under hydrogen or oxidizing treatments under oxygen will lead to a wide range of oxidation states. The advantage of using these organometallics as starting materials is the high degree of dispersion obtained on the surface.

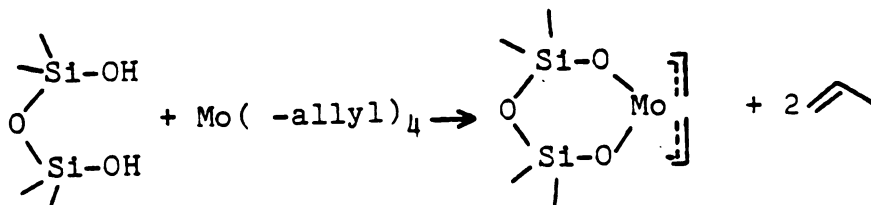
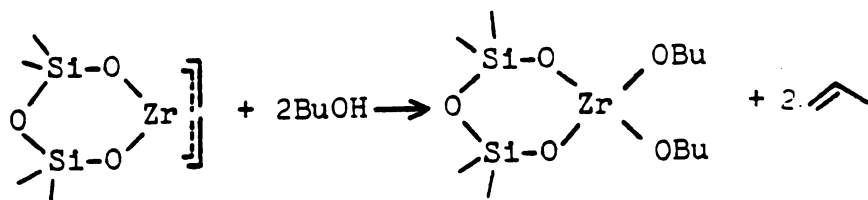
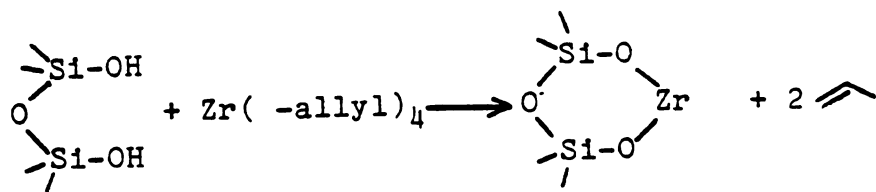


Figure 3. Direct interaction of organometallic compounds with silica surface.

Table 6. Examples of Organometallic Precursor Supported On Inorganic Supports.

Support	Organometallic Precursor	Reaction	Ref.
SiO <sub>2</sub> or Al <sub>2</sub> O <sub>3</sub>	Zr ( $\pi$ -allyl) <sub>4</sub>	Polymerization	61, 62, 63
	Zr ( $\pi$ -allyl) <sub>3</sub> Br	Polymerization	
SiO <sub>2</sub> or Al <sub>2</sub> O <sub>3</sub> or SiO <sub>2</sub> -Al <sub>2</sub> O <sub>3</sub>	Cr(cp) <sub>2</sub>	Polymerization	31c
	Cr ( $\pi$ -allyl) <sub>4</sub>	Polymerization	
	Ni ( $\pi$ -C <sub>3</sub> H <sub>5</sub> )X <sub>2</sub>	Polymerization	
	(x = Cl, Br, I)		
SiO <sub>2</sub> or Al <sub>2</sub> O <sub>3</sub>	Mo ( $\pi$ -allyl) <sub>4</sub>	Disproportionation	31c
	Mo <sub>2</sub> ( $\pi$ -allyl) <sub>4</sub>	Disproportionation	
	W ( $\pi$ -allyl) <sub>4</sub>	Disproportionation	
Al <sub>2</sub> O <sub>3</sub> SiO <sub>2</sub> -Al <sub>2</sub> O <sub>3</sub>	RhCl <sub>3</sub>	Dimerization	64
	RhCl <sub>3</sub>	Dimerization	64

The general types of possible surface reactions are summarized below:

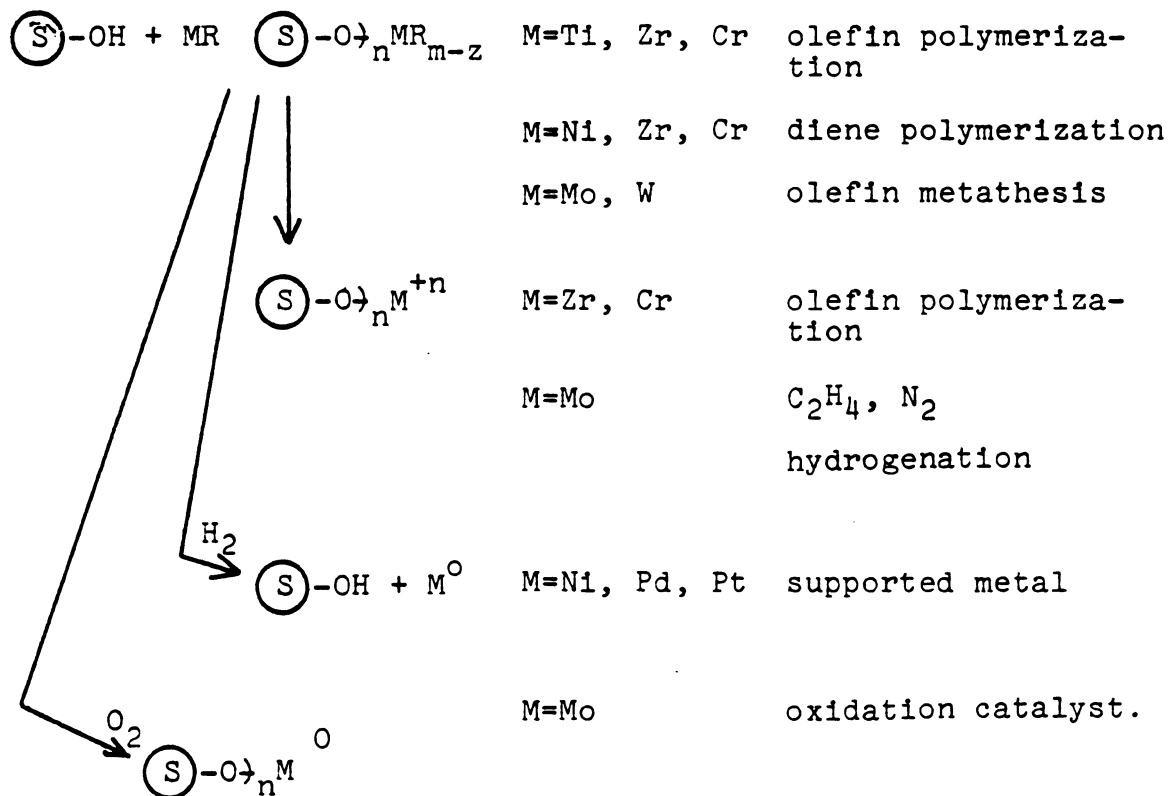


Figure 4. General types of possible surface reactions. (Adapted from Reference 34e).

As has been mentioned, the methods most studied for complexes immobilization is covalent attachment or ionic attachment of transition metal complexes to support via functional group ligands. Electrostatic binding of cationic metal complexes to crystalline inorganic matrices represents

a promising approach to the problem of supported homogeneous catalysts. Unlike covalent methods of attachment, electrostatic binding does not require the support to function as a ligand.

The inorganic matrices best studied for the electrostatic immobilization of metal complexes are the crystalline two-dimensional layered silicates related to the micas (e.g., montmorrillonite or hectorite and the three-dimensional silicates or zeolites. Related classes of compounds such as layered transition metal sulfides<sup>65</sup> and graphite<sup>66</sup> are also capable of intercalating metals and metal complexes of catalytic interest. Although layered silicates and zeolites have been extensively investigated as protic heterogeneous catalysts, studies aimed at their use as supports for metal complex catalysts are in the first stages of development.

Three limitations to the use of an anionic inorganic framework as supports for homogeneous complexes can be anticipated:

- i. The metal complex must be cationic.
- ii. A solution-like environment in the intracrystal regions may be necessary to realize catalytic activity.
- iii. The reaction may be diffusion controlled.

Although a large number of homogeneous metal complexes

Table 7. Physisorption and Ion Exchange Reactions in Zeolites and Layered Silicates.

Silicate	Exchange Cation	Catalytic Application	Ref.
Zeolite (Na <sup>+</sup> /y-Zeolite)	Rh(NH <sub>3</sub> ) <sub>6</sub> <sup>3+</sup>	Hydroformylation	67
Zeolite (Na <sup>+</sup> /y-Zeolite)	Cu <sup>+</sup>	Cyclodimerization	68
	Co <sup>2+</sup>	Oxidation	69
Layered Silicate			
Na <sup>+</sup> -hectorite	Rh <sub>2</sub> (OAc) <sub>4-x</sub> <sup>x</sup> , PPh <sub>3</sub>	hydrogenation	70
	Rh(diene)L <sub>2</sub> <sup>+</sup>	hydrogenation	71
	L=PPh <sub>3</sub> , diphos		
	[Rh(diene)(diop)] <sup>+</sup>	asymmetric hydro- genation	72

of interest are suitable for binding in layered or three-dimensional studies because they are electrically neutral or become neutral during the reaction and readily desorb from the supports. However in zeolites sometimes desorption can be prevented because of the limited pore size.<sup>67</sup>

Research Objectives: to synthesize a positively charged metal complex catalyst suitable for intercalation in layered silicate and to examine the properties of the intercalated complex for catalytic hydroformylation. To provide the necessary background for the research, the structures of layered silicates will be reviewed and the properties of homogeneous hydroformylation catalysts will be surveyed.

## 6. Structural Features of Layered Silicates<sup>73</sup>

The term clay as used in soil science and geology refers to any inorganic material with a particle size  $<2\mu$ . However, the term "clay" which has been used in this thesis, refers to layered-lattice silicate minerals. In all the groups of mineral shown in Table (8) a common structural feature is a hexagonal sheet of linked  $\text{SiO}_4$  tetrahedra. The vertices of the tetrahedra in each sheet point in one way except for polygruskites and members of the serpentine group. If such a sheet is envisaged as being formed by condensation-polymerization of  $\text{Si}(\text{OH})_4$  units, it will be seen that all the vertices are hydroxyl groups and that the composition of the sheet is  $\text{Si}_2\text{O}_3(\text{OH})_2$ . The hydroxyl

Table 8. Some Minerals having the Three-fold Sheets Found in Miccas.

Mineral	Ideal Formula	Interlayer cations (meg/100g)
Pyrophyllite	$\text{Al}_2(\text{Si}_4\text{O}_{10})(\text{OH})_2$	0
Talc	$\text{Mg}_3(\text{Si}_4\text{O}_{10})(\text{OH})_2$	0
<u>Micas</u>		
Muscovite	$\text{KAl}_2(\text{AlSi}_3\text{O}_{10})(\text{OH})_2$	252
Paragonite	$\text{NaAl}_2(\text{AlSi}_3\text{O}_{10})(\text{OH})_2$	262
Phlogopite	$\text{KMg}_3(\text{AlSi}_3\text{O}_{10})(\text{OH})_2$	240
Biotite	$\text{K}(\text{Mg, Fe})_3(\text{AlSi}_3\text{O}_{10})(\text{OH})_2$	240 to 204
Lepidolite	$\text{K}(\text{Li}_2, \text{Al})(\text{Si}_4\text{O}_{10})(\text{F, OH})_2$	279 to 277
Zinnwaldite	$\text{K}(\text{Li, Fe, Al})(\text{AlSi}_3\text{O}_{10})(\text{F, OH})_2$	≈229
<u>Brittle Micas</u>		
Margarite	$\text{CaAl}_2(\text{Al}_2\text{Si}_2\text{O}_{10})(\text{OH})_2$	502
Chloritoid	$(\text{Mg, Fe}^{\text{II}})\text{Al}_2(\text{Al}_2\text{Si}_2\text{O}_{10})(\text{OH})_2$	524 to 440
Seyberite	$\text{Ca}(\text{Mg, Al})_3(\text{Si, Al})_4\text{O}_{10}(\text{OH})_2$	
<u>Vermiculites<sup>a</sup></u>		
General formula	$(\text{Ca, Mg})_{x/2}(\text{Mg, Fe, Al})_3(\text{Al, Si})_4\text{O}_{10}(\text{OH})_2 \cdot n\text{H}_2\text{O}$	≈100 to 165

Table 8. Continued.

Mineral	Ideal Formula	Interlayer cations (meg/100g)
<u>Smeectites</u> <sup>a</sup>		
Montmorillonite	$\text{Na}_x(\text{Al}_{(2-x)}\text{Mg}_x)(\text{Si}_4\text{O}_{10})(\text{OH})_2, \text{mH}_2\text{O}$	
Saponite	$\text{Ca}_{x/2}\text{Mg}_3(\text{Al}_x\text{S}_{(4-x)}\text{O}_{10})(\text{OH})_2, \text{mH}_2\text{O}$	
Nontronite	$\text{M}_x(\text{Fe}^{\text{III}}, \text{Al})_2(\text{Al}_x\text{Si}_{(4-x)}\text{O}_{10})(\text{OH})_2, \text{mH}_2\text{O}$	
Beidellite	$\text{M}_x\text{Al}_2(\text{Al}_x\text{Si}_{(4-x)}\text{O}_{10})(\text{OH})_2, \text{mH}_2\text{O}$	} ≈60 to 100
Sauconite	$\text{M}_x(\text{Zn}, \text{Mg})_3(\text{Al}_x\text{Si}_{(4-x)}\text{O}_{10})(\text{OH})_2, \text{mH}_2\text{O}$	
Hectorite	$(\text{Na}_2, \text{Ca})_{x/2}(\text{Li}, \text{Al})_2(\text{Si}_4\text{O}_{10})(\text{OH})_2, \text{mH}_2\text{O}$	
Fluorhectorite	$(\text{Na}, \text{Ca})_{x/2}(\text{Li}, \text{Al})_2(\text{Si}_4\text{O}_{10})(\text{F}, \text{OH})_2, \text{mH}_2\text{O}$	

<sup>a</sup>M denotes one equivalent of an exchangeable cation such as Na, Ca and Mg, and so x is the number of equivalents of exchangeable cations present. In a typical smectite x in the above formulae is about 0.33, representing around 90 meq per 100 g of clay mineral. The water contents vary with relative humidity and with the cations present. A typical value of m is ~3.5. (Adapted from Reference 73b.)

groups can be thought to undergo further condensation polymerization with  $\text{Al}(\text{OH})_6$  octahedra. Now if one layer of octahedra reacts with one sheet  $(\text{Si}_2\text{O}_3(\text{OH})_2)_n$  the two layer sheet typical of kandites results. This two layer sheet has the composition of  $\text{Al}_2\text{SiO}_5(\text{OH})_4$ . In the minerals of this group there is no net ionic charge on the double sheets and so in the ideal structures there are no interlayer cations. The small cation exchange capacity sometimes found, for example with kaolinite, is probably a result of lattice imperfections associated with the termination of crystal faces.

The  $\text{Si}_4\text{O}_{10}$  unit in pyrophyllite and talc represents the composition after two tetrahedral silica sheets have been condensed with one  $\text{Al}(\text{OH})_3$  sheet to form the triple phase. The octahedral layer contains the Al(pyrophyllite) or Mg (talc) given in the formula. The Al occupies only two out of every six-fold positions (a dioctahedral whereas the Mg in talc occupies all three of these positions (a trioctahedral mineral). In both cases the triple sheet is electrically neutral and the thickness of triple sheet is 9.3 to 9.4 Å.

In the micas, various isomorphous replacements are found. Very important is the substitution of Si by Al in the tetrahedral layers, which introduces one negative charge on the framework for each Al. In addition, Li, Mg, and Fe may replace Al in the octahedral layer with no alteration

in framework charge, to change dioctahedral micas to tri-octahedral micas.

Thus the triple sheets can develop negative charge by substitution either in tetrahedral or in octahedral layers, or in both such as vermiculite or smectite group.

### Smectite

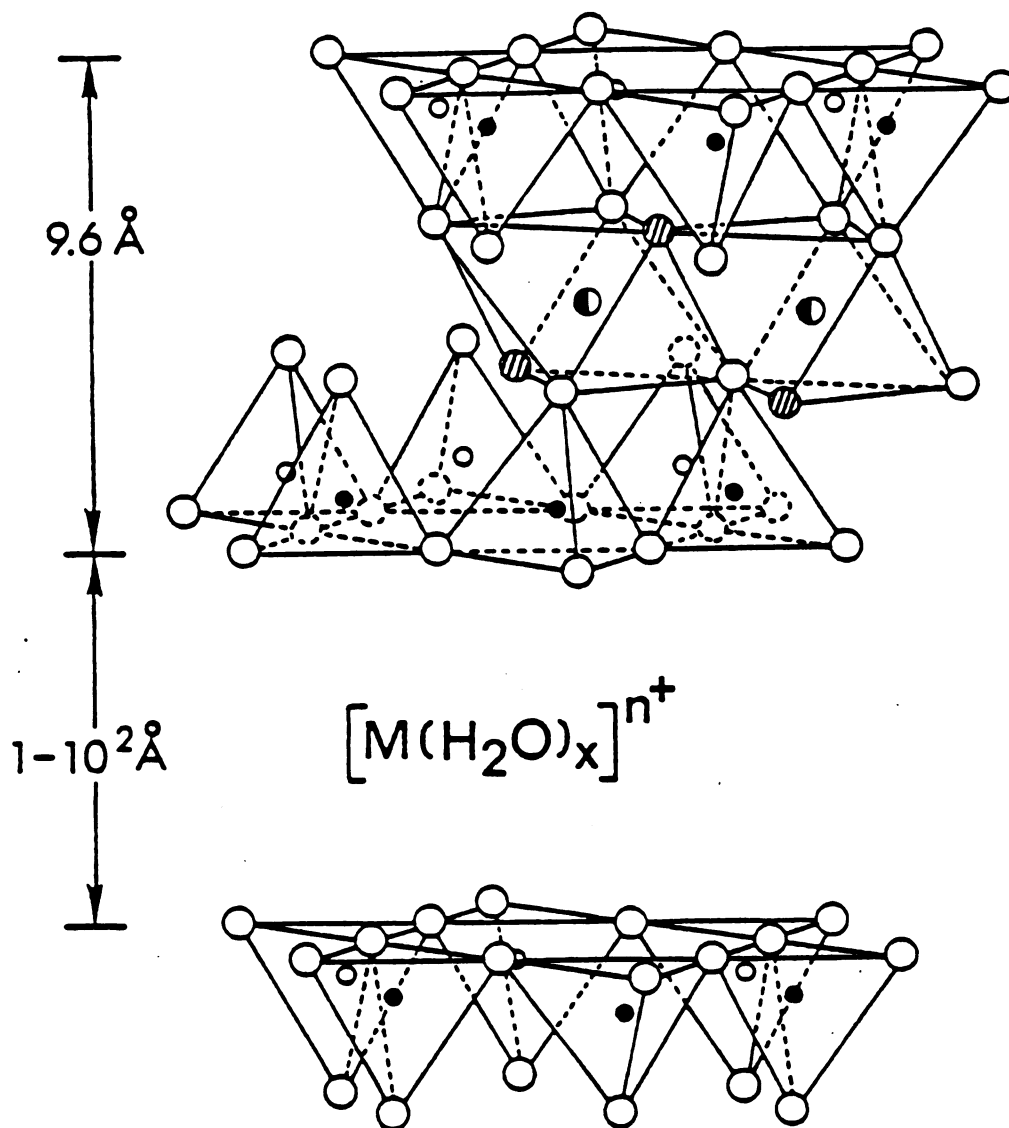
According to the Table (8), smectite clays are divided in two different categories:

1. Dioctahedral (heptaphyllitic) smectite such as montmorillonite.
2. Trioctahedral (octaphyllitic) such as hectorite.

Smectite composed of units made up of two silica tetrahedral sheets with a central alumina octahedral sheets. The tetrahedral and octahedral sheets are combined so that the tips of tetrahedra of each silica sheet and one of hydroxyl layers of the octahedral sheet form a common layer. The layers are continuous in the a and b directions and are stacked one above the other in the c direction. Figure (5) shows the structure of smectite group.

In montmorillonite  $Mg^{2+}$  replaces some  $Al^{3+}$  ions the idealized unit cell formula is  $(Na_{0.66}Al_{3.34}Mg_{0.66})[Si_8]O_{20}(OH)_4$ . Hectorite has a similar substitution where  $Li^+$  replaces some  $Mg^{2+}$  in the Oh positions with idealized unit

Figure 5. Layer structure of smectites illustrating the intracrystalline space which contains the exchangeable cations. (Adapted from Reference 73a.)



- $Al^{3+}$ ,  $Mg^{2+}$ ,  $Fe^{3+}$
- Oxygens
- ◐ Hydroxyls
- }  $Si^{4+}$ , occasionally  $Al^{3+}$
- }

cell formula  $\text{Na}_{0.66} (\text{Mg}_{5.34}\text{Li}_{0.66}) [\text{Si}_8] \text{O}_{20} (\text{OH})_4$ .

Therefore the isomorphous substitution results in negatively charged silicate layers. This charge is compensated by an array of hydrated sodium ions located between these layers. As a consequence, the sodium ions may be readily replaced by a variety of other cations and cationic complexes by simple ion-exchange methods. The mineral will swell to allow two monolayers of water in the intercrystalline space whereas hectorite and montmorillonite will swell to accommodate multiple monolayers of water. In a water slurry hectorite and montmorillonite will swell to approximately 100 Å so that under these conditions the sheets are totally separated. Therefore swollen smectite systems the interlayer cations exist in solution-like environments. Hydrated  $\text{Cu}^{2+}$  and  $\text{Mn}^{2+}$  ions exhibit rapid, solution-like molecular tumbling on the ESR time scale<sup>74</sup> as do protonated amine functionalized nitroxide spin probes.<sup>75</sup>

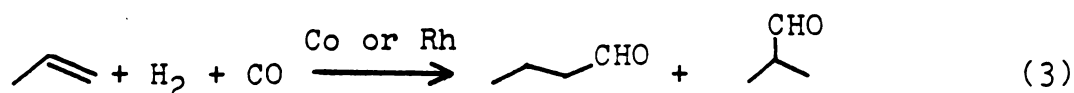
Smectites have been known for many years to be effective heterogeneous catalysts for a number of reactions. Theng has reviewed their use in the petroleum industry as cracking and polymerization catalysts.<sup>76</sup> The active species are of the Bronsted and Lewis acid type. The clay minerals have been used as catalysts for other reactions. Fenn et al. have reported the dimerization of anisole to 4,4'-dimethoxybiphenyl on  $\text{Cu}^{2+}$ -hectorite over  $\text{P}_2\text{O}_5$ ,<sup>77</sup> the formation of

porphyrins and porphyrin montmorillonite on various transition metal ions. Also Pinnavaia *et al.* used  $\text{Rh}(\text{PPh}_3)_x^+$ -Hect,<sup>70</sup>  $\text{Rh}(\text{diene})\text{L}_2^+$ <sup>71</sup> and  $\text{ClRh}(\text{COD})\text{P}-\text{P}^+$ <sup>78</sup> for hydrogenation type reactions. The interlayer regions of smectites often alter the reactivities and stabilities of transition metal complexes, e.g.,  $\text{Cu}^{2+}$ -arene complexes, not found in homogeneous solution, are found and stabilized in smectites.<sup>79</sup>

Recently it has been found that silicon could be introduced into the interlamellar regions by ion exchange of triacetylacetonato silicon (IV) cations ( $\text{Si}(\text{acac})_3^+$ ), by in situ reaction of acetylacetonate-solvated clays with  $\text{SiCl}_4$ , or by formation of polychlorosiloxanes  $(-\text{SiOCl}_2^-)_n$ .<sup>80</sup>

### C. Hydroformylation

Otto Roelen discovered the "oxo" or hydroformylation reaction in 1938,<sup>81</sup> while studying the Fischer-Tropsch reaction, an existing industrial process. The hydroformylation reaction is used to convert olefins to the saturated aldehydes via reaction of the olefin with water gas ( $\text{CO}+\text{H}_2$ )



The reaction is homogeneously catalyzed by a number of transition metal carbonyl complexes. Cobalt is the most

widely used catalytic element for this reaction. Rhodium catalysts increase both the reaction rate and selectivity of the process, but it is very expensive.

Commercial use of the hydroformylation reaction is on a large scale. The ultimate commercial products are alcohols, either 1-butanol or 2-ethylhexanol, which are formed by the hydrogenation of the aldehyde, 2-ethylhexanol is used as a plasticizer<sup>82</sup> component. The oxo products also can be used as solvents, lubricants, detergents and so on.<sup>83</sup>

Despite the highly developed oxo technology based on  $\text{HCo}(\text{CO})_4$  or the catalytic species, there has been no lack of attempts to improve the total yield or the selectivity of the reaction. In addition, efforts have been directed at increasing the activity of the catalysts via variation or modification. Therefore, the oxo reaction has been the subject of a very large number of patents, scientific papers and review articles.<sup>84</sup>

The complexes summarized in Table 9 have been intensively studied as hydroformylation catalyst precursors.

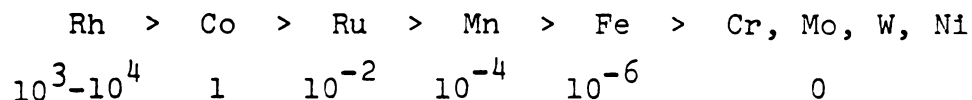
Among these metals, rhodium and its derivatives were found more active and at least as selective as cobalt (as carbonyl form), whereas ruthenium and iridium appeared fairly active but less selective. Recently hydridic platinum complexes<sup>85</sup> were found to have catalytic activity comparable to that of cobalt. Other metals like iron, osmium, nickel, palladium, and their derivatives tested to

Table 9. Hydroformylation Catalysts and Their Variants. (34)

Catalyst Precursor	Modified By
$M_n(CO)_m$	M = Co, Rh, Fe, Ru, Ir, Os, Pd, etc. e.g., $Co_2(CO)_8$ , $Rh_4(CO)_{12}$ , $Ru_3(CO)_{12}$ $Os_3(CO)_{12}$ , $Ir_4(CO)_{12}$
$Hal M(CO)_m L_n$	M = Co, Rh, Fe, Ru, Ir, Os Hal = Cl, Br L = $PR_3$ , $P(OR)_3$ , $AsR_3$ , etc. e.g., $ClRh(CO)(PPh_3)_2$

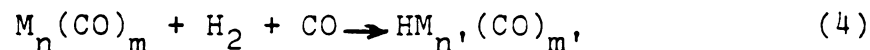
date showed slight to very slight activity. For a number of other metals like copper, chromium, and tungsten the catalytic activity have not been investigated sufficiently.

Reactivities of various metal carbonyls as oxo products relative to cobalt are shown below.

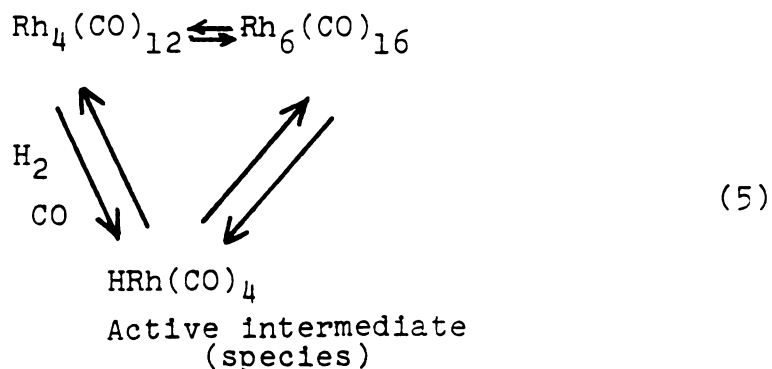


$M_n(CO)_m$  type complexes are precursor catalysts, but by the addition of CO and  $H_2$ , a monohydride carbonyl complex is formed according to Equation (4) which is the active species

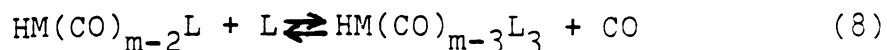
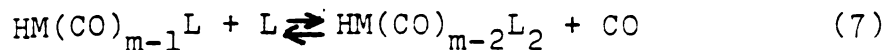
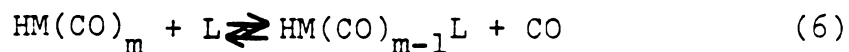
for hydroformylation reactions.



E.g.,<sup>86</sup>



The problem with this type of catalyst is that the selectivity is low, which is not favorable for industrial usage. The normal-to-isomer ratio can be dramatically increased by replacing the CO ligand with organic electron donors such as amines ( $\text{NR}_3$ ), phosphines ( $\text{PR}_3$ ), phosphites ( $\text{P}(\text{OR})_3$ ), arsines ( $\text{AsR}_3$ ), etc., which is called "ligand modification", and has led to industrially relevant development in the catalyst recycle as well as in the oxo process itself.<sup>87</sup>



The ligand modification of  $\text{HCo}(\text{CO})_4$  was used by Reppe et al for the first time in 1941 for stabilizing catalysts. After the basic research conducted by Slauch, Mulineaus and Wilkinson (1966), ligand modified catalysts have been used for industrial applications. Ligand modification has a drastic effect on oxo catalysts where the central atom is Co or Rh.

By replacing some of the CO ligands with other donors such as  $\text{PR}_3$  the selectivity, reactivity and stability of reactions can be changed. For example, the stability of metal hydride carbonyls of Co or Rh modified with electron donors ligands  $\text{PR}_3$  have been increased.

However, the catalyst activity drops when the selectivity increases. Also, the ligand modified oxo catalysts are more active in hydroformylation than their unmodified counterparts.<sup>88</sup> Selectivity usually has been increased by ligand modification.

Recently mixed metals have been used for hydroformylation reactions<sup>89</sup>, i.e., Co-Rh or Co-Pt, Co-Fe. Mixed catalysts are said to exhibit particular effects besides an increase in activity.

However, the homogeneous catalyzed hydroformylation with a metal carbonyl of the type  $\text{HM}(\text{CO})_m\text{L}_n$  requires a step after the actual oxo stage to separate, recover and reprocess the catalyst.

Heterogenized hydroformylation catalysts can be prepared as follows:

- A. Polymerization or Copolymerization of suitable monomers;
- B. Functionalization of formed supports (organic and inorganic);
- C. Precipitation of metals on supports;
- D. Impregnation method such as SLPC.

Method A is rarely used for heterogenized oxo catalysis. The most well-known example is ICI procedure for the polymerization of suitably substituted bis(dialkyl-styrene phosphine) metal halides.<sup>90</sup>

There is a number of standard methods for the functionalization of polymers, silica gels, zeolites or other supports according to method B. This method has been explained before in Section (I-B2).

Method C includes systems in which the complex is chemisorbed to the supports. The SLPC technique in which the oxo catalysts, dissolved in high boiling solvents (in some cases the ligands themselves are used as solvent), are deposited in the pores of suitable supports where they are made available to the gaseous reactants (alkene and  $\text{CO} + \text{H}_2$ ) and the use of Co-Al silicates are examples of Method D. The SLPC Technique is very useful in the gas phase hydroformylation reaction which is the subject of recent studies of hydroformylation reactions. At the moment, oxo active clusters-polynuclear transition metal carbonyls with M-M bonds are also subject of intensive research. This

intensification of the research of the transition metal complex is also exploited in hydroformylations. The results are less surprising than the fact that the clusters  $(\text{Co}_3(\text{CO})_9[\mu_3\text{-}(\text{C}_6\text{H}_5)])$ , and  $\text{Co}_4(\text{CO})_8(\mu_2\text{-CO})_2(\mu_4\text{-P}_6\text{H}_5)_2$  can be recovered unchanged after the reaction.

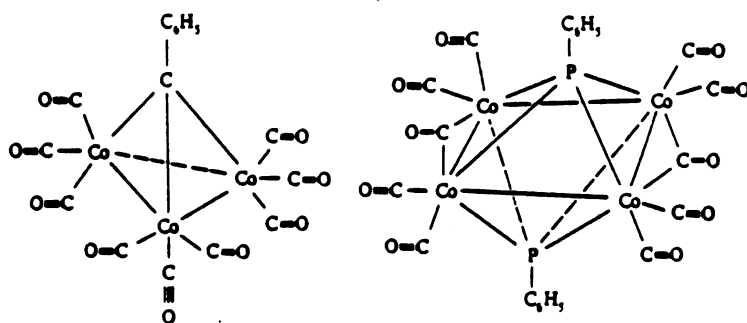


Figure 6. Cobalt clusters for hydroformylation.

Pittman et al.<sup>91</sup> have also studied the hydroformylation reaction with cobalt clusters and postulated a mechanism based on the Heck and Breslow mechanism.

Table 10 provides some examples of these four methods.

The objective of the present study was to examine the properties of intercalated hydroformylation catalysts.

Table 10. Hydroformylation with Immobilized Catalysts.

Method	Support	Linking Agent	Precursor Catalyst	Ref.
A	Poly-(divinyl-styrene phosphine)		$\text{HCo}(\text{CO})_4$	90
B (Polymer)	Polystyrene-DVB	Phosphine	$\text{Mo}(\text{CO})_4(\text{PPh}_3)_2$	92
	Polystyrene-DVB	Phosphine	$\text{Fe}(\text{CO})_3(\text{PPh}_3)_2$	92
	Polystyrene-DVB	Phosphine	$\text{Mn}(\text{CO})_2\text{Cp}(\text{PPh}_3)$	92
	Polystyrene-DVB	Phosphine	$\text{CoCl}_2(\text{PPh}_3)$	92
	Polystyrene-DVB	Phosphine	$\text{Rh}(\text{acac})\text{COPPh}_3$	53b
Silica	Silica	Silyl phosphine	$\text{HRhCOPPh}_3$	46
			$\text{Co}(\text{PPh}_3)(\text{CO})_3$	93
			$[\text{RhCl}(\text{CO})_2]_2$	57, 94
			$\text{RhCl}(\text{CO})(\text{PPh}_3)_2$	53d, 95
B	Silica	Silyl phosphine	$\text{HRh}(\text{CO})_4$	53d
			$\text{HRh}(\text{CO})_4$	53d
			$\text{Rh}(\text{acac})(\text{CO})_2$	53d
			$[\text{Rh}(\text{CO})_2\text{Cl}]_2$	53d, c, 96
			$[\text{RhCl}(\text{COD})]_2$	53d, c, 96

Table 10. Continued.

Method	Support	Linking Agent	Precursor Catalyst	Ref.
B	Silica	Silyl Phosphine	$\text{RhH(CO)(PPh}_3)_2$	97
	$\text{Al}_2\text{O}_3$		$\text{Rh}(\pi\text{-allyl})\text{CO(PPh}_3)_2$	98
	Zeolite	-0-	$\text{HCo(CO)}_4$	99
Method C	Polystyrene DVB	-----	$\text{HCo(CO)}_4$	100
	Silica		$\text{HRh(CO)}_4\text{L}_m\text{N}_n$	101
	Zeolite	-----	$\text{HRh(CO)}_4$	67
	$\text{Al}_2\text{O}_3$	-----	Rh	102
Method D	Silica and other supports	SLPC Technique	$(\text{P}\emptyset_3)_2\text{RhCoCl}$ $(\text{As}\emptyset_3)_2\text{RhCoCl}$ $\text{Co}_2(\text{CO})_6(\text{PBu}_3)_2$	103
	$\text{Al}_2\text{O}_3$ Other Supports	SLPC Technique	$\text{Rh } \pi\text{-allyl Co(PPh}_3)_2$	104

Most hydroformylation catalysts are neutral and are not suitable for use in layered silicates. In fact, to achieve catalyst immobilization in layered silicate, the catalyst should be positively charged. Cationic complexes of type  $\text{Rh}(\text{diene})-(\text{PPh}_3)_2^+$  were selected for hydroformylation in homogeneous and intercalated systems. In 1978, Oro et al.<sup>105</sup> reported these type complexes are active under mild conditions at temperature and pressure. As will be shown later, however, the catalytically active species derived from  $\text{Rh}(\text{diene})-(\text{PPh}_3)_2^+$  precursors are electrically neutral and readily desorb from the silicate surfaces. Nevertheless, complexes suitable for the formation of intercalation catalysts were obtained by replacement of the neutral phosphine ligands in  $\text{RhCl}(\text{diene})\text{PPh}_3$  and  $\text{Rh}(\text{diene})(\text{PPh}_3)_2^+$  catalyst precursors with a positively charged ligand. There are a few examples of positively charged phosphine ligands in the literature, Table 11 lists some of those ligands.

Table 11. Complexes Containing Positively Charged Ligands.

Complex	L <sup>+</sup>	Ref.
MX <sub>3</sub> (L <sup>+</sup> )	Ph <sub>2</sub> PCH <sub>2</sub> CH <sub>2</sub> <sup>+</sup> PPh <sub>2</sub> CH <sub>2</sub> Ph	106
M = Co <sup>2+</sup> or Ni <sup>2+</sup>	Ph <sub>2</sub> PCH <sub>2</sub> <sup>+</sup> PPh <sub>2</sub> CH <sub>2</sub> Ph	
X = Cl, Br, I		
CoBr <sub>3</sub> (L <sup>+</sup> )	Ph <sub>2</sub> PCH <sub>2</sub> CH <sub>2</sub> <sup>+</sup> PPh <sub>2</sub> CH <sub>2</sub> Ph	107
MX <sub>3</sub> L <sup>+</sup>		
M = Co <sup>2+</sup> or Ni <sup>2+</sup>	$\text{Ph}_2\overset{+}{\text{P}}\begin{array}{l} \diagup \text{CH}_2 \\ \diagdown \text{CH}_2 \end{array} \text{C} \begin{array}{l} \diagup \text{CH}_3 \\ \diagdown \text{CH}_2 \end{array} \text{PPh}_2$	108
[Au(L <sup>+</sup> )Cl <sub>3</sub> ]Cl	"	(108)b
[Pd(L <sup>+</sup> ) <sub>2</sub> Cl <sub>2</sub> ](ClO <sub>4</sub> ) <sub>2</sub>	"	(108)b
[W(CO) <sub>5</sub> L <sup>+</sup> ]BF <sub>4</sub>	[P(OCH <sub>2</sub> ) <sub>3</sub> PCH <sub>3</sub> ] <sup>+</sup>	109
	[Ph <sub>2</sub> P(CH <sub>2</sub> ) <sub>2</sub> PPh <sub>2</sub> CH <sub>2</sub> Ph] <sup>+</sup>	110
[W(CO) <sub>5</sub> L <sup>+</sup> ]I	[cis-Ph <sub>2</sub> PCH=CHPPh <sub>2</sub> -CH <sub>3</sub> ] <sup>+</sup>	111
	[TransPh <sub>2</sub> PCH=CHPPh <sub>2</sub> -CH <sub>3</sub> ] <sup>+</sup>	111
[M(CO) <sub>5</sub> L <sup>+</sup> ]BF <sub>4</sub>	[(CH <sub>3</sub> ) <sub>2</sub> PCH <sub>2</sub> CH <sub>2</sub> P(CH <sub>3</sub> ) <sub>3</sub> ] <sup>+</sup>	112
	[Ph <sub>2</sub> PCH <sub>2</sub> PPh <sub>2</sub> CH <sub>3</sub> ] <sup>+</sup>	112
M = Cr, MO, W	[Ph <sub>2</sub> P(CH <sub>2</sub> ) <sub>2</sub> PPh <sub>2</sub> CH <sub>3</sub> ] <sup>+</sup>	112

## II. EXPERIMENTAL

### A. Materials

Sodium Hectorite (Bl-26) was obtained from the Baroid Division of National Lead Co. in the Pre-centrifuged and spray dried form the idealized unit cell formula is  $\text{Na}_{0.42}[\text{Mg}_{5.42}\text{Li}_{0.68}\text{Al}_{0.02}](\text{Si}_{8.00})\text{O}_{20}(\text{OH},\text{F})_4$ <sup>79d</sup> and the experimentally determined cation exchange capacity is 73 meq/100g.<sup>74b</sup> Sodium Montmorillonite (Upton, Wyoming) was obtained from the Source Clay Minerals Depository.

The trichlororhodium(III) hydrate used in this study was either obtained as a gift from Monsanto, Co., or purchased from Engelhard Industries, Inc. The di- $\mu$ -chlorotetracarbonyldirrhodium(I) was obtained from Sterm Chemicals Incorporated. Triphenylphosphine, benzylbromide, 1,5-cyclooctadine were purchased from Aldrich Chemical Company, while sodium tetrafluoroborate and potassium hexafluorophosphate were purchased from Alfa Products-Ventron. Dowex (AG<sub>2</sub>-X<sub>8</sub>) anion (Cl<sup>-</sup>) exchange resin, 50-100 mesh, was a gift from the Dow Chemical Company. Bis(1,2-diphenylphosphino) ethane was obtained from PCR, Inc. Sodium tetraphenylborate and silver tetrafluoroborate were purchased from the Alderich Chemical Company. Sodium perchlorate and activated alumina were obtained from

Matheson, Colman and Bell. 70% Perchloric acid was purchased from the Allied Chemical Company. 1-Hexene was purchased from Pfaltz and Bauer, Incorporated. It was purified by distillation over alumina under argon or nitrogen atmosphere.

All solvents were reagent grade, except that spectrograde solvents were used for the hydroformylation reactions and NMR studies. The solvents were degassed prior to use by standard pump-flush or freeze-pump-thaw techniques. Benzene and toluene were dried over lithium-aluminum hydride for at least 24 hours and freshly distilled before use.

## B. Physical Methods

### 1. Infrared Spectra

Most of the infrared spectra were recorded by employing a Perkin-Elmer Model 457 grating spectrophotometer. The samples were prepared by mulling in fluorolube (Hooker Chemical Company) or mineral oil (Nujol), and then placing the mull sample between CSI plates. Also, some IR samples were prepared as solids in KBr disks. A wire mesh screen served as an attenuator in the reference beam of the spectrometer. Mulls of oxygen sensitive samples were prepared in a nitrogen filled glove box immediately before measurement. Spectra of hectorite and rhodium exchanged

hectorite were obtained by use of a Perkin-Elmer Model 225 IR spectrophotometer. Oriented film samples were prepared by evaporating 1% aqueous slurries of hectorite mineral at room temperature.

## 2. X-Ray Diffraction Studies

A Phillips X-ray diffractometer with Ni-filtered CuK(a) radiation was utilized to determine the 001 basal spacing of samples of the layered silicate before and after exchanged with the desired cationic complex. The basal spacings for the mineral in the dry form were determined by spreading thin films on microscope slides and monitoring the diffraction through  $2^\circ$  to  $14^\circ$  of  $2\theta$ . The X-ray diffraction of mineral wetted with acetone was obtained by replacing the microscope slide with a slab of white, porous, fire brick, and soaking the firebrick in acetone. The peak positions in degrees of  $2\theta$  were converted to d-spacings with a standard chart.

## 3. Proton NMR Studies

Proton nuclear magnetic resonance ( $^1\text{H}$  NMR) spectra were obtained by use of a Varian T-60 (60 MHz) and a Bruker WHM 250 MHz. The spectra provided a check on the purity and identity of solvents and compounds. Chemical shifts were usually measured relative to tetramethyl silane as an

internal standard.

#### 4. Phosphorus-31 NMR Studies

Fourier transform, proton decoupled, phosphorus-31 NMR spectra of cationic rhodium complexes were recorded on a Bruker HFX-10 Spectrometer modified for multinuclear measurements as described by Traficante et al.,<sup>113</sup> and interfaced to a Nicolet 1083 computer with 12K of memory, a Diablo Disc memory unit, and Nicolet 293 I/O Controller. During these measurements an external lock mode was employed, wherein the spectrometer maintained a constant fluorine-19 lock on a sample of hexafluorobenzene contained in a microprobe assembly externally adjacent to the Dewar assembly of the main sample probe. Chemical shifts, relative to 85% phosphoric acid as an external reference, were calculated by taking the irradiation frequency to be 36.43 MHz. Spectra were obtained at approximately 36.44 MHz. The second part of our studies on rhodium complexes with positively charged ligands were carried out on a Bruker WH-180 spectrometer interfaced to a Nicolet 1180 computer with 16K of memory. Spectra were obtained at approximately 53.59 MHz. Samples were prepared by mixing solutions of the desired compounds in 10 mm diameter NMR tubes and sealing them with a few turns of black electrical tape. Spectra obtained under hydroformylation conditions, were obtained by preparing the samples in a glove box, in a 10 mm tube equipped with two side arms

fitted with a female 14/35 pyrex joint. Then the tube was attached to the hydroformylation line and the CO/H<sub>2</sub> mixture was added to the solution prior to conducting the nmr experiment. The sample tube was not spun in the probe in this case.

#### 5. Gas Chromatography

Gas phase chromatography of liquid samples were recorded by employing a Varian Associates Model 90P single column chromatograph with thermal conductivity detector. The output of the detector was recorded with a sargent model SR recorder. The hydroformylation products were separated on 6 ft x 3/16 inch column filled with 20% β,β'-oxidipropionitrile on 80/100 mesh chromosorb W.

For the separation solvent, 1-alkene and 2-alkenes, a 10 ft x 1/8 in 10% UCW-98 (Hewlett-Packard) on 80/100 chromosorb-W (Hewlett-Packard) column was used. The products were identified by GLC comparison with known standards. Also, GC-Mass spectroscopy was used in the identification of products. The percentage of products was determined by integration of the chromatographic peaks. Integrations were carried out by employing the "cutting and weighing" method.

#### 6. Elemental Analysis and Melting Points

All chemical analyses were performed by Galbraith laboratories, Inc., Knoxville, Tenn.

Melting points were determined on a Thomas-Hoover Model 6406-H capillary melting point apparatus.

### C. Synthesis

All the synthesis were carried out under an inert atmosphere, either in a nitrogen-filled dry box or on vacuum line.

#### 1. [RhCl(COD)]<sub>2</sub>

Di- $\mu$ -chlorobis(1,5-cyclooctadiene)dirhodium(I) was prepared by the procedure of Chatt and Venanzi.<sup>114</sup> From the reaction of  $\text{RhCl}_3 \cdot 3\text{H}_2\text{O}$  and COD in refluxing ethanol. The resulting orange crystals were recrystallized from glacial acetic acid. The compound melts at 256°C and decomposes above 258°C with effervescence. <sup>1</sup>H NMR ( $\text{CDCl}_3$ ) 4.2(d), 2.45(m), 1.72(d). Melting point and proton NMR data were in good agreement with literature values.<sup>115</sup>

#### 2. [Rh(NBD)Cl]<sub>2</sub>

Di- $\mu$ -chloro(norbornadiene)dirhodium was prepared from  $\text{RhCl}_3 \cdot 3\text{H}_2\text{O}$  and NBD in aqueous ethanol as known literature procedure. The crystalline complex darkened at 220°C and decomposed above 240°C <sup>1</sup>H NMR ( $\text{CDCl}_3$ ), 3.9t, 3.8(m), 1.16(t). The NMR and melting point was agreed with literature values.<sup>116</sup>

3.  $\underline{[\text{Rh}(\text{COD})(\text{PPh}_3)_2]\text{PF}_6}$ ,  $\underline{[\text{Rh}(\text{COD})(\text{PPh}_3)_2]\text{BF}_4}$ 

The hexafluorophosphate and tetraphenylborate salts of (1,5-cyclooctadiene)bis(triphenylphosphine)rhodium(I), were prepared according to the method of Schrock and Osborn<sup>117</sup> by the reaction of  $[\text{RhCl}(\text{COD})]_2$  and  $\text{PPh}_3$  in the presence of  $\text{KPF}_6$  or  $\text{NaB}(\text{C}_6\text{H}_5)_4$ . The bright orange crystals of the  $\text{PF}_6^-$  salt melted at 193-194°C and decompose above 200°C. The  $\text{B}(\text{C}_6\text{H}_5)_4^-$  salt was obtained as yellow powder which melted at 135-136°C and decomposed above 145°C.

4.  $\underline{[\text{Rh}(\text{NBD})(\text{PPh}_3)_2]\text{PF}_6}$ 

Norbornadiene bis(triphenylphosphine)rhodium(I) hexafluorophosphate was prepared by a previously reported method from  $[\text{Rh}(\text{NBD})\text{Cl}]_2$ ,  $\text{KPF}_6$  and  $\text{PPh}_3$ .<sup>117</sup> The bright orange crystals melted at 183-184°C and decomposed above 190°C.

5.  $\underline{[\text{Rh}(\text{COD})(\text{diphos})]\text{ClO}_4}$ 

1,5-Cyclooctadienebis(diphenylphosphinoethane)rhodium (I) perchlorate was prepared from  $[\text{RhCl}(\text{COD})]_2$  and diphenylphosphinoethane according to previously reported procedures.<sup>117</sup> It melted at 175-176°C. The infrared  $^1\text{H}$  and  $^{31}\text{P}$  NMR spectra of the complex were in agreement with those reported in the literature.

6. RhCl(COD)(PPh<sub>3</sub>)

Chloro(1,5-cyclooctadiene)triphenylphosphine rhodium(I) was prepared from [RhCl(COD)]<sub>2</sub> and PPh<sub>3</sub> without modification of the Chatt and Venanzi<sup>114</sup> method.

7. Ph<sub>2</sub>PCH<sub>2</sub>CH<sub>2</sub>PPh<sub>2</sub>CH<sub>2</sub>PhBr

Diphenylphosphino-2-benzylidiphenylphosphonium ethane bromide abbreviated as P-P<sup>+</sup>Br, was synthesized from diphos and benzyl bromide in benzene or toluene according to known procedures.<sup>106,78</sup> The resulting white crystals melt at 244-247°C.

8. BF<sub>4</sub><sup>-</sup> - Resin

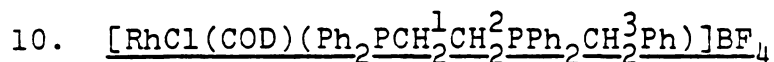
Tetrafluoroborate anion exchange resin was prepared from NaBF<sub>4</sub> and (AG<sub>2</sub>-X<sub>8</sub>) Dowex anion exchange resin according to known procedures.<sup>78</sup>

9. (Ph<sub>2</sub>PCH<sub>2</sub><sup>1</sup>CH<sub>2</sub><sup>2</sup>PPh<sub>2</sub>CH<sub>2</sub><sup>3</sup>Ph)BF<sub>4</sub>

Diphenylphosphino-2-benzyl diphenylphosphoniummethane tetrafluoroborate, abbreviated as [P-P<sup>+</sup>]BF<sub>4</sub> was prepared as follows:<sup>78</sup> In a nitrogen filled glove box, BF<sub>4</sub><sup>-</sup>-resin was added to a solution of P-P<sup>+</sup>Br in methanol. The resulting slurry was stirred for several hours (4 hr) and then filtered. Fresh BF<sub>4</sub><sup>-</sup>-resin was added to the filtrate

solution, and the procedure was repeated three times. The solution was concentrated under vacuum. The white, needle-like crystals were collected and washed with benzene or toluene, m.p. 188-189°C.  $\delta^1\text{H}$  NMR ( $\text{CDCl}_3$ ),  $\delta\text{H}^1 = 2.65$  (ddt),  $\delta\text{H}^2 = 2.1$  (dt),  $\delta\text{H}^3 = 4.37$  (d),  $J_{\text{H}^1\text{H}^2} = 10.6$ ,  $J_{\text{H}^1\text{P}} = \sim 6$  Hz,  $J_{\text{H}^1\text{-P}^+} = \sim 3$  Hz,  $J_{\text{H}^2\text{-P}^+} = 6.4$  Hz and  $J_{\text{H}^3\text{-P}^+} = 14.5$  Hz.

The proton decoupled  $^{31}\text{P}$  NMR spectrum in acetone consists of a doublet at +12.1 ppm upfield from 85%  $\text{H}_3\text{PO}_4$  which is assigned to trivalent phosphorous, another doublet at -27.1 ppm is assigned to the quaternized phosphorus  $J_{\text{P-P}^+} = 46$  Hz.

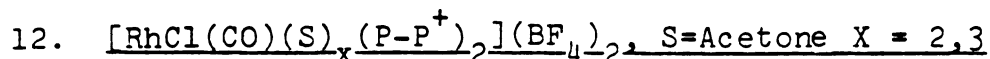


Chloro(1,5-cyclooctadiene)(1-diphenylphosphino-2-benzoyldiphenyl phosphoniummethane)rhodium(I) tetrafluoroborate was prepared from  $[\text{RhCl}(\text{COD})]_2$  and  $\text{P-P}^+\text{BF}_4$  by reported methods.<sup>78</sup> This procedure was also analogous to the Chatt and Venanzi preparation of  $\text{RhCl}(\text{COD})\text{PPh}_3$ .<sup>114</sup> The light-yellow, microcrystalline complex melted at 195-196°C and decomposed at 200°C.  $^1\text{H}$  NMR in ( $\text{CDCl}_3$ ) =  $\delta\text{H}^1 = 3.7$  (m),  $\delta\text{H}^2 = \sim 2.3$  m,  $\delta\text{H}^3 = 4.48$  (d),  $\delta\text{H}^a = 5.5$  (s),  $\delta\text{H}^b = 3.1$  (s); (a,b were assigned to the olefinic protons of 1,5-cyclooctadiene  $\delta_{\text{Ph-ring}} = 6.9-7.9$  (m)

11.  $\underline{[\text{Rh}(\text{CO})_2\text{Cl}(\text{P}-\text{P}^+)]\text{BF}_4}$  and  $\underline{[\text{Rh}(\text{CO})\text{Cl}(\text{P}-\text{P}^+)_2](\text{BF}_4)_2}$

An attempt was made to prepare trans-chlorodicarbonyl-(1-diphenylphosphino-2-benzylidiphenylphosphinoethane) rhodium(I) tetrafluoroborate as follows: In a nitrogen filled glove box,  $[\text{Rh}(\text{CO})_2\text{Cl}]_2$  (0.39 g, 1 mmol) in 20 mL of benzene was treated slowly with  $\text{P}-\text{P}^+$  (1.152 g, 2 mmol) in 20 mL of benzene.<sup>10</sup> After 30 minutes of vigorous stirring, the resulting orange solution was concentrated under a vacuum. The addition of pentane produced a orange yellow product which decomposed at 195°C, ir 1975  $\text{cm}^{-1}$  (S, C≡O). The orange-yellow compound is believed to be  $[\text{Rh}(\text{CO})_2\text{Cl}(\text{P}-\text{P}^+)_2]\text{BF}_4$  based the similarity of the C ≡ O stretching frequency to that reported for  $\text{Rh}(\text{CO})_2\text{Cl}(\text{PPh}_3)$ ,<sup>118</sup>.

The conditions required for carrying out the preparation of the above orange yellow compound are critical, since even a small excess of ligand ( $\text{P}-\text{P}^+$ ) reacts further to give orange  $\text{Rh}(\text{CO})\text{Cl}(\text{P}-\text{P}^+)_2(\text{BF}_4)_2$ . This latter compound was also obtained through disproportionation of  $\text{Rh}(\text{CO})_2\text{Cl}(\text{P}-\text{P}^+)$  in warm benzene solution after two days reaction time. The product was isolated as a precipitate, which was washed with pentane and dried. Chemical analysis of the latter one gave a ratio of 2/1 for  $\text{P}-\text{P}^+/\text{Rh}$  and 1/1 for  $\text{Cl}/\text{Rh}$ , i.r. (KBr) 1975  $\text{cm}^{-1}$  (S, C ≡ O). The yellow compound was formulated as  $[\text{Rh}(\text{CO})_2\text{Cl}(\text{P}-\text{P}^+)_2]^{2+}(\text{BF}_4)_2$ . Anal. Found: P, 8.81; Rh, 6.92; Cl, 3%. Calc: P, 9.4; Rh, 7.8; Cl, 2.7.



Trans-chlorocarbonylbis(1-diphenylphosphino-2-benzyl diphenylphosphinoethane)rhodium(I) tetrphenylborate was prepared as follows: In a nitrogen filled glove box,  $\text{RhCl}(\text{CO})\text{P}-\text{P}^+\text{BF}_4$  (0.2 mmol, 0.164 g) in 10 mL acetone was treated slowly with  $\text{P}-\text{P}^+\text{BF}_4$  (0.2 mmol, 0.115 g) in 10 mL acetone, after being stirred for 30 minutes. The solution was transferred into a stainless steel autoclave and the autoclave was pressurized to 600 psi by addition of 1:1  $\text{CO}:\text{H}_2$ . The autoclave was at 100°C for 1 hr, then it was cooled to room temperature. In a nitrogen filled glove box, the pale yellow solution was concentrated under vacuum. A yellow precipitate was formed by the addition of pentane to the concentrated solution. The yellow precipitate was washed with pentane several times, a yellow solid was obtained. This complex was identified as  $[\text{Rh}(\text{CO})(\text{P}-\text{P}^+)_2](\text{BF}_4)_2 \cdot 3(\text{CH}_3)_2\text{C}=\text{O}$ . Anal. calc: Rh, 6.9%; P, 8.3%, C, 61.1%; H, 5.3%, Cl, 2.4%. Found: Rh, 6.7%, P, 2.8%; C, 61.4%; H, 5.31%; Cl, 2.5%. IR (KBr) 1975  $\text{cm}^{-1}$  (S,  $\text{C} \equiv \text{O}$ ), 1700  $\text{cm}^{-1}$  (C = O, acetone).

Crystallization of the compound from dichloromethane and ether gave yellow crystals in 90% yield. The crystals were free of excess acetone, as judged by the absence of a strong IR absorption band at 1700  $\text{cm}^{-1}$ .

13.  $[\text{Rh}(\text{COD})^+] \text{BF}_4$ 

(Cycloocta-1,5-diene)rhodium(I)tetrafluoroborate was prepared by treatment<sup>119</sup> of  $[\text{RhCl}(\text{COD})]_2$  with  $\text{AgBF}_4$  in acetone.

14.  $[\text{Rh}(\text{NBD})]^+ \text{BF}_4$ 

(Norbornadiene)rhodium(I)tetrafluoroborate was prepared by known procedures from  $[\text{Rh}(\text{NBD})\text{Cl}]_2$  and  $\text{AgBF}_4$  in acetone.<sup>119</sup>

15.  $[\text{Rh}(\text{COD})(\text{PPh}_3)_2]^+ \text{-hectorite}$ 

Hectorite (0.2 g) was stirred for half an hour with 5 mL of the desired solvent (acetone, DMF) in a nitrogen filled glove box.  $[\text{Rh}(\text{COD})(\text{PPh}_3)_2]\text{PF}_6$  (0.014 g) in 5 ml acetone was added to the slurry of hectorite and the mixture was stirred for 15 minutes. The Rh-hectorite was filtered through a medium glass frit, and washed several times with solvent to remove any unexchanged rhodium complex. The yellow  $[\text{Rh}(\text{COD})(\text{PPh}_3)_2]^+ \text{-hectorite}$  showed the amount of rhodium to be 0.016 mmole in 0.2 g hectorite.

16.  $[\text{Rh}(\text{NBD})(\text{PPh}_3)_2]^+ \text{-hectorite}$ 

This rhodium exchanged hectorite was prepared from  $[\text{Rh}(\text{NBD})(\text{PPh}_3)_2]^+ \text{PF}_6$  (0.016 mmol) and hectorite (0.2 g)

by using a method analogous to that used for the preparation of  $[\text{Rh}(\text{COD})(\text{PPh}_3)_2]$ -hectorite.

17.  $\text{RhCl}(\text{COD})\text{P-P}^+$ /Hectorite

The exchanged hectorite was prepared from  $\text{RhCl}(\text{COD})-(\text{P-P})^+\text{BF}_4$  (0.016 mmol) and hectorite (0.2 g) in the desired solvent (acetone) the same way as described for the other cationic complexes.

18. Oriented Film Samples of Hectorite and Montmorillonite

Hectorite or montmorillonite 0.5 g, in 50 mL water, was sonifier for 20 minutes, then it was stirred for 30 minutes. The suspension was placed on a polystyrene sheet stretched across a glass plate. After two days the solvent ( $\text{H}_2\text{O}$ ) was evaporated at room temperature and a thin oriented film of hectorite or montmorillonite was formed.

19. Oriented Films of Rhodium Exchanged Hectorite

In a nitrogen filled glove box, 0.025 g of hectorite as an oriented film was placed in 10 mL acetone. After several hours, 0.043 g  $[\text{Rh}(\text{NBD})(\text{PPh}_3)_2]^+\text{PF}_6$  in 2 mL acetone was added to this film mixture. The mixture was kept in the dry box for two days, then the Rh exchanged hectorite as oriented film was removed from the solution. The film

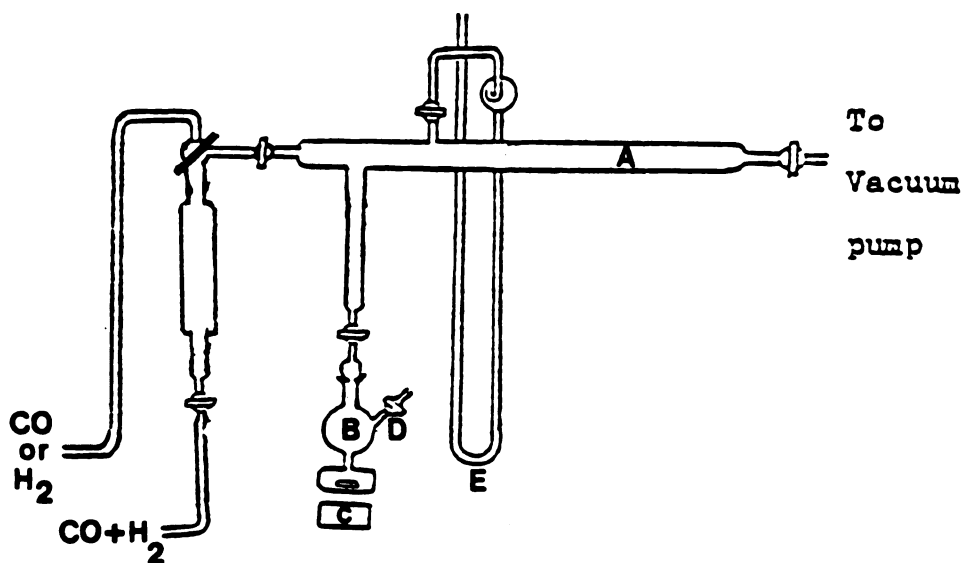
was washed with acetone and dried under vacuum. The oriented film was used for ir studies.

#### 20. P-P<sup>+</sup>/Hectorite

P-P<sup>+</sup>Br (1.12 g, 1.97 mmol) in 200 mL methanol was added to stirred suspension of hectorite (1 g, 0.73 meq, Na<sup>+</sup>) in 40 mL methanol. The mixture was stirred for 24 hr. It was filtered and washed with methanol until the filtrate gave a negative test for bromide. The mineral was allowed to be dry in a nitrogen filled glove box. The 001 basal spacing was 18.8 Å, which agrees with the literature result.<sup>78</sup> Approximately 68% cation exchange was achieved. When P-P<sup>+</sup>BF<sub>4</sub> was used instead of P-P<sup>+</sup>Br and the 001 basal spacing was the same as mentioned for P-P<sup>+</sup>Br (18.8Å).

#### D. Hydroformylation Procedures and Apparatus

1-Hexene as a substrate was hydroformylated under two different conditions of temperature and pressure; 1 atm pressure, 25°C and 37 atm (600 psi), 100°C. The apparatus which was used for hydroformylation at 1 atm is shown in Figure 6. Homogeneous catalysts were prepared in situ in a nitrogen filled glove box immediately prior to use. Stock solutions of the catalyst components were added to the hydroformylation flask containing solvent. The flask



- A. Manifold
- B. Reaction Flask
- C. Magnetic Stirrer
- D. Rubber Septum
- E. Open Hg Manometer with Meter Stick Scale.

Figure 7. Hydroformylation apparatus (schematic) for reaction carried out at 1 atm pressure.

was sealed and attached to the hydroformylation apparatus. The stirrer was set at a moderate rate of rotation (Figure 7). A vacuum was carefully applied to the manifold and then a 1:1 mixture of CO and H<sub>2</sub> was added. This process was repeated several times. The reaction flask (including septum) was then exposed to vacuum sufficient to degas the solvent. When  $[\text{Rh}(\text{COD})(\text{PPh}_3)_2]^+$  was used as a catalyst precursor for hydroformylation reaction, it was first treated with CO for 5 minutes and then 1:1 CO:H<sub>2</sub> was added to the reaction flask. In the case of  $[\text{Rh}(\text{NBD})(\text{PPh}_3)_2]^+$  the complex was treated first with H<sub>2</sub> and then 1:1, CO:H<sub>2</sub> was added to the reaction flask. After 15 minutes, freshly distilled 1-hexene was added to the reaction flask via the rubber septum by inert atmosphere syringe techniques. The reaction was stopped after 24 or 48 hours, and the percent conversion was measured by GC analysis.

In the heterogeneous systems, the rhodium exchanged hectorite was placed in the reaction flask and hydroformylation reaction was carried out the same manner as described for the homogeneous systems.

The second part of our experiments were done at 600 psi and 100°C by using a stainless steel autoclave apparatus (Figure 7). The homogeneous catalysts were prepared in a nitrogen filled glove box immediately prior to use. Stock solutions containing catalysts components were

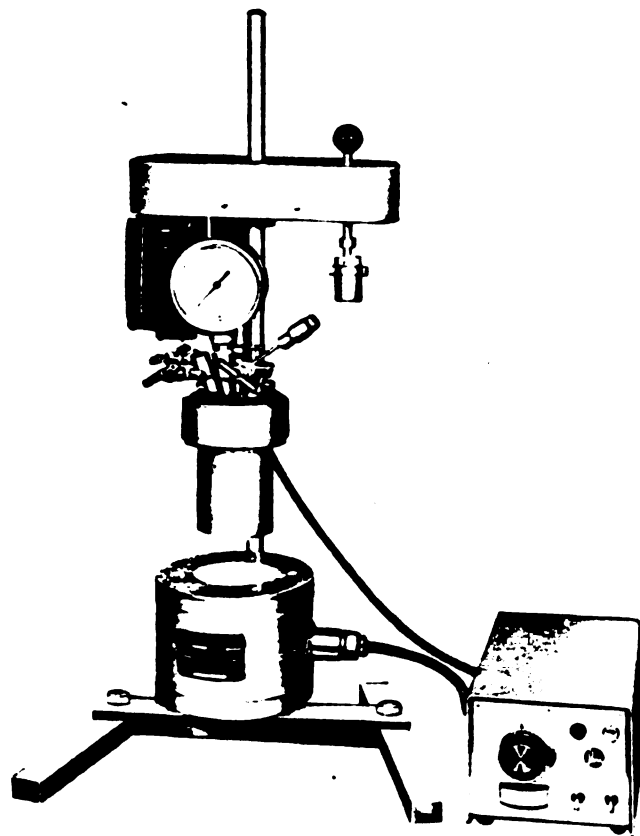


Figure 8. 600 mL Autoclave used for hydroformylation reactions at 600 psi.

transferred to the autoclave. The total volume of solution was 21 mL (20 mL solvent and 1 mL 1-hexene). The pressure was increased to 600 psi by addition of 1:1 CO:H<sub>2</sub> gas.

Several methods were used for preparation of homogeneous catalyst precursors with positively charged ligands. All preparations were conducted in a nitrogen filled glove box.

#### 1. Method I - Homogeneous Catalysts

In a nitrogen filled glove box, 0.014 mmol P-P<sup>+</sup>BF<sub>4</sub> in 5 mL acetone was slowly added to a solution of RhCl(COD)P-P<sup>+</sup>BF<sub>4</sub> (0.014 mmol in 5 mL acetone). The solution was stirred for 30 minutes, then it was transferred to the autoclave, followed by addition of 10 mL acetone and 1 mL of 1-hexene (total volume, 21 mL). The pressure of the autoclave was increased to 600 psi by addition of a 1:1 CO:H<sub>2</sub> gas mixture and the reaction was carried out at 100°C. The reactor was cooled to room temperature and opened to the atmosphere. The solution was then submitted for GC analysis of the reaction products.

#### 2. Method I, Heterogeneous Catalysts

The active species for intercalation was generated in acetone at 100°C and 600 psi by addition of CO:H<sub>2</sub> (1:1) to a solution containing 0.014 mmol each of RhCl(COD)(P-P<sup>+</sup>)BF<sub>4</sub>

and  $P-P^+$  in 20 mL acetone. The reaction was allowed to proceed for 1 hr. The solution then was cooled to room temperature, and the pressure was decreased to 1 atm. Intercalation of the active catalyst precursor was achieved by ion exchange reaction of the freshly generated intermediate with 0.2 g  $Na^+$ -hectorite at 25°C. The exchange reaction was carried out in a nitrogen filled glove box, the exchanged procedure was the same as mentioned earlier for cationic rhodium complex. The yellow mineral was washed with acetone, dried, and then used as a heterogeneous catalyst for hydroformylation reaction. Analysis of the intercalated mineral gave Rh, 0.32%; P, 0.85%,  $P-P^+ : Rh = 4.4 : 1$ .

A second heterogeneous catalyst was prepared from  $RhCl(CO)(P-P^+)_2$  and excess  $P-P^+$ .  $P-P^+BF_4$  (0.014 mmol) in 5 mL acetone was slowly added to 0.014 mmol  $RhCl(CO)(P-P^+)_2$  in 5 ml of acetone. The solution was stirred for 30 minutes and then it was used for a homogeneous hydroformylation. The same solution was used to prepare an intercalated catalyst. The procedure for intercalation of the active species was the same as explained above for the  $RhCl(CO)(P-P^+) + 1P-P^+$  system.

### 3. Method II, Homogeneous Catalysts

$P-P^+BF_4$  (0.028 mmol, in 6 mL acetone) was slowly added to a freshly prepared solution of  $[Rh(COD)]^+BF_4$  (0.014 mmol,

in 3 mL acetone). The solution was allowed to stir for 30 minutes and then it was transferred to the reactor, followed by addition of 10 mL acetone. Hydroformylation reaction was carried out with this catalyst precursor according to the methods outlined above.

#### 4. Method II, Heterogeneous System

The active species was formed by treatment of 0.014 mmol  $[\text{Rh}(\text{COD})]^+\text{BF}_4^-$  and 0.028 mmol in 20 mL of acetone with  $\text{CO}:\text{H}_2$  (1:1) at 600 psi and  $100^\circ\text{C}$ . After 1 hr. the reactor was cooled to room temperature, and the pressure was decreased to 1 atm. Then this solution was added to 0.2 g  $\text{Na}^+$ -hectorite, previously equilibrated in 5 mL acetone. The suspension was stirred for 30 minutes in a nitrogen filled glove box, then it was filtered and washed with acetone several times. The yellow rhodium exchanged hectorite was formed. Chemical analysis of the intercalated mineral gave; Rh, 0.47%; P, 0.57%,  $\text{P}^+:\text{Rh}=2:1$ .

#### 5. Method III, Heterogeneous Catalyst

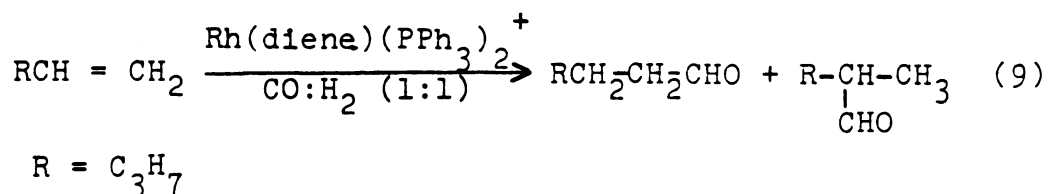
A freshly prepared solution of  $[\text{Rh}(\text{COD})]^+\text{BF}_4^-$  (0.01 mmol, in 2 mL of acetone) was added to 0.2 g  $\text{P}^+$ -hectorite, previously equilibrated with 5 mL acetone for 30 minutes. The suspension was stirred for 30 minutes, and then it was filtered and washed with acetone. The color of the Rh

exchanged hectorite was yellow. The 001 basal spacing of the dry intercalate was 18.8 Å. The yellow mineral was used as a heterogeneous catalyst for hydroformylation reactions.

A second heterogeneous catalyst was prepared by a similar method except that  $[\text{RhCl}(\text{COD})]_2$  was used in place of  $[\text{Rh}(\text{COD})]^+$ .  $[\text{RhCl}(\text{COD})]_2$  (0.01 mmol) in 5 mL acetone was added to the 0.2 g P-P<sup>+</sup>-hectorite, previously equilibrated with 5 mL acetone. The suspension was stirred for 30 minutes. The yellow mineral was filtered and washed with acetone for several times in a nitrogen filled glove box.

### III. RESULTS AND DISCUSSION

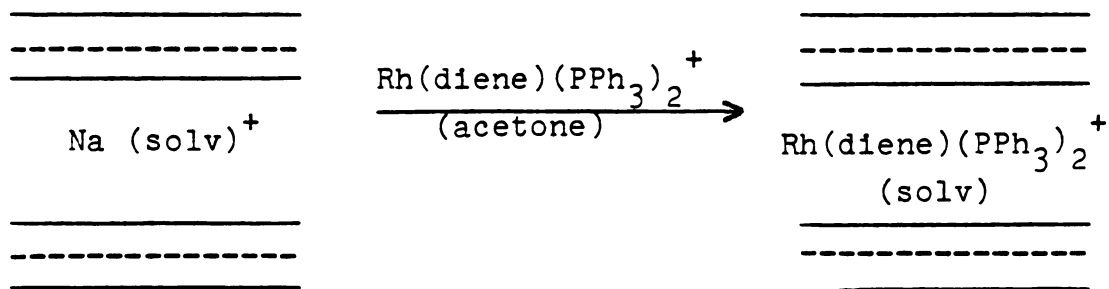
Our objective in this research project was (1) to find cationic rhodium catalysts for homogeneous hydroformylation reaction, (2) to use layer silicates for immobilization of the metal complex catalysts and to conduct hydroformylation with them as heterogeneous systems. For this purpose, known cationic rhodium complexes<sup>117</sup> such as  $[\text{Rh}(\text{COD})(\text{PPh}_3)_2]\text{A}$ ; ( $\text{A} = \text{PF}_6, \text{B}(\text{C}_6\text{H}_5)_4$ ),  $[\text{Rh}(\text{NBD})(\text{PPh}_3)_2]\text{-PF}_6$  and  $[\text{Rh}(\text{COD})(\text{diphos})]\text{ClO}_4$  were examined as catalyst precursors for hydroformylation reactions in homogeneous and intercalated systems. The reaction of interest is the hydroformylation of 1-hexene to give a mixture of normal heptanal and branched 2-methylhexanal



#### A. Characterization of Rhodium Exchanged Hectorite

Solvated sodium ions in the layered silicates  $\text{Na}^+$ -hectorite and  $\text{Na}^+$ -montmorillonite are readily exchanged by other ions of the same charge but different sizes.

Therefore, cationic rhodium complexes such as  $\text{Rh}(\text{diene})\text{L}_2^+$  species can easily be exchanged into the silicate layers: as described below:



(10)

IR and X-ray studies confirm the presence of the exchanged rhodium complex between the silicate sheets.

### 1. Interpretation of Infrared Spectra

Figures 9 and 10 show the IR spectra of the rhodium complex  $[\text{Rh}(\text{NBD})(\text{PPh}_3)_2]\text{PF}_6$ ,  $\text{Na}^+$ -hectorite and  $[\text{Rh}(\text{NBD})(\text{PPh}_3)_2]^+$ -exchanged hectorite. The IR spectrum of the cationic rhodium complex was recorded by using KBr pellet techniques, while infrared spectra of  $\text{Na}^+$ -hectorite and  $\text{Rh}(\text{NBD})(\text{PPh}_3)_2^+$ -hectorite were taken as oriented films. The IR spectrum of the cationic rhodium complex (Figure 9) shows two sharp bands around  $1480$  and  $1440 \text{ cm}^{-1}$ . These bands were assigned to in plane deformation of the phenyl rings bound to phosphorus.<sup>120</sup> In addition, two unassigned bands at  $1310$  and  $1270 \text{ cm}^{-1}$  are also observed. Two multiple

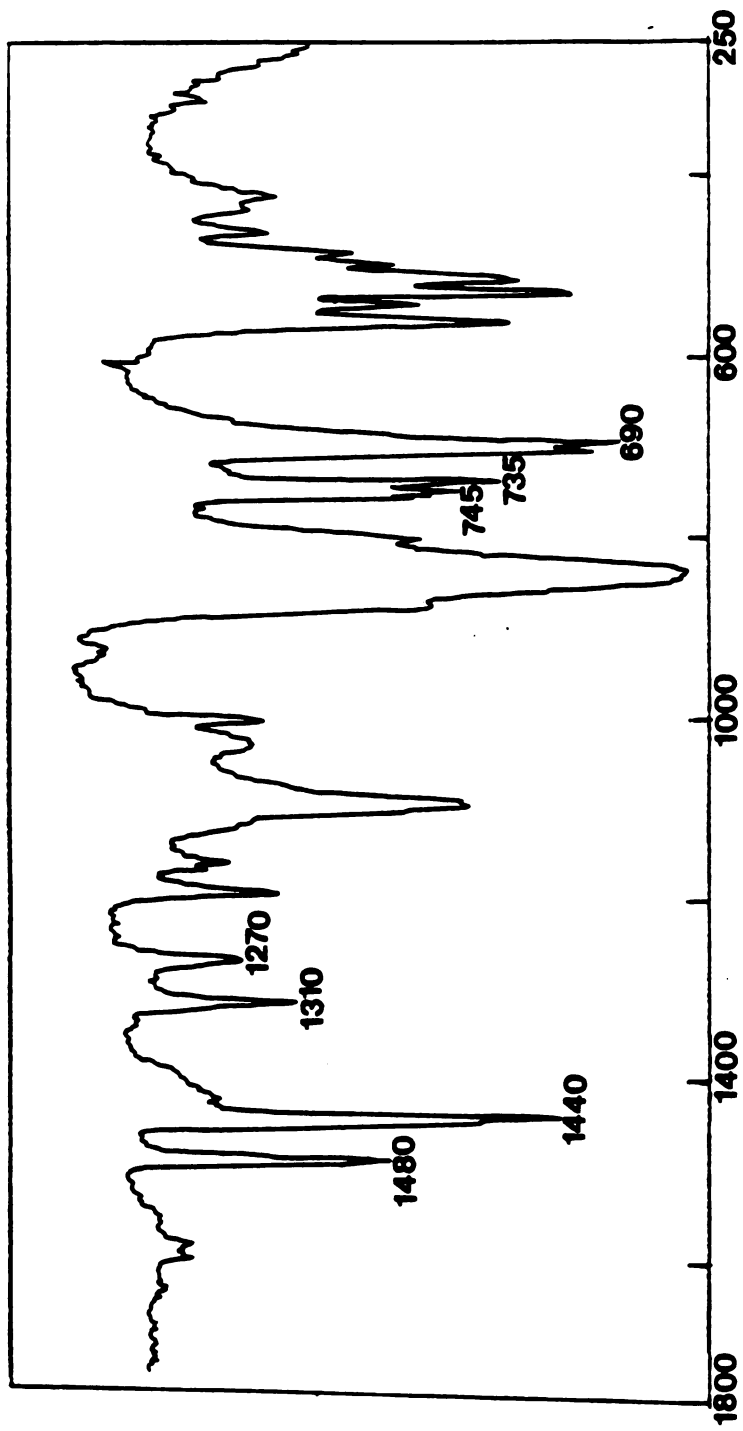


Figure 9. Infrared spectra (KBr pellet) of  $[\text{Rh}(\text{NBD})(\text{PPh}_3)_2]\text{PF}_6$  in the region 1600-250  $\text{cm}^{-1}$ .

Figure 10. Infrared spectra of (A) Na<sup>+</sup>-hectorite and (B) [Rh(NBD)(PPh<sub>3</sub>)<sub>2</sub>]-hectorite as oriented films.

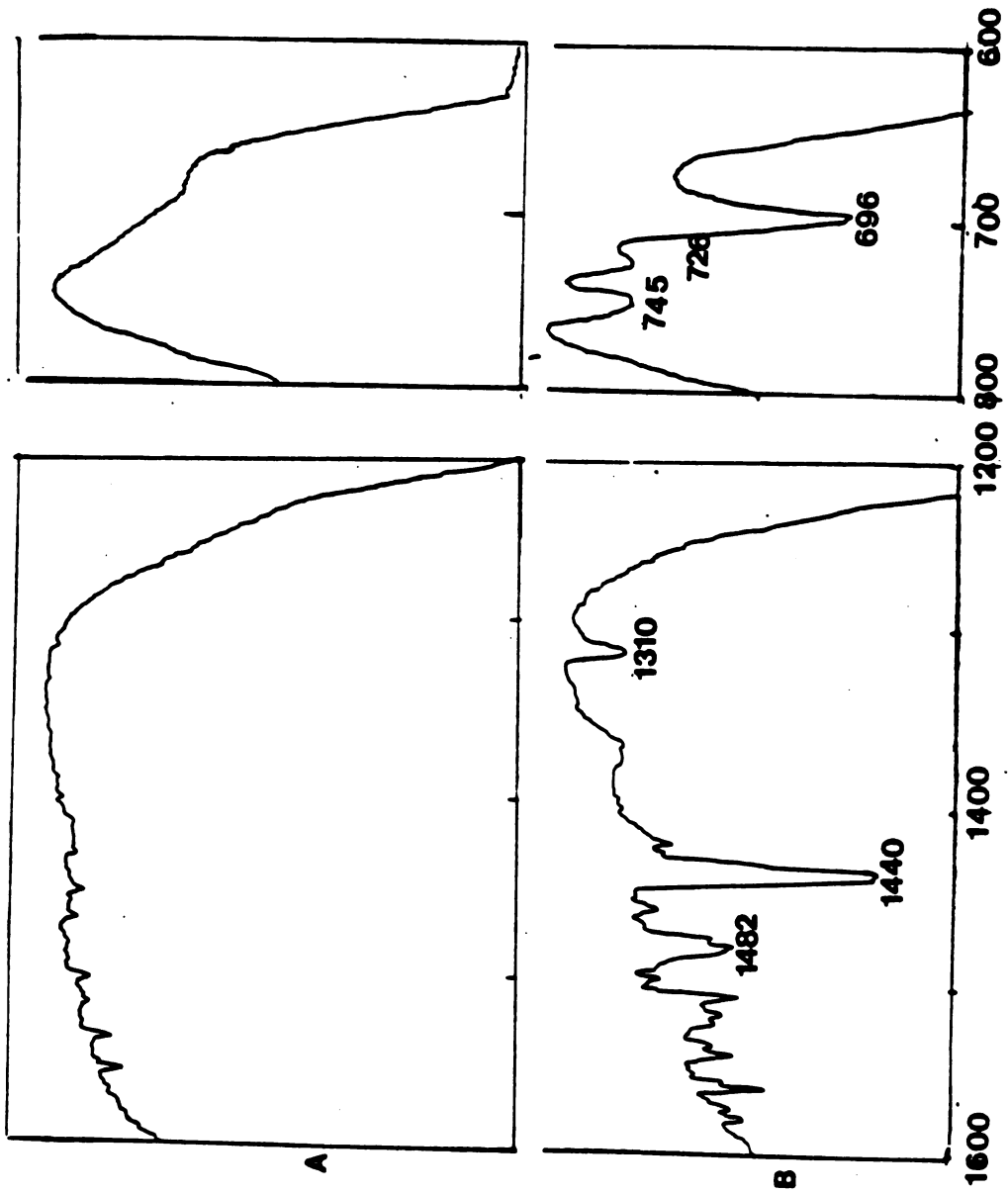


Table 12. Infrared Bands ( $\text{cm}^{-1}$ ) of  $[\text{Rh}(\text{NBD})(\text{PPh}_3)_2]\text{PF}_6$ ,  $\text{Na}^+$ -hectorite and  $\text{Rh}(\text{NBD})-(\text{PPh}_3)_2$ -hectorite.

Complex	1800-1600	1600-1200	800-600
$[\text{Rh}(\text{NBD})(\text{PPh}_3)_2]\text{PF}_6$	-----	1480, 1440, 1310	745, 735, 690
$\text{Na}^+$ -hectorite	1622	-----	-----
$\text{Rh}(\text{NBD})(\text{PPh}_3)_2^+$ -hectorite	1622	1482, 1440, 1310	745, 726, 696

bands located at  $745\text{-}690\text{ cm}^{-1}$  are assigned to C-H out of plane deformation modes of the phenyl rings. The  $\text{Na}^+$ -hectorite spectrum (Figure 10a) is explained in the following way. The band at  $1622\text{ cm}^{-1}$  is due to a deformation mode of water molecules adsorbed between the layers. The mineral exhibits no bands between  $1500\text{-}1400\text{ cm}^{-1}$ . This result indicates that the mineral is free of natural carbonate impurities. The IR spectrum of  $\text{Rh}(\text{NBD})(\text{PPh}_3)_2^+$ -hectorite shows two bands at  $1482\text{ cm}^{-1}$  and  $1440\text{ cm}^{-1}$ . These bands are also assigned to in-plane deformation of phenyl rings bonded to phosphorus, also. The bands located at  $745\text{ cm}^{-1}$ ,  $726\text{ cm}^{-1}$  and  $696\text{ cm}^{-1}$  are assigned to C-H out of plane deformations of the phenyl rings. The band positions for  $\text{Na}^+$ -montmorillonite and  $\text{Rh}(\text{NBD})(\text{PPh}_3)_2^+$ -montmorillonite were the same as those shown for hectorite. These results suggested that the nature of the intercalated cationic rhodium complex is the same as that of the pure rhodium complex salt, these results were summarized in Table 12.

## 2. X-ray Diffraction Studies

Under ordinary conditions, a smectite type mineral with  $\text{Na}^+$  as the exchangeable ion, usually contains one or two molecular layers of water. The X-ray diffraction pattern of natural  $\text{Na}^+$ -hectorite and natural  $\text{Na}^+$ -montmorillonite washed with acetone or methanol and air dried gave a c-axis spacings of  $12.6\text{ \AA}$  and  $12.1\text{ \AA}$ , respectively.

These values are in agreement with the reported values. These results indicated that one molecular layer of solvent water is located between the silicate sheets.

It is possible to exchange most of the sodium ions present between the charged surfaces of the clay minerals by exposure to a concentrated solution of the cationic rhodium complex. Ion exchange was readily accomplished by treating 0.2 g  $\text{Na}^+$ -hectorite with a CEC 70 meq/100 with 0.053 mmol of rhodium complex in acetone. The exchanged rhodium hectorite was submitted for chemical analysis and was found to be 22% exchanged. Table 13 lists the 001 basal spacings of  $\text{Na}^+$ -hectorite and the partially exchanged hectorite.

Based on the difference between the thickness of the silicate sheets (9.6 Å) and the observed 001 reflection for  $\text{Rh}(\text{NBD})(\text{PPh}_3)_2$ -hectorite (17.7 Å), the average thickness of the interlayers is estimated to be 8.1 Å. This expansion agrees well with the value expected from molecular models for a monolayer of complex cations in the interlayer surfaces. It can also be seen in Table 13 that in the case of acetone as a solvent, the interlayer spacing increases from 17.7 Å to 22.1 Å, and indicates that the interlayer can be swelled by one or more molecular layers of acetone.

Table 13. 001 Basal Spacings of  $\text{Na}^+$ -Hectorite and  $\text{Na}^+$ -Hectorite Partially Exchanged with Cationic Rhodium Complexes.

Mineral	Condition	(001) Basal Spacing ( $\text{\AA}$ )	% Rh Exchange
$\text{Na}^+$ -Hectorite	Dry	12.6	0
$\text{Na}^+$ -Montmorillonite	Dry	12.1	0
$[\text{Rh}(\text{NBD})(\text{PPh}_3)_2]^+$ -Hectorite	Dry	17.7	22%
$[\text{Rh}(\text{NBD})(\text{PPh}_3)_2]^+$ -Hectorite	Wet With Acetone	22.1	22%
$[\text{Rh}(\text{COD})(\text{PPh}_3)_2]^+$ -Hectorite	Dry	17.7	22%
$[\text{Rh}(\text{COD})(\text{PPh}_3)_2]^+$ -Hectorite	Wet With Acetone	21.0	22%

## B. Homogeneous Hydroformylation

Three cationic rhodium complexes  $[\text{Rh}(\text{COD})(\text{PPh}_3)_2]\text{PF}_6$ ,  $[\text{Rh}(\text{NBD})(\text{PPh}_3)_2]\text{PF}_6$  and  $[\text{Rh}(\text{COD})(\text{diphos})]\text{ClO}_4$  were used for the hydroformylation of 1-hexene at 25°C, 1 atm. It was found that only the first two complexes were active for hydroformylation reactions under these conditions.

Table 14 lists the results for the homogeneous hydroformylation of 1-hexene under batch reaction conditions with  $\text{Rh}(\text{diene})(\text{PPh}_3)_2^+$  (diene = NBD, COD) as the catalyst precursors. The conversion of 1-hexene at 25°C is appreciably lower in acetone than in DMF, but the distribution of normal and branched aldehyde products (n/b=3/1) is the same for the two solvents (runs 1,2). The reaction with  $\text{Rh}(\text{NBD})(\text{PPh}_3)_2^+$  is faster than with  $\text{Rh}(\text{COD})(\text{PPh}_3)_2^+$ . This effect has also been observed for hydrogenation reactions, too. Also, no significant isomerization or hydrogenation is seen under the reaction conditions employed.

Table 15 lists the results for homogeneous hydroformylation of 1-hexene at 100°C and 600 psi. In this case extensive isomerization occurs along with a decrease of n/b ratio relative to the n/b ratio obtained at 25°C. The addition of excess triphenylphosphine decreases the extent of isomerization and increases the n/b ratio (runs 5, 6,7). The dependence of n/b ratio on  $\text{PPh}_3/\text{Rh}$  ratio agrees with the previously reported ligand dependence of hydroformylation reactions with  $\text{RhH}(\text{CO})(\text{PPh}_3)_3$  or  $\text{ClRh}(\text{CO})(\text{PPh}_3)_2^{121}$  as the

Table 14. Homogeneous Hydroformylation of 1-Hexene with Rh(diene)(PPh<sub>3</sub>)<sub>2</sub><sup>+</sup>PF<sub>6</sub><sup>-</sup> as Catalyst Precursors.<sup>a</sup>

Run	Catalyst	Solvent	Time (hr)	% Conv.	Product Distribution %			n/b
					n-heptanal	2-Methyl-hexanal	2-hexene	
1	Rh(NBD)L <sub>2</sub> <sup>+</sup> PF <sub>6</sub> <sup>-</sup>	Acetone	48	25	74	26	--	2.8
2	Rh(NBD)L <sub>2</sub> <sup>+</sup> PF <sub>6</sub> <sup>-</sup>	DMF	48	80	74	26	--	2.8
3	Rh(COD)L <sub>2</sub> <sup>+</sup> PF <sub>6</sub> <sup>-</sup>	Acetone	48	10	75	25	--	3.0
4	Rh(COD)L <sub>2</sub> <sup>+</sup> PF <sub>6</sub> <sup>-</sup>	DMF	48	70	76	24	--	3.2

<sup>a</sup> Reaction Temp. = 25°C, [1-H exene] = 1.0M; CO : H<sub>2</sub> = 1:1; Total Pressure = 1 atm, 1-Hexene:Rh = 71:1.

Table 15. Homogeneous Hydroformylation of 1-Hexene with  $[\text{Rh}(\text{COD})(\text{PPh}_3)_2]\text{PF}_6$  as Catalyst Precursor.<sup>a</sup>

Run	Moles $\text{PPh}_3$ Added	Time (hr)	% Conv.	Product Distribution (%)				n/b
				n-Heptanal	Hexanal	2-Methyl-2-Hexene		
(5)	0	1	100	52	24	24 <sup>b</sup>		2.2
(6)	2	1	100	59	26	15		2.3
(7)	8	1	100	66	22	12		3.0

<sup>a</sup>[1-Hexene] = 1.0M in acetone;  $\text{CO:H}_2 = 1:1$ ; Total pressure = 600 psi; Reaction Temp. = 100°C; 1-Hexene : Rh = 200:1.

<sup>b</sup>Trans:cis = 2.5:1.

catalyst precursors. In fact, the lower ratio of n/b at 100°C must be associated with the dissociation of triphenylphosphine under such conditions. In 1978, Oro et al reported that  $[\text{Rh}(\text{COD})(\text{APh}_3)_2]\text{ClO}_4$  (A = N, P, As, Sb, Bi) are active catalyst precursors for hydroformylation reactions.<sup>105</sup>

He also mentioned that the IR spectra of the catalytic solutions resulting from experiments with  $(\text{PPh}_3)$  and  $(\text{SbPh}_3)$  show absorptions which clearly indicate the presence of these coordinated  $\text{C}\equiv\text{O}$  ligands along with bands due to non-coordinated  $\text{ClO}_4^-$  (anion).<sup>122</sup> The bands assignable to  $\text{V}(\text{C}\equiv\text{O})$  are located in the 2100-1950  $\text{cm}^{-1}$  region. It was claimed that the  $\text{C}\equiv\text{O}$  bands are characteristic for cationic carbonylated species.<sup>117</sup> He proposed that the active species should be cationic.

Further studies on homogeneous systems are listed in Table 16. According to this table, it is especially noteworthy that the addition of triethylamine ( $\text{NEt}_3$ ) to the reaction mixture at 25°C increases the reaction rate without influencing the aldehyde distribution (runs 8,9), whereas  $\text{HClO}_4$  in DMF as solvent greatly depresses the reaction (run 11). On the other hand, the addition of two moles of  $\text{NEt}_3$  to the solution containing one mole of  $\text{HClO}_4$  restores the catalytic activity. The addition of  $\text{HClO}_4$  to the complex in acetone solution, caused a dark red color to develop and no hydroformylation product was detected (run 10). The formation of the red color might have been

Table 16. Homogeneous Hydroformylation of 1-Hexene with  $[\text{Rh}(\text{COD})(\text{PPh}_3)_2]\text{PF}_6$  as Catalyst Precursor.

Run	Solvent	Time (hr)	% Conv.	Product Distribution %			n/b
				n-Heptanal	2-Methylhexanal	2-Hexene	
8 <sup>a</sup>	Acetone	24	80	78	22	--	3.5
9 <sup>a</sup>	DMF	24	100	78	22	--	3.5
10 <sup>b</sup>	Acetone	24	0	--	--	--	---
11 <sup>b</sup>	DMF	24	0	--	--	--	---

<sup>a</sup>In this run  $\text{NEt}_3$  was added to the reaction,  $\text{NEt}_3$  : Rh = 3:1.

<sup>b</sup>In this run  $\text{HClO}_4$  was added to the reaction,  $\text{HClO}_4$ :Rh = 3:1.

[1-Hexene] = 1.0M; CO:H<sub>2</sub> = 1:1; Total Pressure = 1 atm; Reaction Temp 25°C  
1-Hexene : Rh = 7:1.

Table 17. Hydroformylation of 1-Hexene with  $\text{Rh}(\text{COD})(\text{PPh}_3)_2^+$  Intercalated in Hectorite at 25°C.<sup>a</sup>

Run	Catalyst	Solvent	% Conv.	Time (hr)	Pressure (atm)	Product Distribution %		
						n-heptanal	2-Methyl-Hexanal	n/b
12	$\text{Rh}(\text{COD})(\text{PPh}_3)_2^-$ hectorite	Acetone	75	48	5	75	25	3
13	$\text{Ph}(\text{COD})(\text{PPh}_3)_2^-$ hectorite	DMF	95	24	1	76	24	3.1

<sup>a</sup>[1-Hexene] = 0.4M;  $\text{CO:H}_2 = 1:1$ ; 1-Hexene : Rh  $\geq$  150 : 1.

the result of reaction of acid with acetone under the reaction conditions.

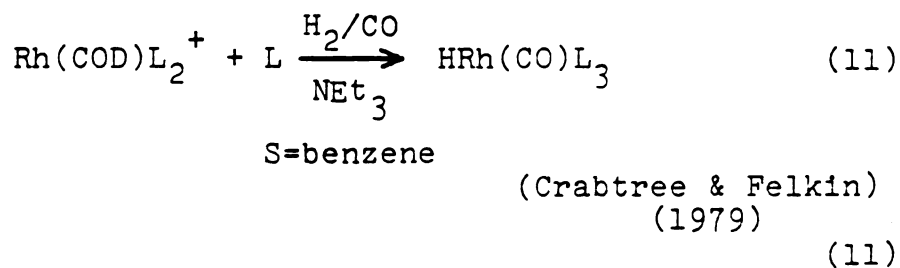
C. Hydroformylation with Intercalated  $\text{Rh}(\text{diene})(\text{PPh}_3)_2^+$ -hectorite

The supported catalysts were generated by passing  $\text{CO:H}_2$  (1:1) through a suspension of  $\text{Rh}(\text{diene})(\text{PPh}_3)_2^+$ -hectorite in acetone or DMF.

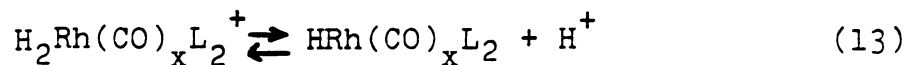
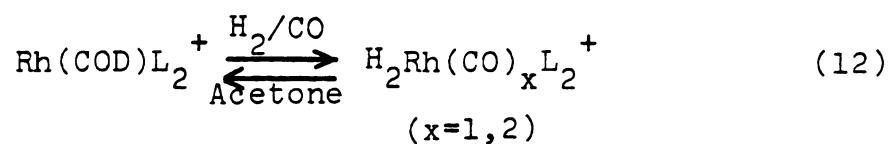
Table 17 lists the results for the heterogeneous hydroformylation of 1-hexene with  $\text{Rh}(\text{COD})(\text{PPh}_3)_2^+$ -hectorite as the supported catalyst. When acetone is used as solvent, the reaction is very slow and unidentified products are formed at 1 atm. By increasing the pressure to 5 atm, the rate of reaction can be significantly increased (run 12). In the case of DMF as solvent the reaction was started immediately (no induction period) (run 13). Therefore, the reaction in DMF was much faster than in acetone. The filtrate from runs 12 and 13 (Table 17) were active toward hydroformylation. These results clearly indicated that such activities were due to the desorption of the active species in the solution. Significantly the desorbed rhodium complex is more active than  $\text{Rh}(\text{COD})(\text{PPh}_3)_2^+$  in homogeneous solution. For example, the desorbed complex in DMF undergoes  $\sim 142$  catalyst turnovers in 24 hours at  $25^\circ\text{C}$  ( $n/b = 3/1$ ), whereas only  $\sim 50$  turnovers occur in 48 hours with  $\text{Rh}(\text{COD})(\text{PPh}_3)_2^+$  as the catalyst precursor (cf. Table 14, run 4 and Table 17, run 13). Since electrical neutrality

must be maintained in the silicate structure, it is clear that the complex which desorbs from the negatively charged silicate surfaces cannot be cationic. At this point two questions can be raised. First, why does  $\text{Rh}(\text{COD})(\text{PPh}_3)_2^+$  desorb during the course of hydroformylation reaction, and second, why desorption in DMF is much greater than in acetone.

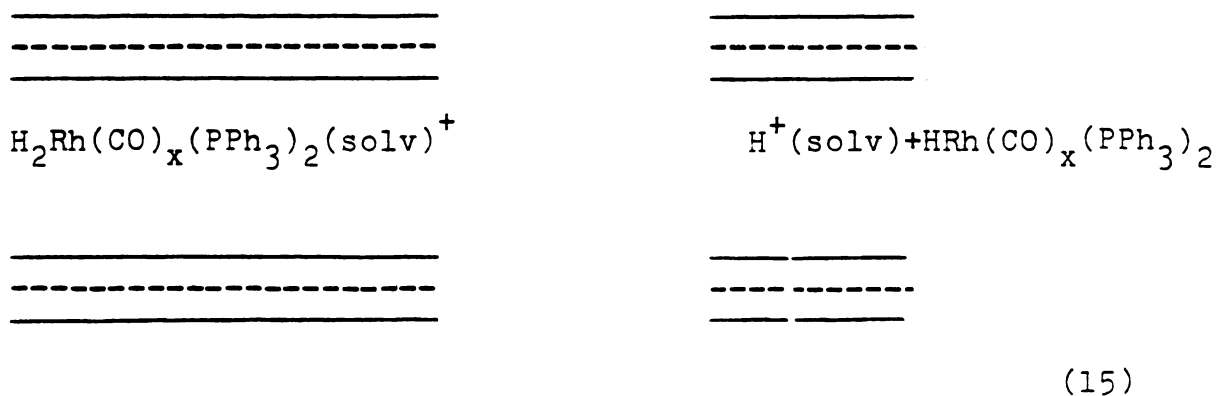
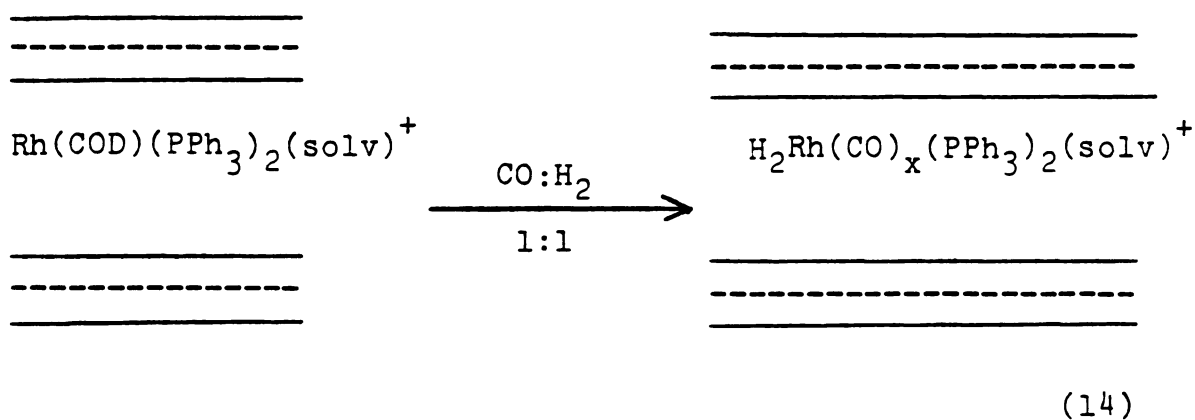
Recently, Crabtree and Felkin<sup>123</sup> found that the hydroformylation of 1-Hexene in benzene with  $\text{Rh}(\text{COD})(\text{PPh}_3)_2^+$  in the presence of triethylamine as base and one mole of triphenylphosphine gave reaction rates and product ratios n/b identical to those obtained with an authentic sample of  $\text{RhH}(\text{CO})(\text{PPh}_3)_3$ . Moreover, they were able to isolate the latter compound from the reaction mixture in high yield.



Based on these results by Crabtree and Felkin together with our findings on the behavior of homogeneous and intercalated systems (Tables 14, 16, 17), it is likely that the active species is a neutral monohydride  $\text{HRh}(\text{CO})_x(\text{PPh}_3)_2$ , which exist in equilibrium with a cationic dihydride  $\text{H}_2\text{-Rh}(\text{CO})_x(\text{PPh}_3)_2^+$  which is not active for hydroformylation:



The proton equilibrium proposed in Equation (13) not only accounts for the observed acid-base dependence of the homogeneous catalyst, but it also provides a mechanism for desorption of rhodium from the intercalation catalyst without loss of electrical neutrality in the silicate structure, or shown in Equation (14) and (15).



Since the silicate sheets act as a base according to the Equation (15), the desorbed monohydride is taken out of equilibrium with the inactive dihydride and consequently the activity of the desorbed catalyst is greater than the activity of the catalyst formed directly from  $\text{Rh}(\text{COD})-(\text{PPh}_3)_2^+$  in homogeneous solution.

According to the results listed in Tables 14 and 17, catalysts showed better activity in DMF than in acetone.

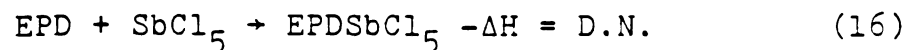
Previous studies of the effects of solvents were shown to have a marked effect upon the rate of hydroformylation reaction and in some cases, alter the product distribution.<sup>124</sup> When  $\text{ClRh}(\text{CO})(\text{PPh}_3)_2$  is used as a catalyst precursor for hydroformylation, as the polarity and concomitant basicity of the solvent increases, the selectivity of the catalyst also increases. The addition of excess triphenylphosphine to the polar solvent such as DMF results in a further increase in selectivity as well as a four-fold acceleration in rate. Also, the reaction in the polar solvent is initially fast and reaction decreases with time. The rate of hydroformylation in a nonpolar solvent such as benzene is initially slow, but reaction becomes faster as the solvent becomes more polar with the presence of product aldehyde.<sup>124</sup> At this stage it can be pointed out that the polarity of the solvent has an effect on the rate of reaction. The difference between acetone and DMF depends on their

acceptor number (AN) and donor number (DN) which are listed as follows:

Table 18. Physical Constants for Acetone and DMF.

Solvent	Dielectric Constant	Acceptor Number	Donor Number
Acetone	20.7	12.5	17.0
DMF	36.1	----	26.6

DMF is more polar than acetone and also has a higher electron donor number and higher electron acceptor number than acetone. The acceptor number (AN) and donor number (DN) were defined by Gutmann et al.<sup>125</sup>. The acceptor and donor number empirically measure the electrophilic and nucleophilic properties of solvents. The acceptor numbers are derived from a change in  $^{31}\text{P}$  nmr chemical shift of  $\text{Et}_3\text{OP}$  dissolved in the solvent relative to  $(\text{C}_6\text{H}_5)_2\text{POCl}$  as a reference. The donor numbers were defined from a negative  $\Delta\text{H}$  value of the Equation (16)



where EPD corresponds to the electron pair donor solvent.

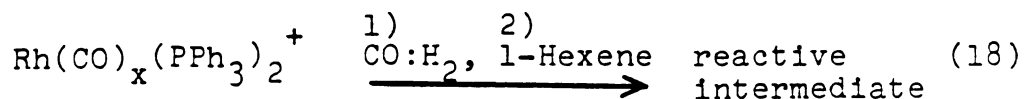
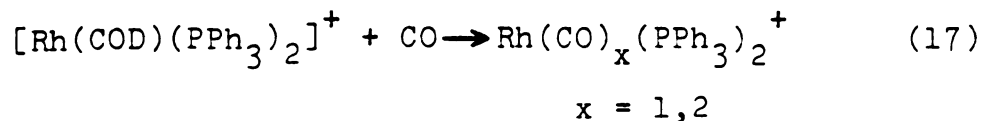
Since DMF has a higher DN and should accept a proton more readily than acetone, it is the more favorable solvent, for formation of a monohydride from the dihydride, which is known to be an active species for hydroformylation reaction.

In the present work, additional studies were done with  $\text{Rh}(\text{diene})(\text{PPh}_3)_2^+$  as the catalyst precursor for hydroformylation reaction of 1-hexene. When  $[\text{Rh}(\text{COD})(\text{PPh}_3)_2]\text{-B}(\text{C}_6\text{H}_5)_4$  was used for hydroformylation reaction, its activity was two times faster than  $[\text{Rh}(\text{COD})(\text{PPh}_3)_2]\text{PF}_6$  as a catalyst precursor. After 48 hr 50% of the 1-hexene was converted to the aldehyde with  $n/b = 2.6$ . No substrate isomerization or hydrogenation was detected. Also, as mentioned before, according to the Equation (12), there is an equilibrium between the dihydride rhodium complex  $\text{H}_2\text{Rh}(\text{CO})_x(\text{PPh}_3)_2^+$ , and the monohydride rhodium complex  $\text{HRh}(\text{CO})_x(\text{PPh}_3)_2$  and either  $\text{HPF}_6$  or  $\text{HB}(\text{C}_6\text{H}_5)_4$ . Since  $\text{HPF}_6$  is a stronger acid than  $\text{HB}(\text{C}_6\text{H}_5)_4$ , solution of  $[\text{Rh}(\text{COD})(\text{PPh}_3)_2]\text{PF}_6$  is more acidic than  $[\text{Rh}(\text{COD})(\text{PPh}_3)_2]\text{B}(\text{C}_6\text{H}_5)_4$ , although the  $\text{B}(\text{C}_6\text{H}_5)_4^-$  salt is initially a more active catalyst than the  $\text{PF}_6^-$  salt, the former salt loses its activity faster than the last named salt. Osborn *et al.*<sup>117</sup> have also reported that anionic groups like  $\text{B}(\text{C}_6\text{H}_5)_4^-$  can readily coordinate with a catalytically active metal center through  $\pi$ -arene bonding. In the present work it was found that trace amounts of oxygen easily converted triphenylphosphine to phosphine oxide and the complex developed

a red color.  $^{31}\text{P}$  nmr spectra of this red solution was only a singlet at -24.9 ppm which can be assigned to triphenylphosphine oxide. The solution was concentrated under vacuum, and crystals were obtained by the addition of the brown solid exhibited a broad peak IR band in the region 1980-1960  $\text{cm}^{-1}$  due to  $\text{C}\equiv\text{O}$  stretching. Other bands were assigned as follows: 1480 and 1440  $\text{cm}^{-1}$  in plane deformation of the phenyl ring of  $\text{B}(\text{C}_6\text{H}_5)_4^-$  anion; broad band at 1070  $\text{cm}^{-1}$ ; tetraphenyl borate anion; 740  $\text{cm}^{-1}$ , 710  $\text{cm}^{-1}$  and 690  $\text{cm}^{-1}$ , C-H out of plane deformations of phenyl rings. It is suggested that the  $\pi$ -bond of the phenyl group of  $(\text{B}(\text{C}_6\text{H}_5)_4^-)$  coordinates to rhodium and converts it to an inactive species.

D. Further Characterization of Homogeneous  $\text{Rh}(\text{COD})(\text{PPh}_3)_2^+$  Catalyst Precursor

A phosphorus-31 NMR study was undertaken in an effort to better understand the nature of homogeneous  $\text{Rh}(\text{COD})(\text{PPh}_3)_2^+$  during the hydroformylation reaction. The results suggest the following scheme:



The proton decoupled  $^{31}\text{P}$  resonance spectra of  $\text{Rh}(\text{COD})-(\text{PPh}_3)_2^+$  consists of a doublet at  $-26.9$  ppm ( $J_{\text{P-Rh}} = 146.5$  Hz) (Figure 11a). The  $^{31}\text{P}$  NMR spectrum of complex  $\text{Rh}(\text{CO})_x-(\text{PPh}_3)_2$  which was formed by addition of CO to the  $\text{Rh}(\text{COD})-(\text{PPh}_3)_2^+$  in acetone, shows a singlet at  $-31.6$  ppm at  $-30^\circ\text{C}$  (Figure 11b), the complex gave a doublet at  $-32$  ppm ( $J_{\text{P-Rh}} = 75.7$  Hz) (Figure 11c). These results indicate that a fast exchange occurs between two phosphine groups at room temperature. The  $^{31}\text{P}$  NMR spectrum of reactive intermediate (Equation 18) formed by addition of  $\text{CO}:\text{H}_2$  (1:1) and 1-hexene to the solution contains  $\text{Rh}(\text{CO})_x(\text{PPh}_3)_2$  consists of a doublet at  $-32.5$  ppm ( $J_{\text{P-Rh}} = 73.2$  Hz) at  $-30^\circ\text{C}$  (Figure 12a). The spectrum of an aged hydroformylation solution (still catalytically active) showed a doublet at  $-31.5$  ppm ( $J_{\text{P-Rh}} = 151.4$  Hz) which was assigned to phosphorus coordinated to the rhodium, and a singlet at  $-24.9$  ppm due to  $\text{OPPh}_3$  (Figure 12b). The hydroformylation solution eventually loses activity, even in the presence of fresh 1-hexene. Catalytically inactive solution was dark red. The  $^{31}\text{P}$  NMR spectrum showed only one singlet at  $-25.0$  ppm (in acetone) due to  $\text{POPh}_3$ . This result shows that no triphenylphosphine was coordinated to rhodium, and as a consequence of this, the catalyst had decomposed. At a ratio of 2.4:1 of  $\text{PPh}_3:\text{Rh}$ , the catalysts did not lose activity and, also, no red solution was formed. As a result, it can be concluded that: 1) the exchange of COD with CO is fast (5 min), 2) in case of  $\text{Rh}(\text{CO})_x(\text{PPh}_3)_2^+$

Figure 11.  $^{31}\text{P}$  NMR spectra of (A)  $[\text{Rh}(\text{COD})(\text{PPh}_3)_2]^+\text{PF}_6^-$  0.01M in acetone at 25°C; (B)  $[\text{Rh}(\text{COD})(\text{PPh}_3)_2]^+$  + CO, 0.01 M in acetone at 25°C, (C) at -30°C number of accumulated scans = 10000.

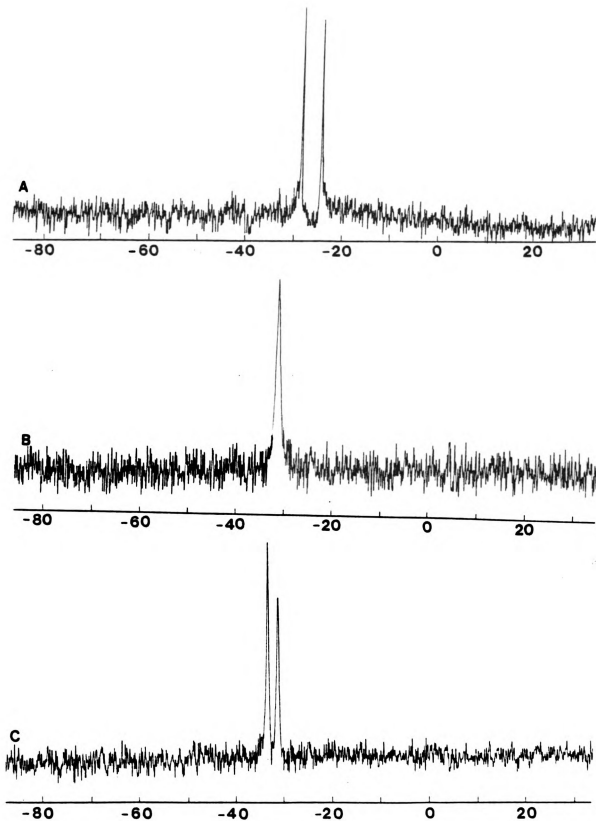
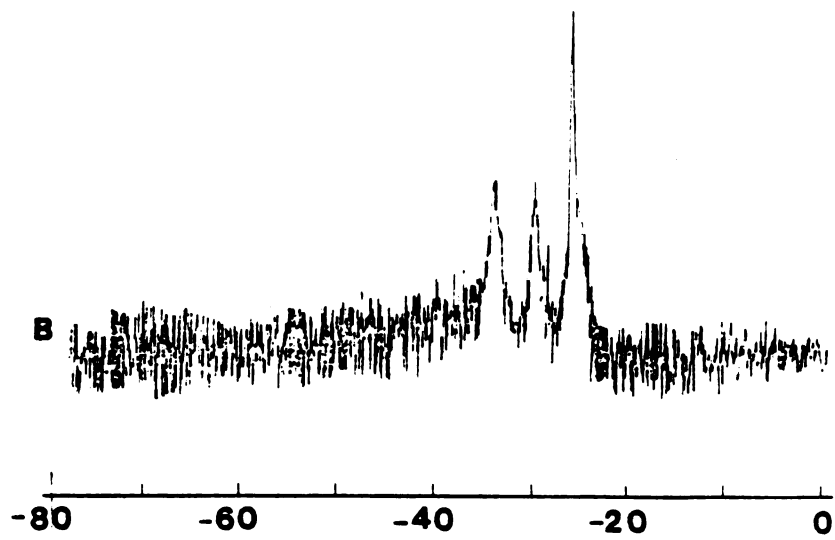
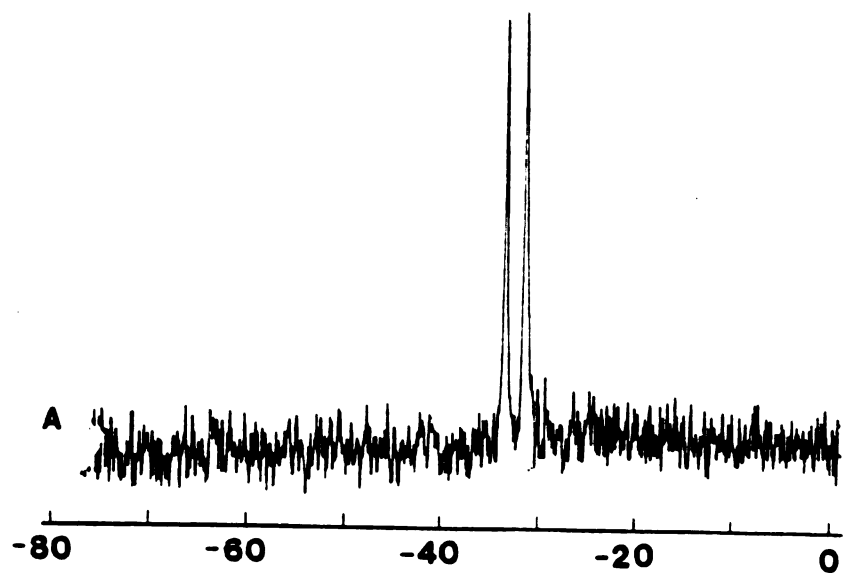


Figure 12.  $^{31}\text{P}$  NMR spectra of  $[\text{Rh}(\text{COD})(\text{PPh}_3)_2]\text{PF}_6 + \text{CO-H}_2$ , 0.01M in acetone under hydroformylation condition at  $-30^\circ\text{C}$  (A) after 2 hr; (B) after 16 hr.



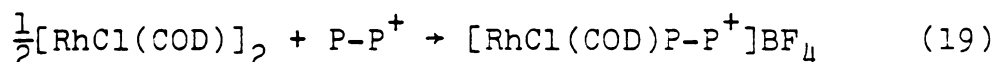
there is a fast exchange between two phosphine groups, 3) as long as two or more triphenylphosphines are coordinated to rhodium, the catalyst is active for hydroformylation reaction, 4) the catalyst is very sensitive to trace amounts of oxygen which depress catalyst activity.

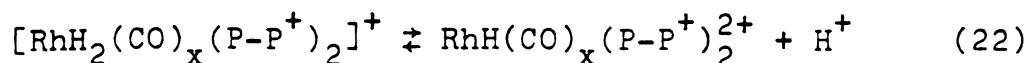
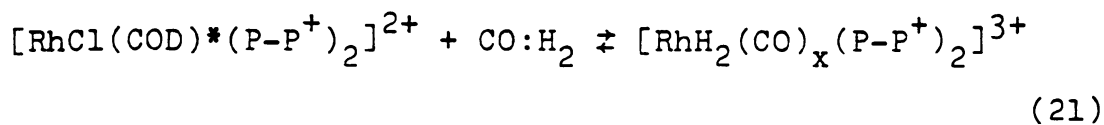
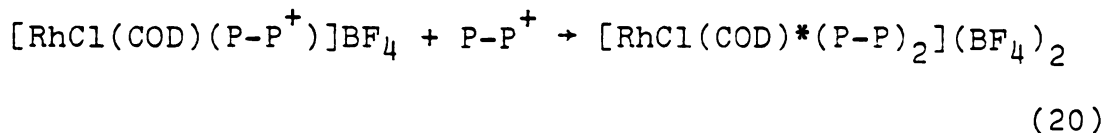
#### E. Utilization of P-P<sup>+</sup> A Cationic Phosphine Ligand

At this point it was felt that the problem of rhodium desorption from the intercalation catalyst could be circumvented by replacing the neutral ligand (PPh<sub>3</sub>) in a known hydroformylation system, RhCl(COD)PPh<sub>3</sub>, with the positively charged ligand such as Ph<sub>2</sub>PCH<sub>2</sub>CH<sub>2</sub>P<sup>+</sup>Ph(CH<sub>2</sub>Ph), abbreviated P-P<sup>+</sup>. A similar approach has been used to prepare layered silicate catalysts for olefin hydrogenation.<sup>78</sup> For this purpose the reactions of rhodium complexes such as [Rh-(diene)Cl]<sub>2</sub>, Rh(diene)<sup>+</sup>, [Rh(CO)Cl]<sub>2</sub> with (P-P<sup>+</sup>) were investigated.

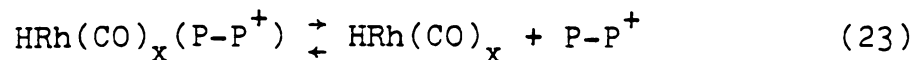
##### 1. [RhCl(COD)]<sub>2</sub> + P-P<sup>+</sup> Precursor Catalyst System

a. Homogeneous - The first system studied is based on RhCl(COD)P-P<sup>+</sup> as the catalyst precursor. A proposed scheme for formation of catalytically active intermediate [RhH<sub>2</sub>(CO)<sub>x</sub>(P-P<sup>+</sup>)<sub>2</sub>]<sup>2+</sup> is described by Equations (19-21).





where COD\* is monodentate COD. Although  $[\text{RhCl}(\text{COD})(\text{P-P}^+)]\text{-BF}_4$  was found not to be active for 1-hexene hydroformylation at 25°C and 1 atm pressure, it showed activity at 100°C and 600 psi. Table 19 lists the results of this catalyst precursor in acetone, dichloromethane and benzene.  $\text{RhCl}(\text{COD})\text{P-P}^+$  is an active hydroformylation catalyst, but it gives low normal to branched aldehyde product ratio ( $n/b \leq 0.6$ ). The low n/b aldehyde ratio may be the result of an equilibrium between  $\text{RhH}(\text{CO})_x(\text{P-P}^+)$  and  $\text{RhH}(\text{CO})_x$ :



$\text{HRh}(\text{CO})_x$  is known to give low n/b aldehyde ratio and significant isomerization under hydroformylation conditions.

At this stage it was thought that increasing the  $\text{P-P}^+ = \text{Rh}$  ratio (from 1:1 to 2:1 or more) might provide higher n/b aldehyde ratios.

Table 20 lists the results for homogeneous

Table 19. Homogeneous Hydroformylation of 1-Hexene with RhCl(COD)P-P<sup>+</sup>BF<sub>4</sub> as Catalyst Precursor.<sup>a</sup>

Run	Solvent	Reaction Time (hr)	% Conv.	Product Distribution %				n/b
				n-heptanal	2-Methyl-hexanal	2-Ethyl-pentanal	2-hexene	
14	Acetone	3	100	30	32	16	22 <sup>b</sup>	0.625
15	CH <sub>2</sub> Cl <sub>2</sub>	3	100	30	40	18	7	0.52
16	C <sub>6</sub> H <sub>6</sub>	3	100	31	44	20	5	0.48

<sup>a</sup>[1-Hexene] = 0.4M; CO = H<sub>2</sub> = 1:1; Total Pressure = 600 psi; Reaction Temperature = 100°C. 1-Hexene:Rh = 200/1.

<sup>b</sup>Trans:cis = 3:1.

Table 20. Homogeneous Hydroformylation of 1-Hexene with ClRh(COD)P-P<sup>+</sup> as Catalyst Precursor.<sup>a</sup>

Run	P-P <sup>+</sup> Rh	RXN Time (h)	% Conv.	Product Distribution				
				n-Heptanal	2-Methyl- hexanal	2-Ethyl- pentanal	2-hexene n/b	
17	2	3	100	45	26	4	25	1.5
18	4	4	97	55	22	--	23	2.5
19	10	4	76	61	18	--	21	3.4

<sup>a</sup>[1-hexene] = 0.4M in acetone; 100°C; 600 psi; CO/H<sub>2</sub> = 1:1, 1-hexene/Rh = 200/1.

hydroformylation of 1-hexene with  $\text{RhCl}(\text{COD})\text{P}-\text{P}^+\text{BF}_4$  as the catalyst precursor with ratios of  $\text{P}-\text{P}^+$  to Rh equal to 2:1, 4:1, and 10:1. No activity was observed at room temperature and 1 atm pressure. The lack of activity at 25°C may be due to the lack of Rh-Cl bond cleavage and formation of a Rh-H bond. However, the catalyst was active at 100°C and 600 psi. The results in Table 20 show that increasing the ligand to rhodium ratio, effects the following:

- 1) aldehyde selectivity (n/b) is increased;
- 2) The rate of reaction is decreased;
- 3) The isomerization of (1-hexene to 2-hexene) is decreased.

These results agree with those obtained when  $\text{trans-RhCl}(\text{CO})(\text{PPh}_3)_2$  is the catalyst precursor for hydroformylation reaction. In 1968, Wilkinson et al.<sup>121a</sup> reported that when  $\text{trans-RhX}(\text{CO})(\text{PPh}_3)_2$ , X = halogene, was used as catalyst precursor, the active species formed by hydrogenolysis is  $\text{RhH}(\text{CO})(\text{PPh}_3)_2$  or  $\text{RhH}(\text{CO})_2(\text{PPh}_3)_2$ . These species were also formed when the stable complex  $\text{RhH}(\text{CO})(\text{PPh}_3)_3$  was used as the catalyst precursor. On the basis of these investigations and comparisons with related systems, two consistent mechanisms were proposed;<sup>121</sup> Dissociative (I) and Associative (II) pathways for the catalytic reaction. These differ in the mode of attack of the alkene on the catalyst. The overall hydroformylation mechanisms proposed by Wilkinson are shown in Figure 13.

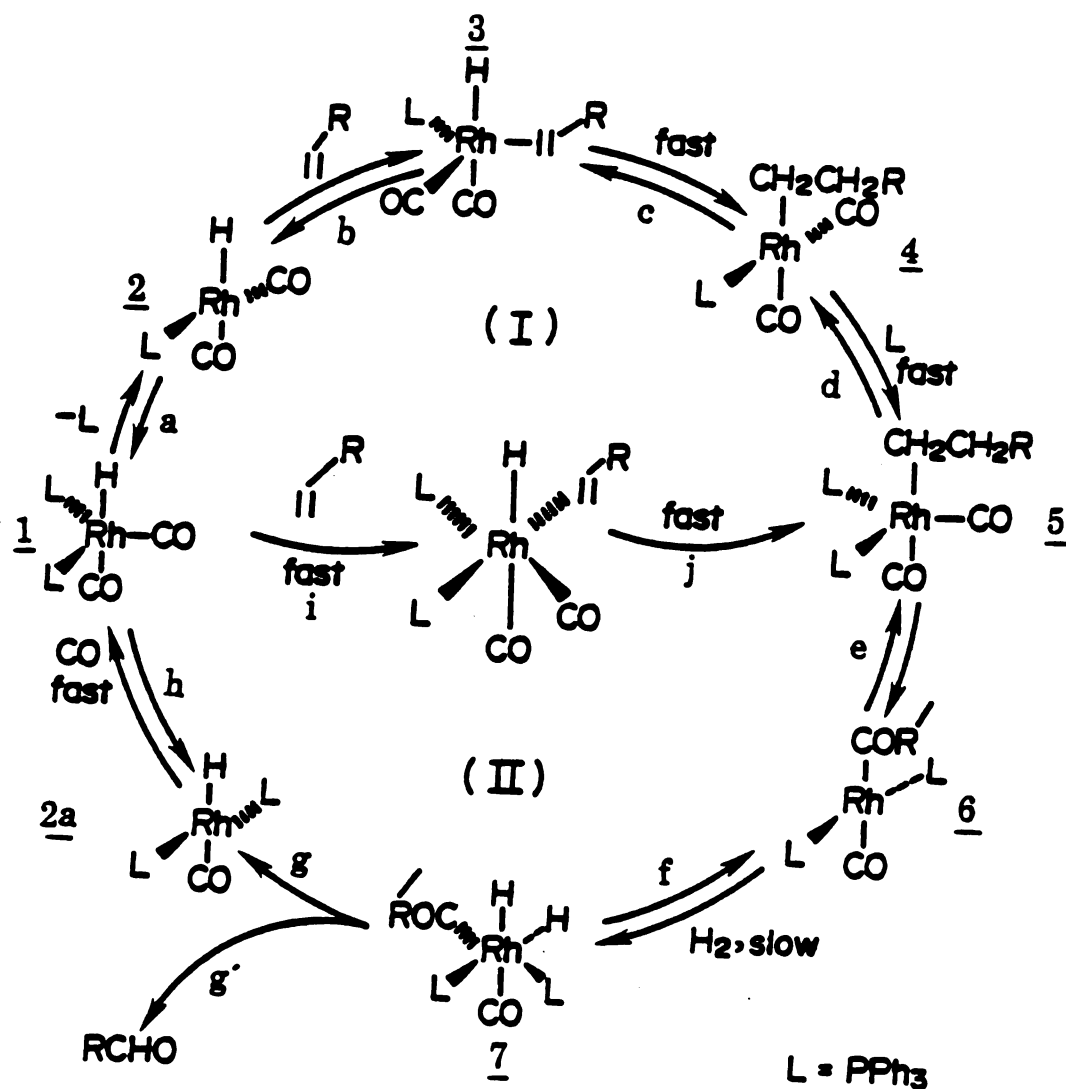


Figure 13. Dissociative (I) and Associative (II) mechanism of hydroformylation reactions (according to G. Wilkinson, et al. 1968).

In the "dissociative" pathway the complex  $\overset{1}{\underset{\sim}{\text{Pt}}}$  loses one phosphine, (path I<sub>a</sub>) and affords the unsaturated hydride  $\overset{2}{\underset{\sim}{\text{Pt}}}$  which coordinates to an olefin forming  $\overset{3}{\underset{\sim}{\text{Pt}}}$  (path b). Insertion (path c) affords the unsaturated alkyl,  $\overset{4}{\underset{\sim}{\text{Pt}}}$ , which adds a phosphine to form the saturated alkyl,  $\overset{5}{\underset{\sim}{\text{Pt}}}$ , (path d). Wilkinson speculates that in step 5 the opposite mode of addition may be favored. Carbonyl migratory insertion (path e) affords the unsaturated acyl,  $\overset{6}{\underset{\sim}{\text{Pt}}}$ . Oxidative addition of hydrogen to the unsaturated acyl,  $\overset{7}{\underset{\sim}{\text{Pt}}}$  (path f), is proposed to be the rate determining step. This is plausible in the sense that the overall reaction rate is first order in [H<sub>2</sub>]. Such an oxidative-addition should be accelerated by phosphine ligands. However, the available evidence does not rule out a binuclear elimination as the product-forming step (g, h). The final step in Wilkinson's proposed mechanism is a fast, irreversible, intramolecular, reductive-elimination of,  $\overset{7}{\underset{\sim}{\text{Pt}}}$  (path g) affording,  $\overset{2}{\underset{\sim}{\text{Pt}}}$  which acquires CO regenerating  $\overset{1}{\underset{\sim}{\text{Pt}}}$  (path h) and thus completing the catalytic cycle. Note also the unusual cis orientation of phosphines, which Wilkinson postulates for this cycle. Wilkinson also proposed a questionable associative mechanism (Figure 13, path II), path i, which involves an unprecedented 20-electron intermediate,  $\overset{9}{\underset{\sim}{\text{Pt}}}$ . The remaining steps (J, . . .) are the same as those in the dissociative-reaction cycle.

Therefore, on the basis of the results which were obtained by positively charged ligands (Table 20) and those

reported for rhodium  $-PPh_3$  complexes, it can be mentioned that by increasing the concentration of free ligand, the associative pathway is favored over the dissociative pathway and more product selectivity is observed.

Wilkinson also reported in the reversible addition of  $L_n M-H$  to alkene to give an alkyl complex, there are two main factors which are not independent.<sup>121</sup> The direction of addition may be Markownikov or anti-Markownikov. Only Markownikov-addition leads to isomerization. The direction of addition will depend on the polarity of the M-H bond and steric effects in the presence on the metal of ligands of high  $\pi$ -acidity, such as carbon monoxide will increase the polarity of the M-H bond in the direction  $M^{\delta-}-H^{\delta+}$ . This will increase the extent of Markownikov addition. The presence of weaker  $\pi$ -acid ligands will have the opposite effect. The presence of bulky ligands such as  $R_3P$  can generate substantial steric inhibition to the formation of the metal alkyl, especially where R is aryl. The steric interaction will be at a maximum when such groups are trans to each other and mutually cis to the hydride group or the alkyl formed from it as in (Figure 13, 2a). When  $R_3P$  groups are cis as in (Figure 13, 1), the steric inhibition to alkyl formation will be minimized though probably not negligible. An increase in  $L^+/Rh$  ratio will form the associative pathway and more steric  $\pi$  inhibition. Therefore, more product selectivity is observed and the

rate of hydroformylation reaction is decreased, because the associative pathway is slower than the dissociative pathway. Also, isomerization of 1-hexene to 2-hexene is decreased because steric inhibition is increased.

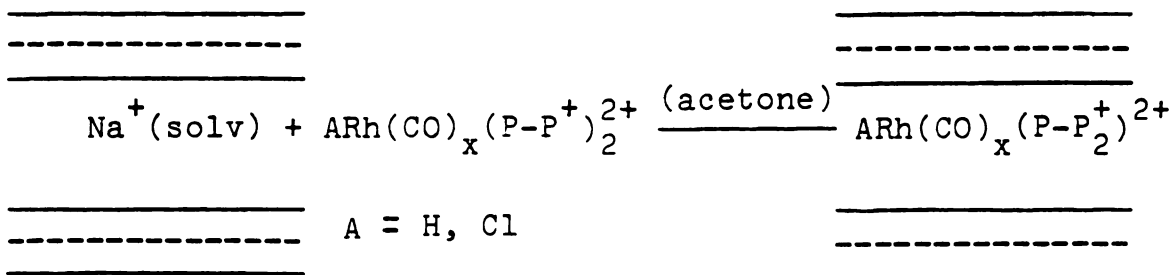
In conclusion, it can be mentioned that electronic and steric factors both have effect on selectivity. In the case of bulky ligands such as  $R_3P$ , steric factor is probably more important than electronic factors, but in some cases the electronic factor can play an important role on selectivity. For example, when  $RhClCO(PPh_2NR_1R_2)^{126}$  is used as a catalyst precursor for hydroformylation of 1-hexene, the selectivity is dependent on the nature of  $R_1$  and  $R_2$ . In fact, the highest aldehyde selectivities are obtained with electron withdrawing aminophosphine ( $\phi_2P-N \begin{array}{|c|} \hline \square \\ \hline \end{array}$ ) and the lowest aldehyde selectivities are observed with  $\phi_2P-NMe_2$ .

On the basis of these investigations and those we obtained, it can be mentioned that by increasing the concentration of bulky ligands in solution, aldehyde selectivities can be increased. Also by changing the nature of substituents on the ligands, it is possible to change the selectivities.

## 2. Hydroformylation of 1-hexene with Intercalated Catalysts

The active species for hydroformylation was generated by the addition of  $CO:H_2$  (1:1) to a solution of

RhCl(COD)P-P<sup>+</sup>+P-P<sup>+</sup> at 600 psi and 100°C. Then it was intercalated as follows:



(24)

Table 21 lists the results which were obtained by the homogeneous and heterogeneous systems. By comparing runs 20, 21, it can be seen that the product distribution of the heterogeneous system is different from the homogeneous system. Although the rate of hydroformylation with the supported system is lower than the homogeneous system, the ratio of normal to branched aldehyde is increased. In runs 22 and 23 in which the ratio of P-P<sup>+</sup>:Rh is 4:1, isomerization of 1-hexene to 2-hexene (cis + trans) is significantly decreased and selectivity is increased. In the supported catalyst system, the production of linear aldehyde is increased considerably in comparison to the homogeneous hydroformylation.

Previous studies on homogeneous hydroformylation of olefins indicated that there are several pathways for olefin insertion into the metal hydride bond. Figure 14

Table 21. Homogeneous and Heterogeneous Hydroformylation of 1-Hexene with ClRh(COD)-P-P.<sup>a</sup>

Run	Catalyst	RXN Time (h)	% Conv.	Product Distribution					Other n/b
				n-Heptanal	2-Methyl-Hexanal	2-Ethyl-Pentanal	2-Hexene		
20	ClRh(COD)P-P <sup>+</sup> 1 P-P <sup>+</sup> (Homogeneous) <sup>b</sup>	3	100	45	26	4	25	--	1.5
21	Intercalated <sup>c</sup>	12	80	53	22	--	25	--	2.4
22	ClRh(COD)P-P <sup>+</sup> 3 P-P <sup>+</sup> (Homogeneous) <sup>b</sup>	4	97	56	22	--	22	--	2.5
23	Intercalated <sup>c</sup>	18	87	63	23	--	8	6	2.8

<sup>a</sup>[1-hexene] = 0.4M in acetone; 100°C; 600 psi; CO/H<sub>2</sub> = 1:1.

<sup>b</sup>1-Hexene:Rh = 200:1.

<sup>c</sup>1-Hexene:Rh ≥ 570:1.



shows the mechanism of hydroformylation with possible isomerization with  $(HM(CO)_m = H_m)$ . Three isomeric aldehydes can arise from a metal carbonyl hydride complex. Further studies showed that the coordination of two or more bulky ligands to the central atom would lead to the formation of aldehyde (15,16). By increasing the concentration of ligand ( $PR_3$ ) in solution the selectivity of linear aldehyde was increased. It can be concluded that more bulky groups in rhodium carbonyl complex would favor intermediate 5. This in turn leads to the formation of linear aldehyde as a major hydroformylation product. By comparing the supported catalyst with homogeneous system, a similar explanation can be proposed as follows:

Two intermediates 3 and 9 in Figure 15 would lead to the formation of branched and linear aldehyde respectively. The methyl group in intermediate 3 has interacted sterically with both the  $P-P^+$  ligands and the silicate layers. On the other hand the latter interaction should be reduced in intermediate 9. Thus intermediate 9 should be favored in the intercalated state and should favor formation of linear aldehyde.

Also it was observed that in the supported catalyst systems the substrate isomerization was decreased, and the rate of hydroformylation was lower than the homogeneous system.

Previously reported investigations of homogeneous hydroformylation have indicated that in the case of olefins

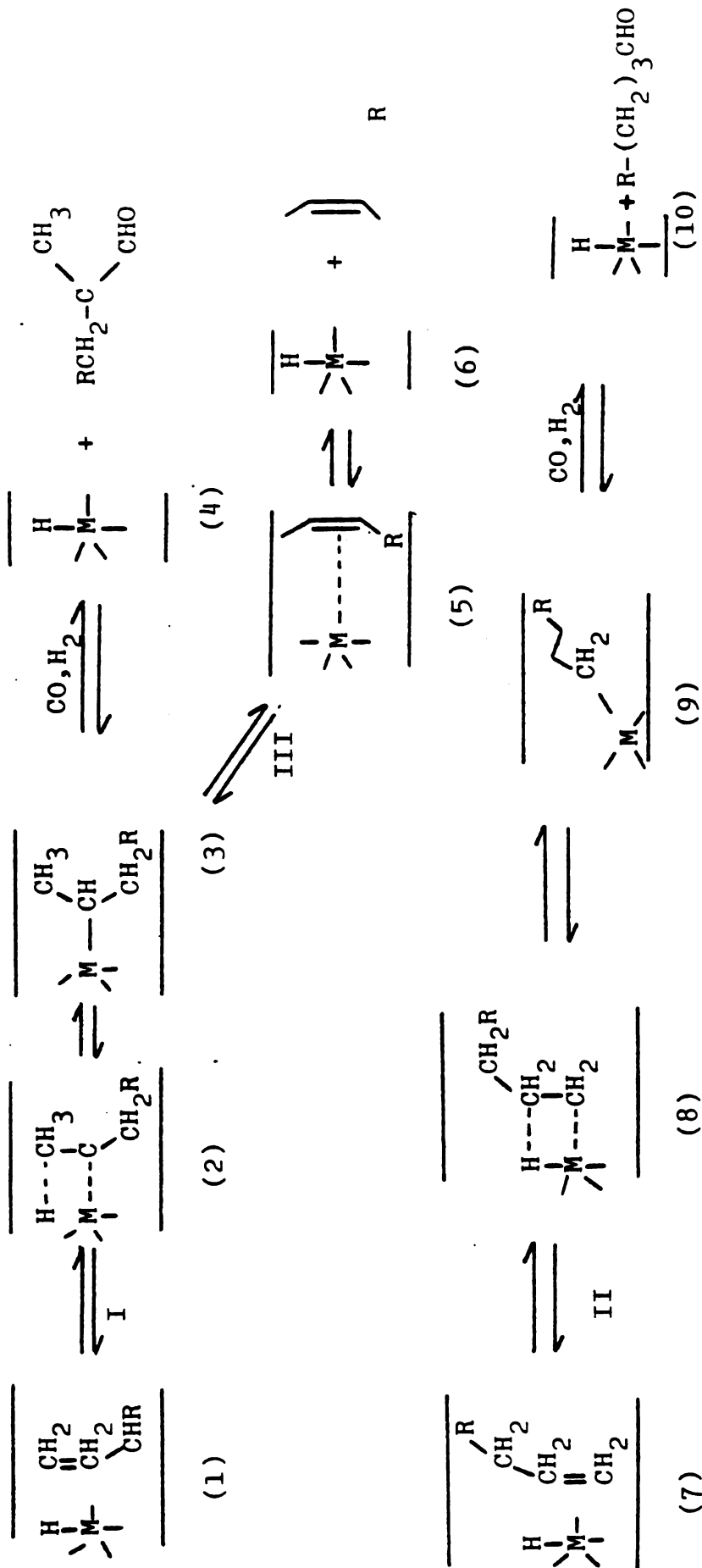


Figure 15. Possible pathways for hydroformylation and isomerization of 1-hexene between the silicate sheets.

higher than propylene in chain length, double bond shifts can occur.<sup>84f</sup> Isomerization in cobalt catalyzed hydroformylation reaction is enhanced by low carbon monoxide partial pressures (50 atm) and higher reaction temperatures (150-190°C).<sup>127</sup> Complete isomerization of 1-dodecene was observed by Asinger and Berg under hydroformylation conditions at 150-200°C.<sup>128</sup>

In contrast, when organophosphines or organoarsines are added to rhodium catalyst systems, isomerization can be completely suppressed so that the products obtained corresponds directly to the olefin charged. Asinger, Fell, and Rupilius<sup>129</sup> demonstrated the complete inhibition of isomerization using octene-1 and octene-4 and a  $\text{Bu}_3\text{P}$  complex of rhodium in the presence of excess  $\text{Bu}_3\text{P}$ . They obtained substantially the same results when they used tricyclohexylphosphine as a ligand. The phenomenon of nearly complete retardation of double bond migration was also observed under nonhydroformylating conditions using octene-1 and  $\text{HRh}(\text{CO})(\text{PBu})_3$  in the presence of excess  $\text{Bu}_3\text{P}$ . Under the same conditions, a phosphine free system yielded an equilibrium distribution of isomers. Similarly, Evans, Osborn and Wilkinson<sup>121a</sup> observed the inhibition of isomerization of 1-pentene by using  $\text{HRh}(\text{CO})(\text{PPh}_3)_3$  in the presence of excess  $\text{Ph}_3\text{P}$ . In addition, they found that H-atom exchange was much more rapid than isomerization using  $\text{DRhCO}(\text{PPh}_3)_2$  and 1-pentene, but that exchange was completely eliminated

in the presence of excess  $\text{PPh}_3$ . Apparently, the formation of a five-coordinate tris-triphenylphosphine complex prevents coordination of the olefin to the metal and therefore only subsequent isomerization.

According to this evidence and the possible pathways (Figure 14) for isomerization of olefins under hydroformylation conditions, it can be proposed that the isomerization pathways are also available under intercalation conditions, (Figure 15, pathway III).

As explained before, the intermediate 8 leads to linear aldehyde while the intermediate 2 would result in both branched aldehyde and isomerization of 1-hexene to 2-hexene. In fact the presence of a methyl group in intermediate 3 and its steric interaction with the other ligands and silicate layers should cause this intermediate to be less favored intermediate 3. Therefore the hydroformylation reaction gives linear aldehyde as a major product, in all intercalated catalyst system. By increasing the concentration of bulky positively charged ligands between the layers the amount of isomerized olefin is significantly decreased.

### 3. Solvent Effects

To investigate the effects of solvents, the active species which was generated from  $\text{RhCl}(\text{COD})\text{P-P}^+ + \text{1P-P}^+$  and  $\text{CO:H}_2$  at 600 psi and  $100^\circ\text{C}$  was utilized for hydroformylation in DMF and in benzene. Table 22 lists the results

Table 22. Homogeneous and Heterogeneous Hydroformylation of 1-Hexene with ClRh(COD)-P-P<sup>+</sup> as Catalyst Precursor in DMF, and C<sub>6</sub>H<sub>6</sub>.<sup>a</sup>

Run	Catalyst Precursor	RXN Time (h)	% Conv.	Product Distribution %				Other n/b Solv.
				n-Heptanal	2-Methyl-Hexanal	2-Hexene		
24	ClRh(COD)P-P <sup>+</sup> 1 P-P <sup>+</sup> (Homogeneous) <sup>b</sup>	2	100	52	22	9	10	1.75 DMF
25	Intercalated <sup>c</sup>	24	92	42	45	2	11	0.9 DMF*
26	ClRh(COD)P-P <sup>+</sup> 1 P-P <sup>+</sup> Homogeneous <sup>b</sup>	2	70	29	14	57	--	2 C <sub>6</sub> H <sub>6</sub>
27	Intercalated <sup>c</sup>	18	No significant reaction					C <sub>6</sub> H <sub>6</sub>

<sup>a</sup>[1-Hexene] = 0.4M in acetone; 100°C; 600 psi; CO/H<sub>2</sub> = 1:1.

<sup>b</sup>1-Hexene:Rh = 570:1.

<sup>c</sup>1-Hexene:Rh ≥ 570:1.

\* In this case significant desorption has been seen.

of these experiments.

The results of Table 22 show that the activity of the catalyst and the product distribution depends on solvent. Homogeneous hydroformylation in DMF is faster than in benzene, because the solvation of the positively charged catalysts in polar solvent (DMF) is better than in nonpolar solvent (benzene) runs (24,26). In the supported catalyst system the aldehyde selectivity and the rate of reaction depends on two factors:

- 1) The extent of swelling of the interlayer.
- 2) The polarity of solvent.

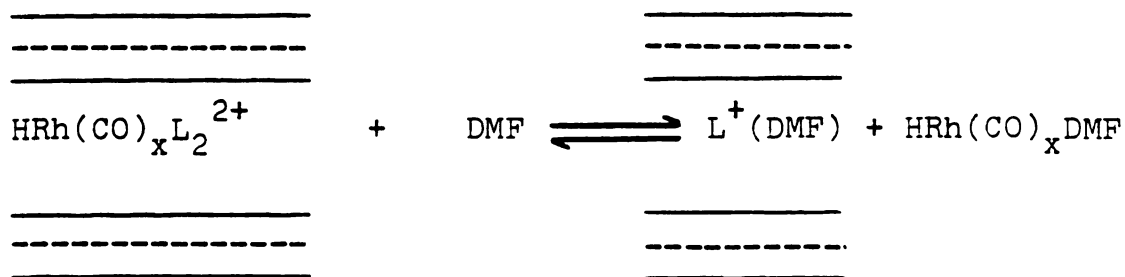
In the supported catalyst system when DMF was used as the solvent (run 25) a low n/b ratio is observed. Also, significant desorption occurs during the hydroformylation reaction. In benzene no significant reaction ( 5%), (run 27) is observed. In acetone (Table 21, run 21) the n/b ratio is higher than in DMF and no desorption occurs.

Table 23 lists the 001 basal spacings of  $\text{Na}^+$ -hectorite partially exchanged with the positively charged rhodium complex. According to this table and previous studies; the interlayer spacing increases as the polarity of the solvent increases. In benzene, which is a nonpolar solvent, no significant swelling is observed. When acetone is used as solvent the interlayer spacing increases from 23.1 to 25.1 Å, which agrees with the existence of solvent between the layers. Based on the difference between the thickness

Table 23. 001 Basal Spacing of  $\text{Na}^+$ -Hectorite After Partial Exchanged with  $\text{RhCl}(\text{COD})\text{P}-\text{P}^+$  +  $\text{P}-\text{P}^+$  Under Hydroformylation Condition.

Condition	001 Basal Spacing ( $\text{\AA}$ )
Dry	18.4
Wet (Acetone)	20.5
Wet (Benzene)	18.4
Wet (DMF)	24.5

of the silicate sheets (9.6 Å) and the observed (001 X-ray reflection (18.4 Å), it can be estimated that the average thickness of the interlayers (8.8 Å) agrees well with the values expected from molecular models for a monolayer of Rh complex with positively charged ligands. In the case of DMF as solvent, the thickness between silicate layers is larger than acetone because of its higher polarity relative to the acetone. The desorption problem with DMF, probably is due to its higher DN numbers relative to the other solvents (Table 18). According to the Equation (25) DMF can be coordinated to the central atom by displacement of some P-P<sup>+</sup>. Finally, the resulting complex was neutral and it was desorbed from the layered silicate and P-P<sup>+</sup> was remained between the silicate sheets. The IR studies of the filtrate solution didn't show any P-P<sup>+</sup> band positions although (C≡O) stretching was observed at the region 2000 cm<sup>-1</sup>. At this stage it can be concluded that DMF and benzene are not good solvents for hydroformylation of 1-hexene with supported positively charged rhodium complex.



(25)

4. Characterization of the Homogeneous Hydroformylation Catalysts Containing P-P<sup>+</sup>

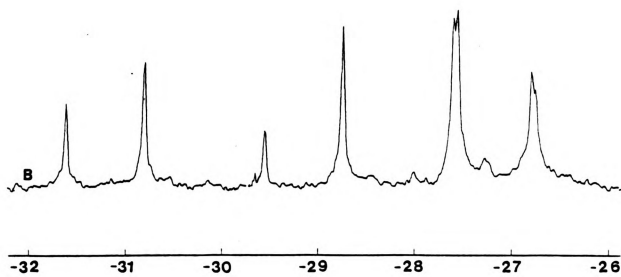
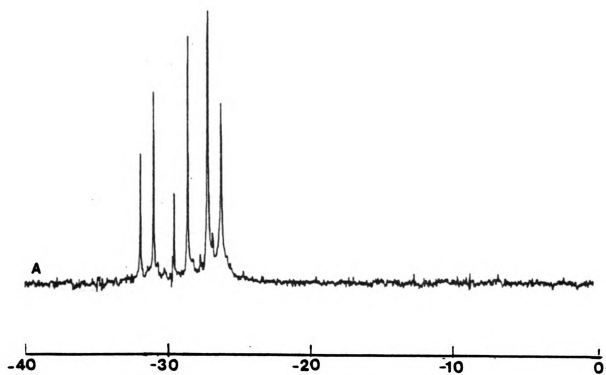
A <sup>31</sup>P NMR study was undertaken in an effort to better understand the nature of the homogeneous hydroformylation catalysts containing P-P<sup>+</sup>, an attempt was made to compare these results with those as obtained for triphenylphosphine rhodium complexes.

It was felt that <sup>31</sup>P NMR studies would allow the characterization of the catalyst precursors and the active species which was exchanged into the Na<sup>+</sup>-hectorite structure. Acetone d<sub>6</sub> was used as the solvent in these studies. As it is described in the literature,<sup>78</sup> P-P<sup>+</sup> cleaves the chloride bridge of [RhCl(COD)]<sub>2</sub> to produce RhCl(COD)(P-P<sup>+</sup>)BF<sub>4</sub> at 1:1 P-P<sup>+</sup>:Rh ratio.



Figure (16a,b) show the <sup>31</sup>P NMR spectrum of RhCl(COD)-P-P<sup>+</sup> at -30°C. The two non-equivalent phosphorus atoms and the rhodium give rise to an ABX pattern. The spectrum was analyzed according to Becker's treatment.<sup>130</sup> At -30° in acetone, δ<sub>p</sub> = -30.1 ppm, δ<sub>p<sup>+</sup></sub> = -27.1 ppm, J<sub>PRh</sub> = 150 Hz, J<sub>P-P<sup>+</sup></sub> = 58.9 Hz, and J<sub>P<sup>+</sup>-Rh</sub> = -5.6 Hz. These results were similar with those reported (lit.,<sup>131</sup> at 28°C, p = -29.5 ppm, δ<sub>p<sup>+</sup></sub> = -27.3 ppm, J<sub>PRh</sub> = 149 Hz, J<sub>P-P<sup>+</sup></sub> = 54 Hz, J<sub>P<sup>+</sup>-Rh</sub> = 7 Hz and at -80°C δ<sub>p</sub> = -31.8 ppm,

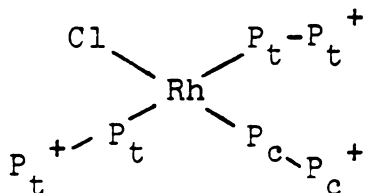
Figure 16.  $^{31}\text{P}$  NMR spectra (A,B) of  $\text{RhCl}(\text{COD})\text{P}-\text{P}^+\text{BF}_4$   
0.01M in acetone ( $d_6$ ) at  $-30^\circ\text{C}$ , number of  
accumulated scans, NS = 10000.



$\delta p^+ = -27.3$  ppm,  $J_{P-Rh} = 153$  Hz,  $J_{P-P^+} = 62$  Hz and  $J_{P^+-Rh} = -6$  Hz in  $CH_2Cl_2$  as solvent).

A solution formed by the addition of another equivalent of  $P-P^+$  to  $RhCl(COD)(P-P^+)$  give the  $^{31}P$  NMR spectrum, shown in Figure 14.

The spectrum consists of a multiplet  $\delta_{P_c} = -42.4$  ppm  $J_{P_c-Rh} = 214.8$  Hz, a doublet at  $\delta p = -27.6$  ppm  $J_{P-P^+} = 34$  Hz and a multiplet ABX pattern between  $-29.9$  to  $-28.8$  ppm ( $\delta p = -29.6$  ppm and  $\delta p^+ = -28.7$  ppm). Based on NMR results the structure formed from 1:1  $RhCl(COD)P-P^+$  :  $P-P^+$  is proposed to be the  $P_c P_c^+$  NMR lines are assigned to the positively charged ligand which is cis to the two trans ligands ( $P_t-P_t^+$ ). Also, no free positively charged ligand ( $P-P^+$ ) was detected by  $^{31}P$  nmr spectra.



Similar behavior has been reported in literature for tri-phenylphosphine:<sup>78</sup>

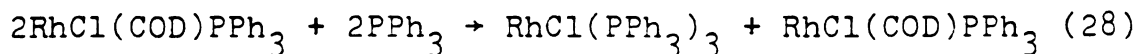
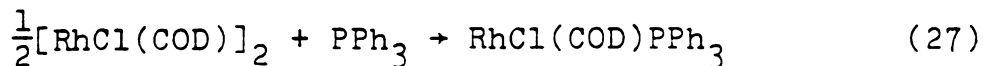
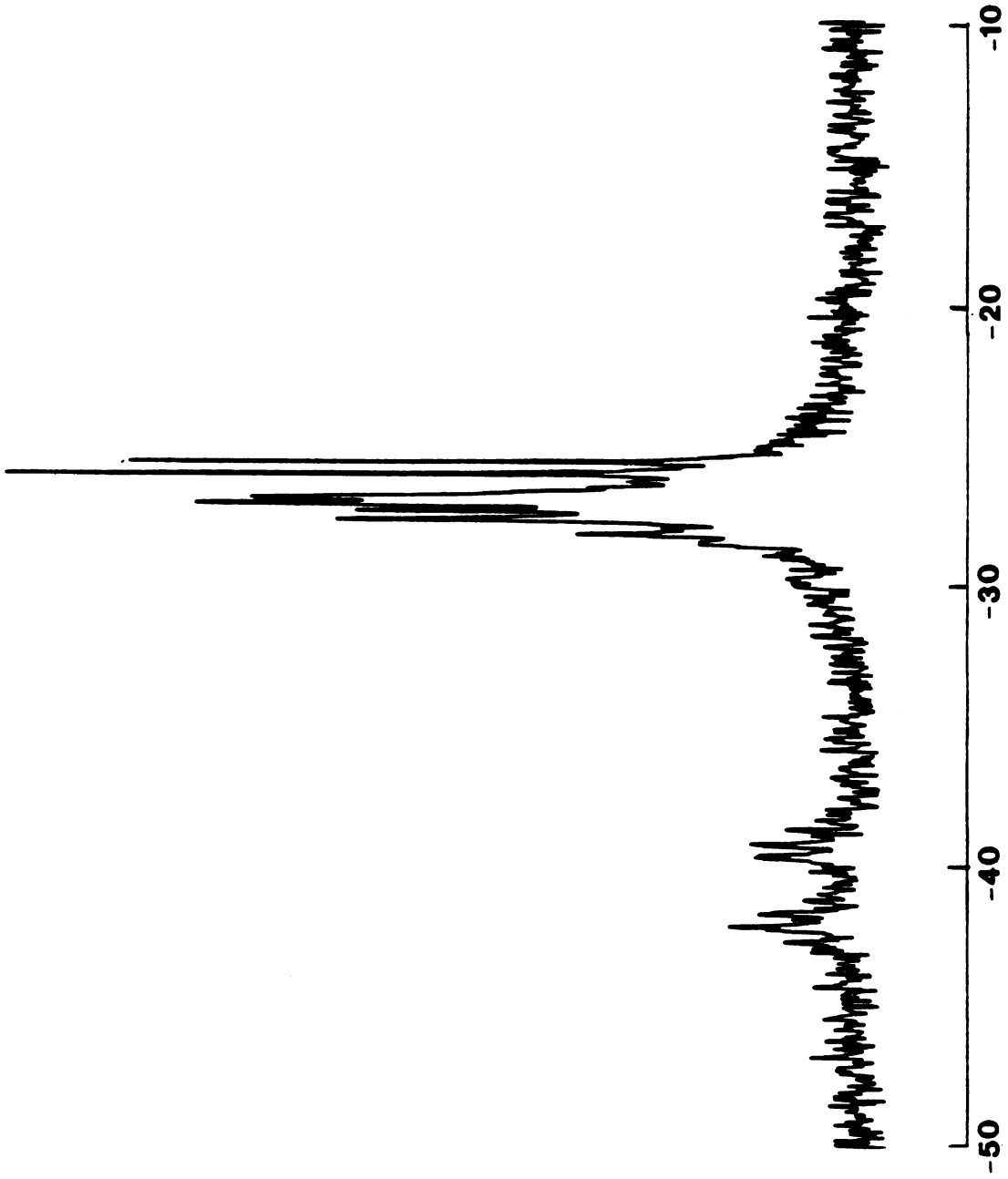
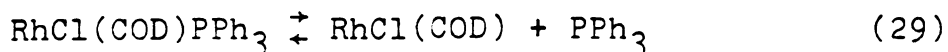


Figure 17.  $^{31}\text{P}$  NMR spectrum of  $\text{RhCl}(\text{COD})\text{P}-\text{P}^+-\text{P}-\text{P}^+$  in  
0.01M solution of acetone ( $\text{d}_6$ ), NS = 10000.



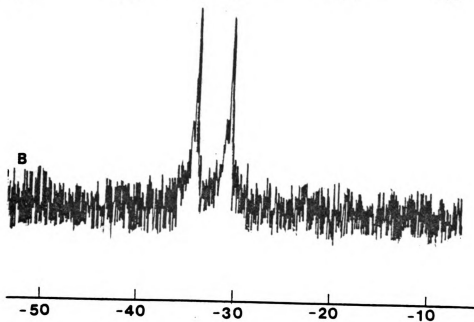
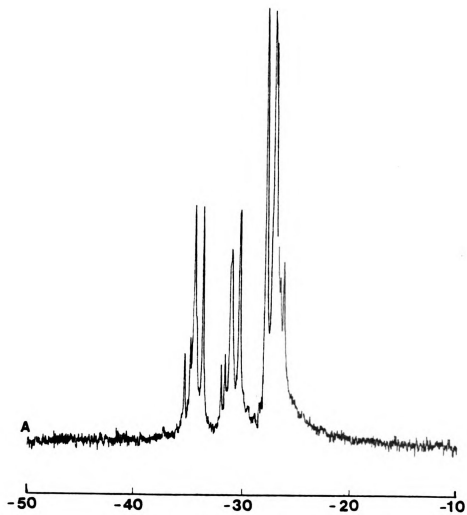


The  $^{31}\text{P}$  NMR spectrum of a  $\text{RhCl}(\text{COD})\text{PPh}_3$  at  $30^\circ\text{C}$  showed a doublet at  $\delta\text{p} = -30.6$  ( $J_{\text{P-Rh}} = 151$  Hz in  $\text{CH}_2\text{Cl}_2$ ). The addition of another mole of triphenylphosphine produced  $\text{RhCl}(\text{PPh}_3)_3$  as a major product. No free triphenylphosphine was detected at  $28^\circ\text{C}$  by  $^{31}\text{P}$  NMR. On the other hand, by lowering the temperature to the  $-80^\circ\text{C}$  some free triphenylphosphine was detected, (lit<sup>78</sup>  $^{31}\text{P}$  NMR.  $\delta\text{p}_\text{c} = -48.9$  ppm,  $\delta\text{p}_\text{t} = -32.2$  ppm,  $J_{\text{P}_\text{c}\text{Rh}} = 192$  Hz,  $J_{\text{P}_\text{c}\text{P}_\text{t}} = 38$  Hz,  $J_{\text{P}_\text{t}\text{Rh}} = 146$  Hz).

A solution of 1:1  $\text{RhCl}(\text{COD})\text{P-P}^+:\text{P-P}^+$  was treated with  $\text{CO:H}_2$  at 600 psi and  $100^\circ\text{C}$ . The final solution was divided into two fractions under nitrogen. The first fraction was used directly for  $^{31}\text{P}$  NMR studies and the second fraction was taken to dryness in vacuum and then it was redissolved in acetone- $\text{d}_6$ . The  $^{31}\text{P}$  NMR spectra of both fraction were the same. Figure 18a shows the  $^{31}\text{P}$  NMR spectrum of mentioned solution. There are two sets of resonances, each containing six lines. Chemical shifts and coupling constants are listed in Table 24.

No free  $(\text{P-P}^+)$  was detected. Therefore, two  $\text{P-P}^+$  ligands are coordinated to rhodium as the central atom. In addition a solution of 1:1  $\text{RhCl}(\text{COD})\text{PPh}_3:\text{PPh}_3$  was treated with  $\text{CO:H}_2$  at 600 psi and  $100^\circ\text{C}$ . The  $^{31}\text{P}$  NMR spectra of that solution shows a doublet at  $\delta\text{p} = -31$  ppm

Figure 13.  $^{31}\text{P}$  NMR spectra of (A)  $\text{RhCl}(\text{COD})\text{P-P}^+$  +  $\text{P-P}^+$  +  $\text{CO-H}_2$  (1:1) 0.01M in acetone ( $\text{d}_6$ ) at  $-30^\circ\text{C}$ . (B)  $\text{RhCl}(\text{COD})\text{PPh}_3$  +  $\text{PPh}_3$  +  $\text{CO/H}_2$  (1:1), 0.01M in benzene at  $25^\circ\text{C}$ . NS = 10000.



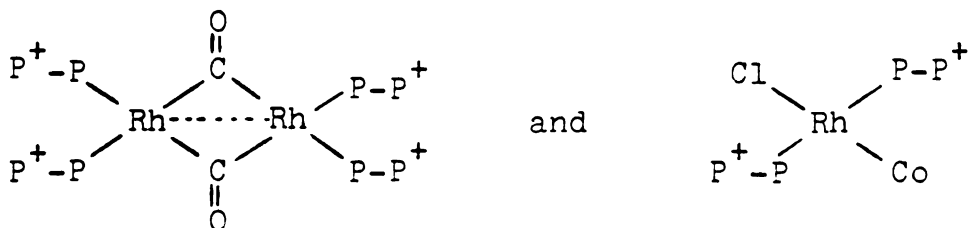
( $J_{P-Rh} = 128$  Hz), and another doublet with lower intensity at  $p = -31.1$  ppm ( $J_{P-Rh} = 128$  Hz) at room temperature in benzene. No free triphenyl was detected in the  $^{31}P$  NMR spectra (Figure 18b). Also, no signal belonging to hydrogen attached to rhodium was detected by NMR studies.

Table 24.  $^{31}P$  NMR Data for 1:1  $RhCl(COD)(P-P^+):P-P^+$  Under Hydroformylation Conditions.

Set	p (ppm)	p <sup>+</sup> (ppm)	$J_{P-Rh}$ (Hz)	$J_{P-P^+}$ (Hz)
1	-31.5	-29.1	124.9	31.2
2	-32	-28.5	124.9	18.7

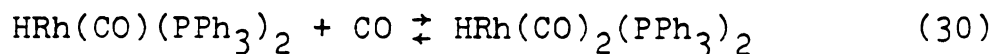
By comparing this spectrum with the one obtained for solution of 1:1  $RhClCODP-P^+:P-P^+ + (CO:H_2)$  in Figure 18a, it can be concluded that the active species which is formed by positively charged ligand, has the same structure and chemical behavior as triphenylphosphine.

On the basis of this evidence, two structures can be proposed under hydroformylation conditions.

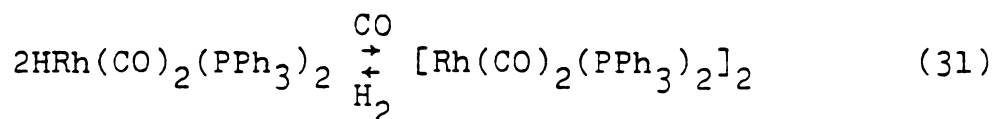


The dimeric structure is analogous to that of  $[\text{Rh}(\text{CO})(\text{PPh}_3)_2]_2$ , which has been proposed by Wilkinson,<sup>87a</sup> to form when  $\text{HRh}(\text{CO})(\text{PPh}_3)_3$  is used as a catalyst precursor for hydroformylation reaction.

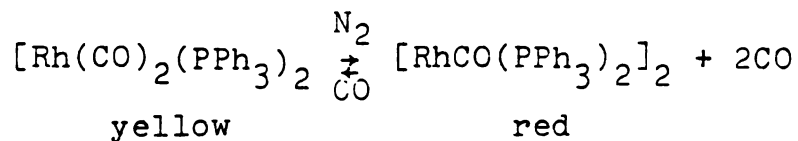
In the presence of carbon monoxide a dicarbonyl complex was formed:



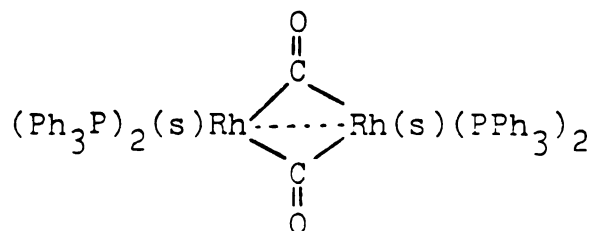
which can then dimerize according to the reaction



Wilkinson also reported that a red dimer is formed by bubbling nitrogen or argon gas through a solution of  $[\text{Rh}(\text{CO})_2(\text{PPh}_3)_2]_2$



In the presence of dichloromethane or ethanol the red dimer can be isolated as  $[\text{Rh}(\text{CO})(\text{PPh}_3)_2\text{S}]_2$



The red dimer exhibit the following IR C≡O stretching.

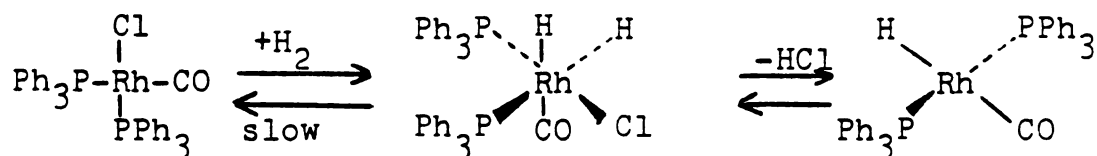
Lit:<sup>87a</sup> IR for  $[\text{Rh}(\text{CO})(\text{PPh}_3)_2, \text{CH}_2\text{Cl}_2]_2$  compound.

In Solid	In Solution
1765 W	1980 S
1739 S	1740 S

The difference in the solid state and solution IR bands was attributed to the presence of only dimeric in the solid state and the presence of both monomeric and dimeric in solution.

The monomeric and dimeric carbonyl dimers are formed from  $\text{HRh}(\text{CO})(\text{PPh}_3)_3$  in the absence of coordinated chlorine.

In 1970 Evans et al.<sup>121a</sup> suggested that rhodium catalyst precursors containing chlorine can form from an active hydride complex by the following reaction sequence:



The  $^{31}\text{P}$  NMR spectrum of  $\text{RhCl}(\text{CO})(\text{PPh}_3)_2$  shows a doublet at  $\delta_{\text{p}} = -29.1$  ppm ( $J_{\text{P-Rh}} = 125$  Hz) in  $\text{CDCl}_3$ . This coupling constant is the same as that obtained for 1:1  $\text{RhCl}(\text{COD})\text{P-P}^+$ :  $\text{P-P}^+ + (\text{CO}+\text{H}_2)$ . However, it was realized that for identification of exact structure of the active species further information was needed.

For this purpose an attempt was made to crystallize the complex from solution. Crystallization was achieved by concentration of an acetone solution of  $\text{RhCl}(\text{CO})\text{P}-\text{P}^+ + \text{P}-\text{P}^+$ , followed by separation of solid from pentane or from a mixture of dichloromethane and ether or  $\text{CHCl}_3$ , (yield 80%). The color of the solid product was yellow. Figure 19a shows the IR spectrum of this species crystallized from pentane. A strong band at  $1975 \text{ cm}^{-1}$  is assigned to a  $\text{C}\equiv\text{O}$  stretching vibration, and the band at  $1700 \text{ cm}^{-1}$  is attributed to the carbonyl stretching vibration of acetone. The bands around  $1600 \text{ cm}^{-1}$  are most likely due to phenyl group skeletal vibrations. Bands around  $1500 \text{ cm}^{-1}$ ,  $1480 \text{ cm}^{-1}$  and  $1440 \text{ cm}^{-1}$  could be assigned to the methyl group scissoring vibrations also might be due to aryl skeletal vibrations. The bands at  $1340-1150 \text{ cm}^{-1}$  are probably due to phenyl group in plane C-H bending vibration. The broad band at  $1120 \text{ cm}^{-1}$  to  $1000 \text{ cm}^{-1}$  is characteristic of tetraphenyl borate anion.<sup>119</sup> In the region  $850$  to  $600 \text{ cm}^{-1}$  the three relatively sharp bands are assigned to phenyl group C-H out of plane bending vibrations. The spectrum confirms the presence of  $\text{P}-\text{P}^+$ , CO and solvent (acetone) which are coordinated to the rhodium as central atom. A sample prepared by crystallization from concentrated solution in pentane gave the following chemical analysis for  $[\text{RhCl}(\text{CO})(\text{P}-\text{P}^+)_2(\text{acetone})_2](\text{BF}_4)_2$

Found: Rh, 6.7%; P, 8.28%; C, 61.4%; H, 5.31%, Cl, 2.5%

Calc.: Rh, 6.9%; P, 8.3%; C, 61.1%; H, 5.38%; Cl, 2.4%.

Figure 19. Infrared spectra of 1:1 mixture of  $\text{RhCl}(\text{COD}) - \text{P}-\text{P}^+:\text{P}-\text{P}^+$  in acetone under hydroformylation condition (A) crystallized in pentane; (B) *re-*crystallized in  $\text{CHCl}_3$ .

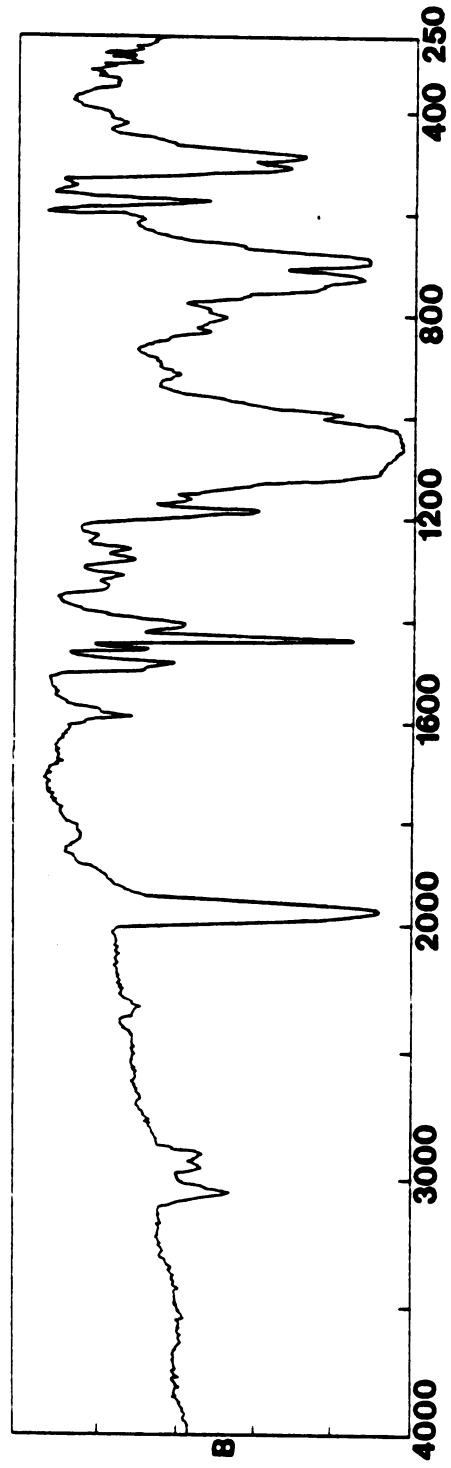
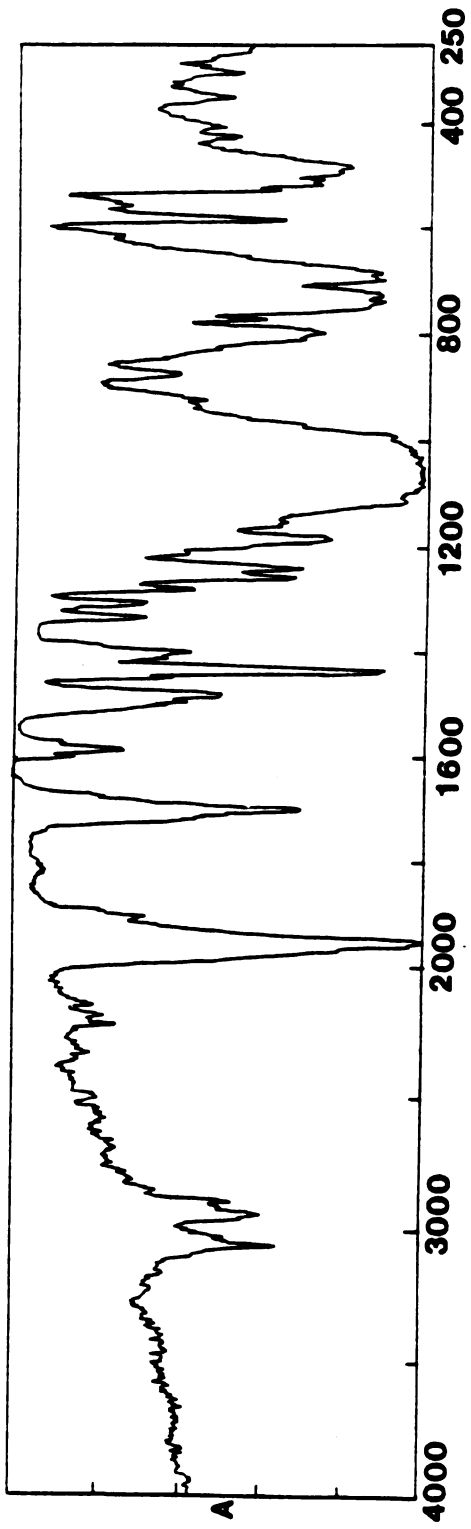
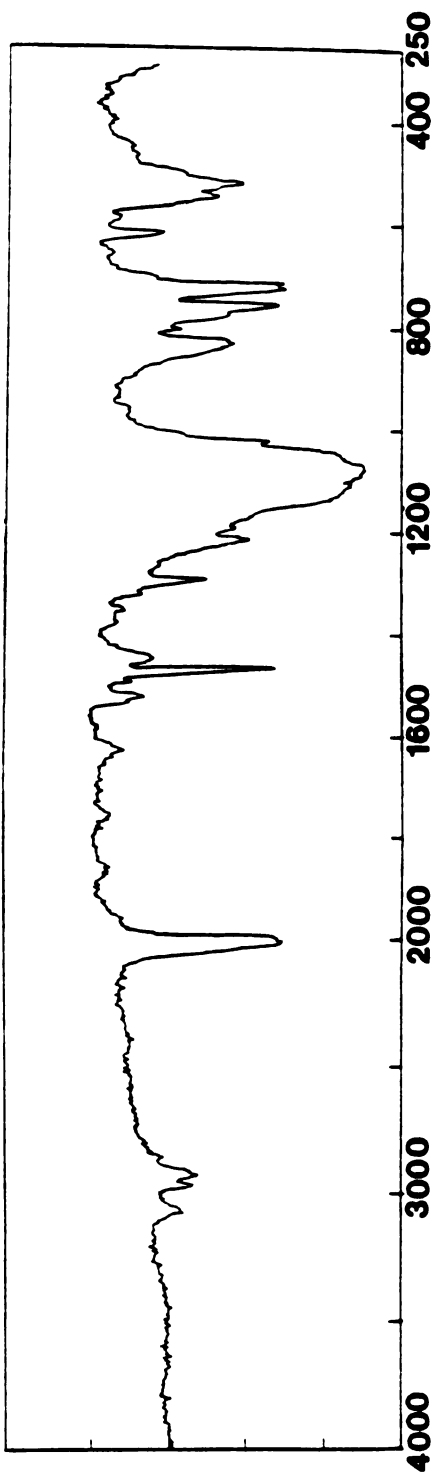


Figure 20. Infrared spectra of 1:1 mixture of  $\text{RhCl}(\text{COD})\text{-P-P}^+:\text{P-P}^+$  + 1-Hexene under hydroformylation condition (recrystallized in  $\text{CHCl}_3$ ).

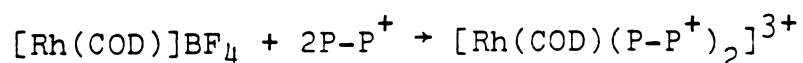
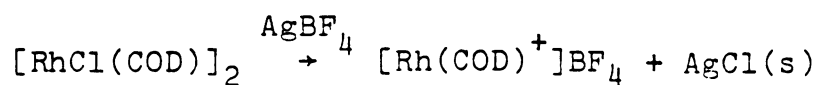


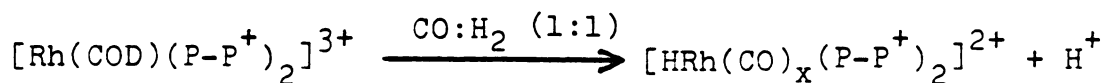
The single, strong CO band at  $1975\text{ cm}^{-1}$  in the IR spectrum confirms the presence of a terminal carbonyl group, not a bridging carbonyl. Also, when the complex is recrystallized in  $\text{CHCl}_3$  or mixture of  $\text{CH}_2\text{Cl}_2$  and ether no strong bands due to bridging CO are seen around  $1800$  to  $1700\text{ cm}^{-1}$  (Figure 19b). Figure 20 also shows the IR spectrum of  $\text{ClRh}(\text{COD})\text{P-P}^+ + \text{P-P}^+$  under hydroformylation conditions. Therefore the IR evidences and chemical analysis suggests that the product is best formulated as  $[\text{RhCl}(\text{CO})(\text{P-P}^+)_2](\text{B}(\text{C}_6\text{H}_5)_4)_2 \cdot \text{X Acetone}$  ( $\text{X} = 2, 3$ ).

#### 5. $\text{Rh}(\text{diene})^+$ , $\text{P-P}^+$ Precursor System

Since hydrochloric acid is formed in the conversion of the  $[\text{RhCl}(\text{COD})]_2$  precursors to  $[\text{RhH}(\text{CO})(\text{P-P}^+)_2]^{2+}$ , the hydroformylation reaction occurs under acidic condition. The acidic solution does not favor hydroformylation reaction of 1-hexene, but it favors isomerization of 1-hexene to 2-hexene. At this stage it was thought that  $\text{Rh}(\text{diene})^+$  complexes (diene = COD, NBD) which do not contain chlorine, would be a better precursor for hydroformylation and might decrease the extent of isomerization of olefin.

The reaction sequence which was examined is described below





Catalyst intercalation was achieved by exchange of the active species with  $\text{Na}^+$ -hectorite:

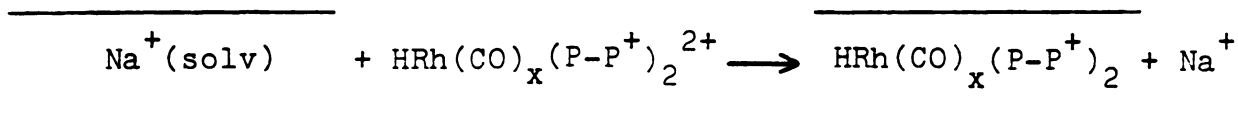


Table 25 lists the results for hydroformylation of 1-hexene with the catalyst at 600 psi and 100°C. The hydroformylation rate and selectivity were found to be the same in case of  $\text{Rh}(\text{COD})^+$ , 2P-P<sup>+</sup> and  $\text{Rh}(\text{NBD})^+$ , 2P-P<sup>+</sup> in both homogeneous system (runs 28, 30) and also in heterogeneous case (runs 29, 31). By comparing homogeneous (runs 28, 30) and intercalated system (runs 29, 31), one may conclude that intercalation significantly decreases the extent of olefin isomerization and increases the n/b aldehyde ratio. These results clearly show that the absence of chlorine in the catalyst system, which has the potentiality to produce hydrochloric acid, decreases the amount of olefin isomerization. No desorption of rhodium complex occurred in these systems, since the filtrate was inactive. Chemical analysis of the intercalated catalyst shows: Rh, 0.27%; P, 0.50%. This means the ratio of P-P<sup>+</sup>:Rh = 2:1.

$\text{Rh}(\text{COD})^+$  and  $\text{Rh}(\text{NBD})^+$  react readily with trace amounts

Table 25. Hydroformylation of 1-Hexene with Rh(diene)<sup>+</sup> Complexes as Catalyst Precursors in Homogeneous and Intercalated Systems.<sup>a</sup>

Run	System Precursor	RXN Time (h)	% Conv.	Product Distribution %				
				n-Heptanal	2-Methyl-Hexanal	2-Hexene	Other <sup>b</sup>	n/b
28	[Rh(COD)] <sup>+</sup> , 2 P-P <sup>+</sup> (Homogeneous)	2	100	60	30	10	--	2.0
29	Intercalated*	24	60	70	23	--	7	3.0
30	[Rh(NBD)] <sup>+</sup> , 2 P-P <sup>+</sup> (Homogeneous)	2	100	64	34	2	--	1.9
31	Intercalated	24	60	73	27	--	--	2.7

<sup>a</sup>[1-Hexene] = 0.4M in acetone; 100°C; 600 psi; CO/H<sub>2</sub> = 1:1; 1-Hexene:Rh = 570:1.

<sup>b</sup>Unidentified reaction products.

of oxygen at  $P-P^+ = Rh(\text{diene})^+ = 2:1$ . The active species is still very sensitive to oxygen. The oxygen sensitivity limits the utility of these systems. Increasing the  $P-P^+ : Rh$  ratio from 2:1 to 10:1 allowed the catalyst to be recycled several times without a significant decrease in activity (Table 26, run 32). Also, it is found that the rates of hydroformylation reaction with  $[Rh(\text{COD})]BF_4 + 10 P-P^+$  and  $[Rh(\text{COD})]BF_4 + 10 PPh_3$  were approximately the same (runs 32, 33). For the intercalated catalyst system, the active catalyst was generated by the addition of CO and  $H_2$  to a solution of  $Rh(\text{COD})^+$ ,  $10 P-P^+$  and then allowing the active species to exchange with hectorite. However, 1-hexene hydroformylation with this intercalated catalyst in acetone was immeasurably slow.

It was thought that by saturating the interlayers of  $Na^+$ -hectorite with positively charged ligand ( $P-P^+$ ), and then allowing the surface-bound ligand to complex  $Rh(\text{diene})^+$ , one might be able to achieve better accessibility of the intercalated rhodium. Therefore  $Na^+$ -hectorite was exchanged with positively  $P-P^+$ . X-ray analysis showed the 001 basal spacing to be  $18.8 \text{ \AA}$ , which indicates one monolayer of positively charged ligand between the silicate sheets.

Figure 21 shows the IR spectrum of  $Na^+$ -hectorite (A) and of  $P-P^+/\text{hectorite} + Rh(\text{COD})^+$  before hydroformylation (B) and after hydroformylation (C). By comparing the three spectra, one can identify the presence of coordinated  $C=O$

Table 26. Hydroformylation of 1-Hexene with  $\text{Rh}(\text{diene})^+$  as Catalyst Precursor in Homogeneous and Intercalated System.

Run	System Precursor	RXN Time (h)	% Conv.	Product Distribution %				n/b
				n-Heptanal	2-Methyl-Hexanal	2-Hexene	Other <sup>b</sup>	
32	$[\text{Rh}(\text{COD})]^+$ + $10\text{PPh}_3$	1	100	60	28	8	4	2.1
33	$[\text{Rh}(\text{COD})]^+$ + $10\text{P-P}^+$	1	100	64	30	4	2	2.1
34	$\overline{\text{P-P}^+}, \text{Rh}(\text{COD})^+$	48	50	70	20	--	10	3.5

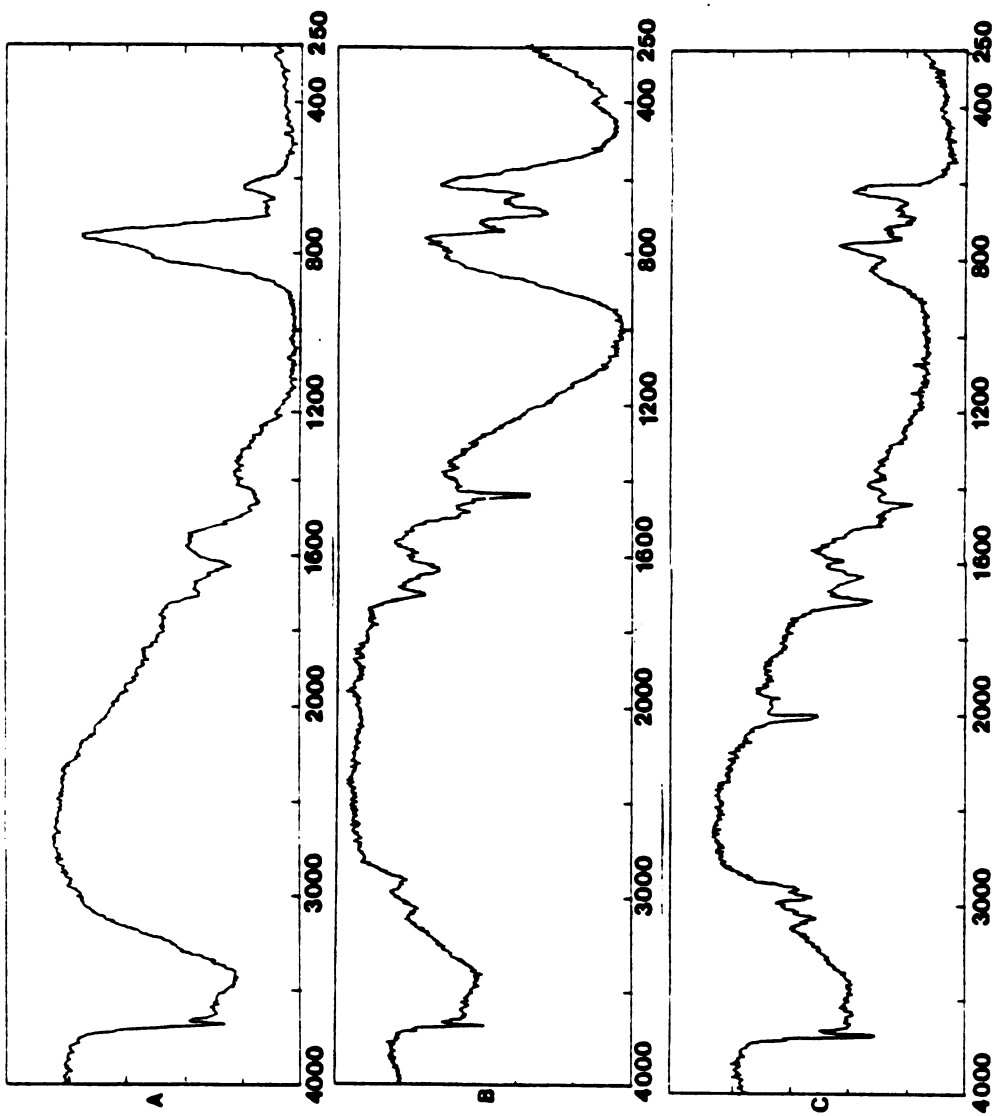
<sup>a</sup>[1-Hexene] = 0.4M in acetone; 100°C; 600 psi;

In Homogeneous; 1-Hexene:Rh = 200:1.

In Run (34); 1-Hexene:Rh  $\geq$  200:1.

In Run 34 Na-Hectorite has been saturated with  $\text{P-P}^+$ , then exchanged with  $[\text{Rh}(\text{COD})]^+$  after addition  $\text{CO}/\text{H}_2 = 1:1$  at 600 psi; 100°C, a very stable complex has been formed.

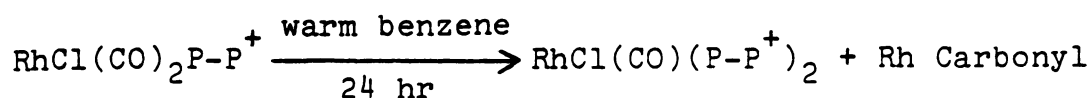
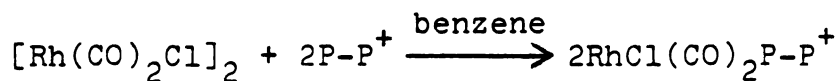
Figure 21. Infrared spectra (KBr disks) of A, Na-hectorite, and (B) the P-P<sup>+</sup>-hectorite + Rh(COD)<sup>+</sup> system before hydroformylation. Spectrum C is for the P-P<sup>+</sup>-hectorite + Rh(COD)<sup>+</sup> system after hydroformylation.



in the spectrum after hydroformylation due to the strong band at  $2000\text{ cm}^{-1}$ . The bands at 1480, 1440 are assigned to methylene group scissoring vibrations ( $\text{P-P}^+$  ligand) and three bands around  $750\text{-}650\text{ cm}^{-1}$  can also be assigned to the phenyl group of the positively charged ligands. The  $\text{P-P}^+$ -hectorite +  $\text{Rh}(\text{COD})^+$  system was active for hydroformylation reaction as shown in Table 26, run 34, it can be seen that (a) the n/b aldehyde selectivity was increased relative to homogeneous solution, (b) no isomerization of 1-hexene to 2-hexene occurred and (c) the rate of hydroformylation was relatively slow. Also, no desorption of rhodium complex was observed. This supported catalyst was found to be one of the best systems for hydroformylation reaction.

#### 6. $[\text{Rh}(\text{CO})_2\text{Cl}]_2 + \text{P-P}^+$ Catalyst Precursor System

A catalyst precursor was prepared by allowing  $[\text{Rh}(\text{CO})_2\text{Cl}]_2$  to react with  $\text{P-P}^+$  as proposed below:



The IR spectra of  $\text{RhCl}(\text{CO})_2\text{P-P}^+$  and  $\text{RhCl}(\text{CO})(\text{P-P}^+)_2$  exhibit a band at  $1975\text{ cm}^{-1}$  which is assigned to a terminal  $\text{C}\equiv\text{O}$  stretching frequency and two bands around 1480 and  $1440\text{ cm}^{-1}$

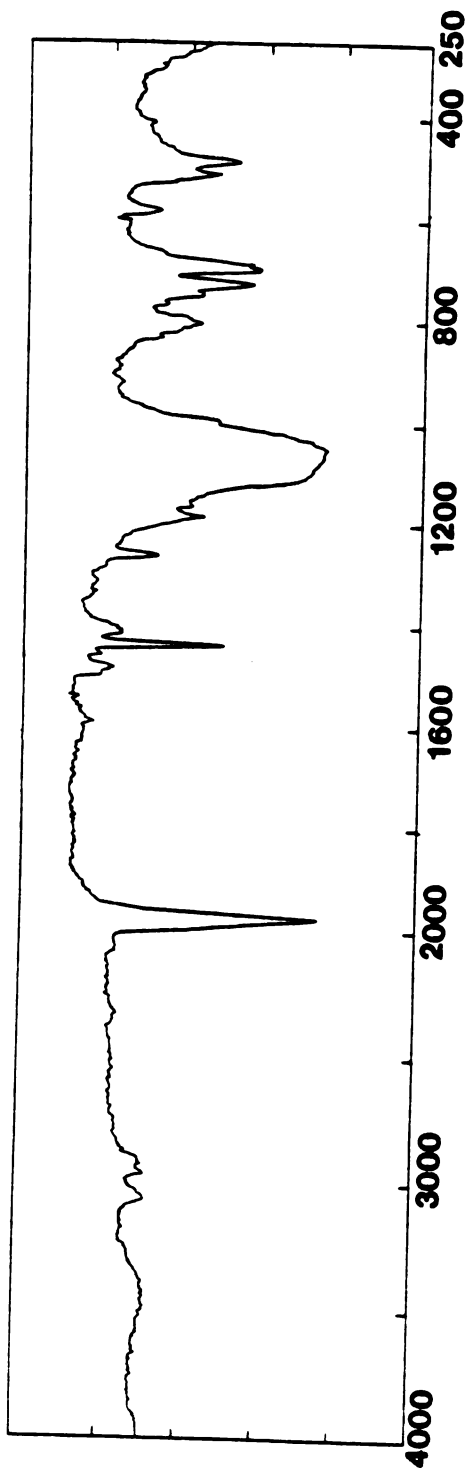


Table 27. Hydroformylation of 1-Hexene with  $[\text{Rh}(\text{CO})\text{Cl}]_2$ , P-P<sup>+</sup> as Catalyst Pre-cursor.<sup>a</sup>

System	RXN Time (h)	% Conv.	Product Distribution %		
			Heptanal	2-Methyl-Hexanal	2-Hexene n/I
<u>a</u> $\text{ClRh}(\text{CO})_2(\text{P-P}^+)$ 2P-P <sup>+</sup>					
Homogeneous	2	100	54	26	20
Intercalated	18	75	71	23	≤6

<sup>a</sup>[1-Hexene] = 0.4M in acetone; 600 psi and 100°C. 1-Hexene:Rh = 570:1.

Figure 22. Infrared spectra (KBr disks) of  $\text{RhCl}(\text{CO})_2\text{-P-P}^+\text{BF}_4$ .



hydroformylation of 1-hexene with the homogeneous and intercalated catalyst systems. The results indicate that the n/b aldehyde selectivity was increased and the isomerization of 1-hexene was decreased by intercalation.

In all of the intercalated catalyst systems investigated in this work, it was observed that the actual rate of hydroformylation was always slower than the corresponding rate of hydroformylation in homogeneous conditions. The immobilization of the homogeneous catalyst probably results in loss of mobility and accessibility of the metal complex, which should have a great influence on the rate of reactions.

#### SUMMARY

This dissertation has shown that cationic rhodium complexes such as  $[\text{Rh}(\text{diene})(\text{PPh}_3)_2]^+\text{A}^-$ , where diene = NBD or COD and  $\text{A}^- = \text{PF}_6^-$ ,  $\text{B}(\text{C}_6\text{H}_5)_4^-$ , are active catalyst precursor for hydroformylation reaction at 25°C and 1 atm. The conversion of 1-hexene was appreciably lower in acetone than in DMF. The rate of reaction at 600 psi and 100°C was faster than at room temperature and 1 atm Pressure, but the amount of isomerization increased and the normal to branched aldehyde ratio decreased. By increasing the  $\text{PPh}_3:\text{Rh}$  ratios to 10:1, aldehyde selectivity was increased and isomerization was decreased.

Solvated sodium ions in the layer silicate hectorite were readily exchanged by  $\text{Rh}(\text{diene})(\text{PPh}_3)_2^+$  rhodium complexes.

IR and X-ray studies confirmed this result. The supported catalyst systems were active for hydroformylation of 1-hexene, but extensive rhodium desorption occurred under hydroformylation conditions. It was clear that the complex which desorbs from the negatively charged silicate surfaces could not be cationic. Further studies of the effects of acid ( $\text{HClO}_4$ ) and base ( $\text{NEt}_3$ ) on the activity of the homogeneous catalysts showed that the reactive intermediate was a neutral monohydride complex which was in equilibrium with inactive rhodium dihydride complex,  $\text{H}_2\text{Rh}(\text{CO})_x(\text{PPh}_3)_2^+$ . Therefore, the neutral intermediate was readily desorbed from the silicate surfaces.

Positively charged rhodium complex analogs  $\text{RhH}(\text{CO})_x(\text{PPh}_3)_2$  suitable for intercalation was prepared first by reaction of  $\text{Ph}_2\text{P}(\text{CH}_2)_2\text{P}^+\text{Ph}_2(\text{CH}_2\text{Ph})$  with rhodium(I) complexes such as  $[\text{RhCl}(\text{diene})]_2$ ,  $\text{Rh}(\text{diene})^+$  where diene = COD or NBD under hydroformylation conditions. These catalysts were active both in homogeneous and intercalated systems. In all of supported catalysts n/b aldehyde selectivity increased and isomerization of 1-hexene to 2-hexene decreased relative to homogeneous solution.

$^{31}\text{P}$  NMR studies confirmed that the coordinating ability of the positively charged ligand ( $\text{P-P}^+$ ) in solution is similar to triphenyl phosphine ( $\text{PPh}_3$ ). Also,  $\text{ClRh}(\text{CO})(\text{S})_2(\text{P-P}^+)_2$ , S = acetone was isolated as one of the major reactive intermediates during the course of hydroformylation reaction.

REFERENCES

## REFERENCES

1. A. Nakamura, M. Tsutsur, "Principles and Applications of Homogeneous Catalysis", John Wiley & Sons, N.Y., 1980, pp. 1-9, and references therein.
2. K. F. Purcell and J. C. Kotz, Inorganic Chemistry, p. 963, and references therein.
3. (a) G. W. Parshall, J. Mol. Catal., 4, 243-270 (1978).  
(b) F. R. Hartley, CHEMTECH, 686 (1980).
4. P. Pino, F. Piacenti, M. Bianchi, I. Inwender and P. Pino (Eds), "Organic Syntheses Via Metal Carbonyls", Wiley-Interscience, New York, 1977, Vol. 2, p. 43.
5. R. Fowler, H. Connor, R. A. Baehl, CHEMTECH, 722, 1976.
6. R. L. Pruett, J. A. Smith, U.S. Patent, 3,917,661 (1975), Chem. Abs., 84, 30433 (1976).
7. C. S. Cronan, Chem. Eng., 84 (26), 109 (1977).
8. F. E. Paulik, Catal. Rev., 6, 49 (1972).
9. H. Hohenschutz, N. VonKutepow, W. Hummele, Hydrocarbon Process., 45 (11), 141 (1966).
10. J. F. Roth; J. H. Craddock, A. Hershman; F. E. Paulik, CHEMTECH., 1, 600 (1971).
11. J. Smidt, W. Hafner, R. Jira, R. Sieber, J. Sedlmeier, A. Sabel, Angew. Chem. Int. Ed., 1, 80 (1962).
12. S. A. Miller, Chem. Process. Eng. 50(6), 63 (1969).
13. J. A. Blay, U.S. Patent, 3,983,208 (1976); Chem. Abs., 86, 20025 (1977).
14. G. E. Welton, German Patent, 2,027,280 (1970); Chem. Abs., 74, 63983 (1971).
15. C. N. Winnick, German Patent, 1,914,572 (1969): Chem. Abs., 72, 54773 (1970).

16. P. H. Towle, R. H. Balwin, Hydrocarbon Process, 43 (11), 149 (1964).
17. R. P. Lowery, A. Aguilo, Hydrocarbon Process., 53 (11), 103 (1974).
18. G. H. Twig, Chem. Ind., 476 (1966).
19. R. B. Stobaugh, V. A. Calarco, R. A. Morris, L. W. Stroud, Hydrocarbon Process., 52, 99 (1973).
20. G. Wilke, Angew Chem. Int. Ed., 2, 105 (1963).
21. T. Alderson, E. L. Jenner, R. V. Lindsey, J. Am. Chem. Soc., 87, 5638 (1965).
22. Dupont, Chem. Eng. New (April 26) 30, 1971.
23. F. J. Bellringer, C. E. Hollis, Hydrocarbon Process, 47, 127 (1968).
24. M. W. Farlow, U. S. Patent, 2,518,608 (1950), Chem. Abs. 45, 639 b (1951).
25. G. Alexmills, CATAL-Rev. SCI. ENG. 14(1), 69 (1976).
26. E. L. Muetterties and J. Stein, Chem. Rev., V. 79(6) 479, (1979), and references therein.
27. (a) R. L. Pruett, Ann. N.Y. Acad. Sci., 295, 239 (1977).  
(b) E. L. Muttterties, Science, 196, 839 (1977).
28. (a) B. L. Hoymore and J. A. Ibers, J. Am. Chem. Soc., 96, 3325 (1974).  
(b) C. D. Meyer and R. Eisenberg, J. Am. Chem. Soc., 98, 1364 (1976).  
(c) S. Bhaduri and B. F. G. Johnson, Trans. Met. Chem., 3, 156 (1978).
29. (a) L. Marko and B. Heil, CATAL. REV. SCI. ENG., 8(2), 269 (1973).  
(b) W. S. Knowles, M. J. Sabacky, B. D. Vineyard, Adv. Chem. Ser., 132, 275 (1974).  
(c) B. D. Vineyard, W. S. Knowels, M. J. Sabacky, G. L. Bachman and D. J. Weinkauff, J. Am. Chem. Soc., 99, 5946 (1977).

30. (a) F. A. Cotton, G. Wilkinson, "Advanced Inorganic Chemistry", John Wiley & Sons, 1980, pp. 163-165, 264-265.
- (b) G. A. Cotton, et al. J. C. S. Dalton, 181, 1978.
- (c) D. E. Fenton, Chem. Soc. Rev., 6, 325 (1977).
31. (a) J. Manassen (1973), In "Catalysis, Progress in Research" (F. Basolo and R. L. Burwell, Jr., eds), pp. 177-188, Plenum, New York.
- (b) J. C. Bailor, Jr., Catal. Rev. Sci. Eng. 10(1), 17 (1974).
- (c) J. P. Candlin and H. Thomas, Adv. Chem. Ser., 132, 212 (1974).
32. (a) F. R. Hartley and P. N. Vezey, Advan. Organometal. Chem., 17, 189 (1977).
- (b) Z. M. Michalska, D. E. Webster, Chemtech, 2, 117 (1975).
- (c) R. L. Pruett, Advances in Organometal. Chem., 17, 1-57, Academic Press, New York, San Francisco, London, 1979.
33. C. N. Satterfield "Heterogeneous Catalysis in Practice", p. 5-7, copyright 1980.
34. (a) D. G. H. Ballard, Advan. Catal. 23, 269 (1973).
- (b) L. L. Murrell "Advanced Materials in Catalysis" (Ed. J. J. Burton and R. L. Garton, p. 239-265 and references therein (1977)).
- (c) M. S. Scurrrell "Catalysis", p. 215-241 and references therein.
- (d) See Reference (31b), (32a).
- (e) J. M. Basset and A. K. Smith, "Fundamental Homogeneous Catalysis", ed. by M. Tsutsui and R. Ugo. Plenum Press, N.Y., p. 69, and references therein.
- (f) M. S. Scurrrell, Platinum Metals Rev., 21, 92 1977.
- (g) R. H. Grubbs, Chemtech, 512 (1977).
- (h) Yu. I. Yermakov, Cat. Rev. Sci. Eng., 13, 77 (1976).

- (i) D. D. Whitehurst, Chemtech, 44 (1980).
- (j) B. C. Gates and J. Lieto, Chemtech, 195 (1980).
35. J. Villadsen and H. Liveberg, Catal. Rev. Sci. Eng. 17, 203 (1978).
36. R. R. Rony and J. F. Roth, J. Mol. Catal., 1, 13 (1975/76).
37. (a) R. H. Grubbs and R. C. Kroll, J. Am. Chem. Soc., 93, 3062 (1971).
- (b) R. H. Grubbs, C. Gibbons, R. C. Kroll and C. Brubaker, J. Am. Chem. Soc., 95, 2373 (1973).
38. (a) C. U. Pittman, L. R. Smith and R. M. Hanes, J. Am. Chem. Soc., 97, 1742 (1975).
- (b) C. U. Pittman and L. R. Smith, ibid, 97, 1749 (1975).
39. G. Braca, G. Sbrana, C. Carlini and F. Ciardelli, "Catalysis, Homogeneous and Heterogeneous", Delmon and Jannes, 307 (1975) and references therein.
40. M. Graziani, G. Strukul, M. Bonivento, F. Pina, E. Cernia and N. Palladino, ibid., p. 33.
41. R. F. Batchelder, B. C. Gates and F. P. Kuijpers, "Proceedings of the Sixth International Congress on Catalysis, 1976", Ed. G. C. Bond, P. B. Wells and F. C. Tompkins, The Chemical Society, London 1, 499 (1977)
42. C. U. Pittman, Jr., B. T. Kim, and W. M. Douglas, 40, 590 (1975), J. Org. Chem.
43. W. Dumont, J. C. Poulin, T. P. Dang and H. B. Kagan, J. Am. Chem. Soc., 95, 8295 (1973).
44. T. H. Kim and H. F. Rase, Ind. and Eng. Chem., (Product Res. and Development), 15, 249 (1976).
45. S. Jacobson, W. Clementz, H. Hiramoto and C. U. Pittman, J. Mol. Catal., 1, 73 (1975/76).
46. C. U. Pittman, Jr. and R. M. Hanes, J. Am. Chem. Soc., 98, 5402 (1976).
47. W. O. Haag and D. D. Whitehurst, "Proceedings 5th International Congress on Catalysis 1972". North Holland, Amsterdam, 1, 465 (1973).

48. A. Gupta, A. Rembaum and H. Gray, Organomet. Poly [Symp], 1977 Pub. 1978, p. 155.
49. F. Hojabri, J. Appl. Chem., Biotchnol., 26, 362 (1976).
50. I. Dietzman, D. Tomanova and J. Hetflejs, Coll. Czech. Chem. Comm. 39, 123 (1974).
51. M. Mejstrikova, R. Reriche and M. Kraus, ibid, 39, 135 (1974).
52. C. U. Pittman, Jr., S. K. Wu, and S. E. Jacobson, J. Catal., 44, 87 (1976).
53. (a) I. V. Howell, R. D. Hancock, R. C. Pitketly and P. J. Robinson, "Catalysis Homogeneous and Heterogeneous", Delmon and Jannes, ed., pp. 349 (1975).  
(b) K. G. Allum, R. D. Hancock, S. M. Kenzi, R. C. Pitketly and P. J. Robinson, J. Organomet. Chem., 87, 189 (1975).  
(c) Ibid, 87, 203 (1975).  
(d) K. G. Allum, R. O. Hancock, I. V. Howell, R. C. Pitketly and P. J. Robinson, J. Catalysis, 43, 322 (1976).  
(e) T. J. Pinnavaia, J. G. S. Lee and M. Abedini, "Silylated Surfaces", D. Leyden, ed., Morden and Breach, N.Y., pp. 333 (1980).
54. R. Jackson, J. Raddlesden, D. J. Thompson and R. Whelan, J. Organomet. Chem., 125, 57 (1977).
55. M. Capka and J. Hetfljls, Coll. Czech. Chem. Comm., 39, 154 (1974).
56. K. G. Allum, R. D. Hancock, I. V. Howell, T. E. Lester, S. McKenzie, R. C. Pitketly and P. J. Robinson, J. Organomet. Chem., 107, 393 (1976).
57. L. L. Murrel, A. A. Oswald and R. L. Hartherink, Preprints, Div. Petr. Chem. National Meeting, Am. Chem. Soc., Chicago, p. 1226 (1977).
58. F. R. W. P. Wild, G. Gubitosa and H. H. Brintzinger, J. Organomet. Chem., 148, 73 (1978).
59. K. G. Allum, R. D. Hancock, S. McKenzie and P. C. Picketly, Proc. 5th Int. Congress Catal. 1972, 477 (1973).

60. K. G. Allum, R. D. Hancock, I. V. Howell, T. E. Lester, S. McKenzie, R. C. Pitkethy and R. J. Robinson, J. Catal. 43, 331 (1976).
61. D. G. H. Ballard, Adv. Cat., 23, 263 (1973) and references therein.
62. Y. I. Yermakov, Cat. Rev., 13, 77 (1976) and references therein.
63. V. A. Zakharov and Y. I. Yermakov, Catal. Rev., Sci. Eng., 19 (1), 67 (1979).
64. N. Takahashi, I. Okura, and T. Keii, J. Am. Chem. Soc., 97, 7489 (1975).
65. Ref. 30(a), p. 514-515 and references therein.
66. M. A. Boersma, Advanced Materials in Catalysis, p. 67-99 (1977) (ed. by J. J. Burton and R. L. Garten).
67. E. Mantovani, N. Palladiano, A. Zanobi, J. of Mol. Catal., 3, 285 (1977/78).
68. (a) I. E. Maxwell, R. S. Dowings and S. A. J. Van-Langer, J. of Catal., 61, 485 (1980).  
(b) Ibid, 61, 493 (1980).
69. S. Tsuruya, H. Miyamoto, T. Sakae and M. Masai, J. of Cat., 64, 260 (1980).
70. T. J. Pinnavaia, R. Raythatha, J. G. S. Lee, L. J. Hollaran, and J. F. Hoffman, J. Am. Chem. Soc., 101, 6891 (1979).
71. T. J. Pinnavaia and R. Rahthatha, submitted for publication.
72. T. J. Pinnavaia and Han Min Chang, unpublished.
73. (a) R. E. Grim, "Clay Mineralogy", 2nd ed., McGraw-Hill, New York, 1968, pp. 77-92.  
(b) R. M. Barrer, FRS "Zeolites and Clay Minerals as Sorbents and Molecular Sieves", Academic Press, 1978, pp. 407-486 and references therein.
74. (a) D. M. Clementz, T. J. Pinnavaia, M. M. Mortland, J. Phys. Chem., 77, 196 (1973).

74. (b) M. McBride, T. J. Pinnavaia, M. M. Mortland, Am. Mineralogist, 60, 66 (1975).
- (c) T. J. Pinnavaia, "Magnetic Resonance in Colloid and Interface Science", ACS Symp. Ser., 34, H-A. Resing, C. G. Wade, eds., 1976, p. 94.
75. S. I. Zones M. R. Palmer, J. G. Palmer, J. M. Doemeny, G. N. Schrauzer, J. Am. Chem. Soc., 100, 2113 (1978).
76. B. K. G. Theng, "The Chemistry of Clay-Organic Reactions", John Wiley & Sons, Inc., New York, NY, 1974.
77. D. B. Fenn, M. M. Mortland and T. J. Pinnavaia, Clays and Clay Minerals, 21, 315 (1973).
78. W. H. Quayl and T. J. Pinnavaia, Inorg. Chem., 18, 2840 (1979).
79. (a) H. E. Doner, M. M. Mortland, Science, 166, 1406 (1969).
- (b) M. M. Mortland, T. J. Pinnavaia, Nature Phys. Sci, 229, 75 (1971).
- (c) T. J. Pinnavaia, M. M. Mortland, J. Phys. Chem., 75, 3957 (1971).
- (d) D. B. Fenn, M. M. Mortland, T. J. Pinnavaia, Clays, Clay Minerals 21, 315 (1973).
80. (a) T. Endo, M. M. Mortland and T. J. Pinnavaia, Clays and Clay Minerals, 28, 105 (1980).
- (b) T. Endo, M. M. Mortland and T. J. Pinnavaia, Clays and Clay Minerals, 29 (2), 153 (1981).
81. Otto Roelen, Ger. Pat. 84 9548 (1938); Chem. Zentr., 1953, 927.
82. E. J. Wickson, H. P. Dengler, No. 11, 69 (1972) "Hydrocarbon Process".
83. B. Conils, "New Synthesis with Carbon Monoxide", (ed. J. Falbe), N. Y. (1980), 11, p. 1 and references therein.
84. (a) F. E. Paulik, 6(1), 49-84 (1972)., Catal. Rev.
- (b) R. Lai and E. Ucciani, Advances in Chemistry Series, 132, 1-26 (1974).

84. (c) A. T. Jurewicz, L. D. Rollmann and D. D. Whitehurst, ibid, pp. 240-251.
- (d) P. Pino, G. Consiglio, C. Botteghi and C. Salmon, ibid, pp. 295-323.
- (e) P. Pino, F. Piacenti and M. Bianchi, V. 2, pp. 43-231, (1977) "Organic Synthesis via Metal Carbonyls", (ed. by I. Wender and P. Pino).
- (f) Roy L. Pruett, V. 17, pp. 1-60 (1979), Advances in Organometallic Chemistry.
- (g) See footnote cited in 83 pp. 1-225.
85. G. Y. Hsu and M. Orchin, J. Am. Chem. Soc., 97, 3553 (1975).
86. G. Sontos, B. Heil and L. Marko, Ann. N.Y. Acad. Sci., 239, 47 (1974).
87. (a) D. Evans, G. Yagupsky, G. Wilkinson, J. Chem. Soc (A), 2660 (1968).
- (b) G. Yauupsky, C. K. Brown, G. Wilkinson, J. Chem. Soc., Chem. Commun. 1244 (1969).
- (c) Ibid, 1392 (1970).
- (d) D. E. Moris, H. B. Tinker, 2, 554 (1972).
- (e) A. J. Draesmith, R. Whyman, J. Chem. Soc., 362 (1973).
- (f) R. Whyman, J. Organomet. Chem., 66, C23-C25, 1974, 81, 97 (1974), 94, 303 (1975).
- (g) F. Calderazzo, Angew Chem., 89, 305 (1977).
88. (a) F. Piacenti, et al., J. Organomet. Chem., 23, 257 (1970).
- (b) J. P. Grima, F. Choplin, G. Kaufman, J. Organomet. Chem., 129, 221 (1977).
89. T. Kitmura, T. Joh, J. Organomet. Chem., 65, 235 (1974).
90. P. L. Ragg, ICI (Ltd), DE-As 2000 829 (1972).
91. (a) R. C. Ryan, C. U. Pittman, J. P. O'Connor, J. Am. Chem. Soc., 99, 1986 (1977).
- (b) C. U. Pittman, R. C. Ryan, CHEMTECH (3), 170 (1978).

92. C. U. Pittman, G. O. Evans, CHEMTECH, Sept. 1973, p. 560.
93. C. U. Pittman, Jr., S. E. Jacobson, H. Hiramoto, J. Am. Chem. Soc., 97, 4774 (1975).
94. M. O. Farrell, C. H. VanDyke, L. J. Boucher, S. J. Metlin, J. Organomet. Chem., 169, 199 (1979).
95. R. L. Burwell, CHEMTECH, June, (1974) 370.
96. R. D. Hancock, I. V. Howell, R. C. Pitkethy and P. J. Robinson, "Catalysis: Heterogeneous and Homogeneous", (ed. by, B. Delmon and G. Janes) (1975) pp. 361-371.
97. O. Johnson, ibid, p. 497.
98. G. C. Bond, P. B. Wells, F. C. Tompkins, The Chemical Society London, V. 1, 488 (1977).
99. E. H. Homeier, UOP, Inc. U.S. 4,070,403 (1978).
100. J. S. Yoo, U.S. 3,940,447 (1976), Atlantic Richfield Co.
102. J. P. Friedrich, Ind. Eng. Chem., Prod. Res. Div., 17, 205 (1978).
103. P. R. Rony and J. F. Roth, J. of Mol. Catal., 1, 13 (1975/76).
104. (a) L. A. Gerritsen, A. VanMeerkerk, M. H. Vreugdenhil, J. J. F. Scholten, J. Mol. Catal., 9, 139 (1980).  
(b) L. A. Gerritsen, J. M. Herman, W. Klut and J. J. F. Scholten, J. Mol. Catal., 9, 157 (1980).  
(c) L. A. Gerritsen, J. M. Herman, W. Klut and J. J. F. Scholten, J. Mol. Catal., 9, 241 (1980).  
(d) L. A. Gerritsen, W. Klut, M. H. Vreugdenhil, and J. J. F. Scholten, J. Mol. Catal., 9, 257 (1980).  
(d) L. A. Gerritsen, W. Klut, M. H. Vreugdenhil and J. J. F. Scholten, J. Mol. Catal., 9, 265 (1980).
105. R. Uson, L. A. Oro, C. Claver, M. A. Garrolda, J. Mol. Catal., 4, 231 (1978).

106. C. Ercolani, J. V. Quagliano, L. M. Vallariano, Inorg. Chim. Acta, 3, 421 (1969).
107. R. C. Taylor, R. A. Kolodny, Inorg. Nucl. Chem. Letters, 7, 1063 (1971).
108. (a) D. Berglund, D. W. Meek, J. Am. Chem. Soc., 90, 518, (1968).  
(b) D. Berglund, D. W. Meek, Inorg. Chem., 8, 2602 (1969).
109. R. D. Bertrand, D. A. Allison, J. G. Verkade, J. Am. Chem. Soc., 92, 71 (1970).
110. (a) R. L. Keiter, D. P. Shah, Inorg. Chem., 11, 191 (1972).  
(b) R. L. Keiter, L. W. Cary, J. Am. Chem. Soc., 94, 9232 (1972).
111. R. C. Taylor, R. L. Keiter, L. W. Carry, Inorg. Chem. 13, 1928 (1974).
112. J. A. Connor, J. P. Day, E. M. Jones, G. K. McEwen, J. Chem. Soc. (D), 347 (1973).
113. D. D. Traficante, J. A. Sims, M. Mulcahy, J. Magn. Res., 15, 484 (1974).
114. J. Chatt and L. M. Venanzi, J. Chem. Soc. (A), 4735 (1975).
115. H. C. Volger, M. M. P. Guasbeek, H. Hogeveen and K. Varieze, Inorg. Chim. Acta., 3, 145 (1969).
116. H. C. Volger and H. Hogeveen, Rec. Trav. Chim., B6, 1066 (1967).
117. R. R. Schrock and J. A. Osborn, J. Am. Chem. Soc., 93, 2397 (1971).
118. P. Uguagliati, G. Deganello, L. Busetto and U. Belluco, Inorg. Chem., 1625 (1969).
119. M. Green, T. A. Kuc and S. H. Taylor, J. Chem. Soc. (A), 2334 (1971).
120. H. G. Horn and K. Sommer, Spectrochim. Acta. A., 27, 1049 (1971).
121. (a) D. Evans, J. A. Osborn and G. Wilkinson, J. Chem. Soc. (A), 3133 (1968).

121. (b) C. K. Brown and G. Wilkinson, J. Chem. Soc. (A), 2753 (1970).
122. J. Peone and L. Vaska, Angew. Chem., 10, 511 (1971).
123. R. H. Crabtree and H. Felkin, J. Mol. Catal., 5, 75 (1979).
124. See Reference 84(f), pp. 29-32.
125. (a) U. Mayer, V. Gutmann and W. Gerger, Monat. fur Chem., 106, 1235 (1975).
- (b) V. Gutmann and R. Schmid, Coord. Chem. Rev., 12, 263 (1974).
126. J. Grimbolt, J. P. Bonnelle, C. Vaccher, A. Movtreux, F. Petit, J. Mol. Catal., 9, 357 (1980).
127. F. Piacenti, P. Pino, R. Lazzaroni and M. Bianchi, J. Chem. Soc. C, 488 (1966).
128. F. Asinger and O. Berg, Chem. Ber., 88, 445 (1955).
129. (a) B. Fell, W. Rupilius, and F. Asinger, Tetrahedron Lett., 3261 (1968).
- (b) F. Asing, B. Fell, and W. Rupilius, Ind. Eng. Chem., Prod. Res. Develop., 8, 214 (1969).
130. E. D. Becker, "High Resolution NMR - Theory and Chemical Applications" Academic Press, New York, Ch. 7 (1969).
131. T. Quayle, Ph.D. Thesis, Michigan State University, 1979.
132. T. H. Brown and P. J. Green, J.A.C.S., 92, 2359 (1970).
133. P. Uguagliati, G. Deganeli, L. Busetto and U. Belluco, Inorg. Chem., 8, 1625 (1969).